Spring 2009

Interdependent Regulation of Cytomegalovirus Proteins in Complex

Lisa L. Bolin
Old Dominion University

INTERDEPENDENT REGULATION OF CYTOMEGALOVIRUS PROTEINS IN COMPLEX

by

Lisa L. Bolin
B.S. August 2002, Old Dominion University

A Dissertation Submitted to the Faculty of
Eastern Virginia Medical School and Old Dominion University in Partial Fulfillment of the
Requirement for the Degree of

DOCTOR OF PHILOSOPHY

BIOMEDICAL SCIENCES

EASTERN VIRGINIA MEDICAL SCHOOL
OLD DOMINION UNIVERSITY
May 2009

Approved by:

Ann E. Campbell (Director)

Julie A. Kerry (Member)

Laura K. Hanson (Member)

Neel K. Krishna (Member)

ABSTRACT

INTERDEPENDENT REGULATION OF CYTOMEGALOVIRUS PROTEINS IN COMPLEX

Lisa L. Bolin
Eastern Virginia Medical School and Old Dominion University, 2009
Director: Dr. Ann E. Campbell

Human cytomegalovirus (HCMV) is a ubiquitous herpesvirus that causes significant morbidity and mortality in the immune compromised. Using the murine cytomegalovirus (MCMV) model, we identified two genes, M140 and M141, which are determinants of macrophage tropism. Monocytes/macrophages are a critical cell type for cytomegalovirus (CMV) pathogenesis as sites of viral latency and by supporting viral replication and disseminating virus throughout the body. We previously found that the localization of the M140/M141 gene products (pM140/pM141) is different when the proteins are co-expressed as compared to their individual expression. When the proteins are individually expressed pM141 localizes diffusely throughout the cytoplasm and, to a lesser extent, the nucleus while pM140 localizes almost exclusively in the nucleus. Co-expression alters the localization of either protein, as they co-localize to a distinct perinuclear region. The proteins form a stable complex and in the absence of pM140, pM141 is significantly destabilized. These results imply a complex regulation and interdependence of the proteins.

The purpose of this study was to identify protein domains within pM140 and pM141 that are required for the interdependent regulation of the proteins and to determine the mechanism of pM141 protein degradation. We identified an interaction

domain within pM140 at the extreme N terminus of the protein that is required foroptimal complexing with *in vitro* expressed pM141. We found that pM141 is degraded in a proteasome-dependent, but ubiquitin-independent pathway. The M141 protein is stabilized by pM140 in a concentration-dependent manner and we identified the region of pM140 required to stabilize pM141. However, direct complexing between pM140 and pM141 is not sufficient to stabilize the protein. Thus, our results support a model in which pM140 protects pM141 from proteasomal degradation by recruiting an additional viral or cellular protein to the pM140 and pM141 complex and this as yet unidentified protein is strictly required for pM141 stability.

This thesis is dedicated to the friend who brought me here. You will live in my heart and soul as long I have life.

ACKNOWLEDGMENTS

No graduate student project would be possible without the assistance, guidance, and encouragement of a great many people. I have great friends who helped with moral support. Steven: thanks for bandaging the blood, drying the sweat, and wiping the tears. Thanks for the pride, encouragement, tolerance, and for your love. There is no doubt that I would not be here without you. Siabhon Harris and Gaurav Basu: thanks for your support, encouragement, sanity, and tolerance. I consider us "brothers" and without you I might have quit...several times. Siabhon: also thanks for many helpful discussions about experiments and for all your technical assitance on this document and others.

I have a fantastic committee who helped in more ways than I could possibly fit on this page. Dr. Campbell: thanks for being an amazing scientist and model mentor. I learn just by being in your presence, but I also thank you for your active guidance and support. Thanks for your wisdom, confidence and encouragement. Thanks also for your critical assistance in helping me with my long-term goals. Dr. Kerry: thanks for serving as my co-mentor on the project, for your contagious enthusiasm for science, and for being a fantastic teacher in the lab and in the many classes that you instructed. Thank you also for your generosity in lab and desk space. Dr. Hanson: thanks for years of kind, patient instruction and mentoring as early as my undergraduate studies, for insightful discussions, and for allowing me access to your vast store of knowledge. Dr. Krishna: thank you for your encouragement and for many valuable suggestions on my project. I also acknowledge the late Timothy Bos. Dr. Bos was an amazing teacher in the lab or classroom. His contributions as a committee member were numerous and his wisdom, encouragement, and enthusiasm as a mentor helped to mold me during my studies and

will continue to inspire me throughout my career.

I have great co-workers and friends. Victoria Cavanaugh and Jackie Slater: thank you for you answering many questions and for your encouragement and support as early as my undergraduate project in Dr. Campbell's lab. Thanks also for making me feel at home in the lab. Lisa Fetters: thank you for all your assitance in the lab and for always giving me encouragement with a smile. Joe Briggs: thanks for your encouragement and guidance when I worked with you before entering graduate school. Thanks for taking the time and for serving as an exemplary model of a graduate student. Liz Westgard, Chuck Frost, and Jodi Osborne: thank you for all you do or have done. Your help has been instrumental in my experiments.

This work was supported by the National Cancer Institute PHS grant (R01-CA41451) awarded to Ann E. Campbell.

TABLE OF CONTENTS

Page

LIST OF TABLES

LIST OF FIGURES

Figure Page

Figure Page

CHAPTER I

INTRODUCTION

The Family *Herpesviridae*

Herpesviruses are widely distributed in nature and have been isolated from most animal species (150). Acute infection, accompanied by cytopathic effects, is followed by lifelong latency (150). The family *Herpesviridae* contains three subfamilies based on biological properties of the viruses. The *alphaherpesvirinae* contain members that establish latency in sensory ganglia and exhibit variable host range (150). Compared to other subfamilies, the *alphaherpesvirinae* have an abbreviated life cycle and rapidly destroy infected host cells (150). The subfamily is represented by viruses such as herpes simplex virus types 1 and 2, varicella-zoster virus, and feline rhinotracheitis herpesvirus. The *betaherpesvirinae*, to which human cytomegalovirus (HCMV) and murine cytomegalovirus (MCMV) belong, exhibit strict species-specificity and cause enlargement of infected host cells (150). Compared to other subfamilies the *betaherpesvirinae* have a long reproductive cycle (150). The *gammaherpesvirinae*, represented by members such as Epstein-Barr virus and Kaposi's sarcoma-associated herpesvirus, consist of viruses that typically exhibit limited host range and are lymphotropic with specificity for either T- or B-lymphocytes (150).

CMV virion and genome

The HCMV and MCMV virions are similar in structure (Fig. 1A (114)). The

---

The model journal for this dissertation is Journal of Virology.

linear, double-stranded DNA genome is enclosed in an icosahedral capsid composed of at least four viral proteins (85, 114, 176). The capsid is surround by a host cell-derived lipid membrane studded with numerous viral glycoproteins that serve as attachment proteins (114). Between the capsid and outer membrane is a tegument layer composed of viral proteins that assist the virus in establishing infection upon entry into a host cell (114).

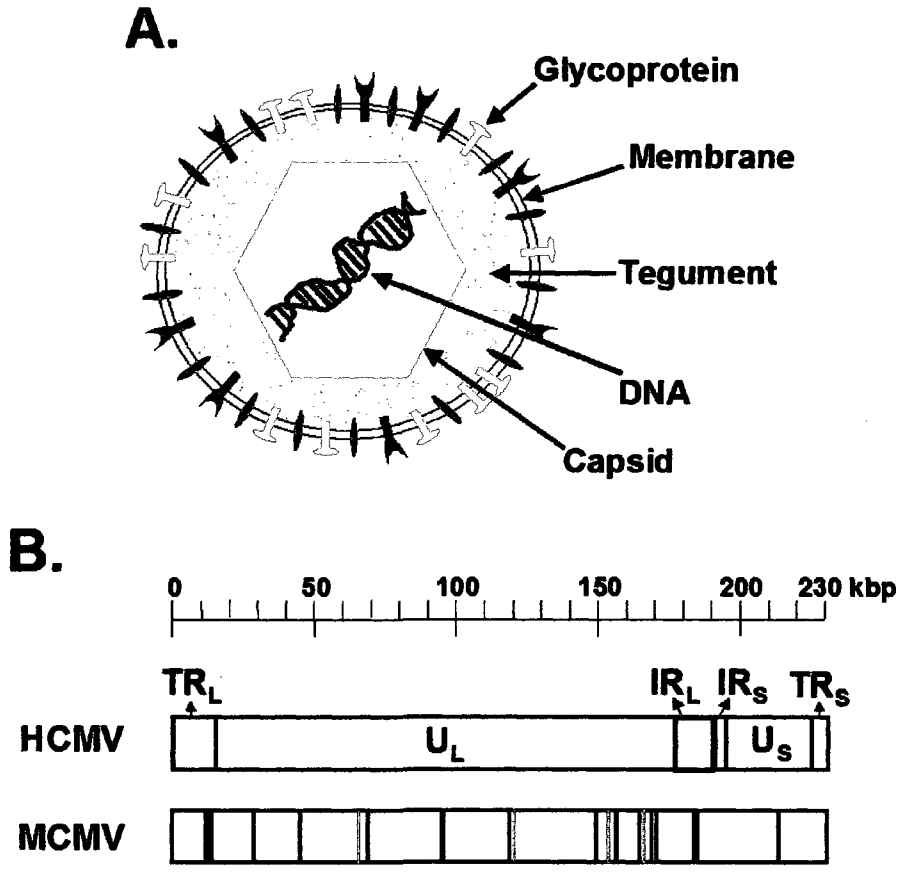

FIG. 1. CMV virion and genome. A. Diagram of a CMV virion. Arrows show the location of the glycoproteins, membrane, tegument, DNA, and capsid. B. Schematic representation of the HCMV and MCMV genomes. A scale is shown at top where each tick mark is 10 kbp. The HCMV genome (middle) is shown with the locations of the unique long (U_L) and short (U_S) regions as open boxes. The internal (IR_L, IR_S) and terminal repeats (TR_L, TR_S) are displayed as gray boxes. The MCMV genome (bottom) contains short terminal repeats (not shown), clusters of direct repeats (black lines where thickness represents relative cluster size), and inverted repeats (gray lines).

The genomes of HCMV and MCMV are similarly sized at just over 230 kilobase pairs (kbp) of DNA (Fig. 1B (21, 143)). The HCMV genome is predicted to contain over 200 open reading frames (ORFs) while the number of MCMV ORFs is predicted to be a little lower, at 170 (21, 37, 85, 116, 143, 201). The HCMV genome is composed of two unique segments designated U_L (unique long) and U_S (unique short) each flanked by a terminal repeat element (TR_L or TR_S) on one side and an inverted repeat (IR_L or IR_S) on the other side (114). The terminal repeat elements can isomerize giving rise to four genome arrangements (114). Nomenclature of HCMV ORFs is based on their location within the unique or repeated regions and within each region the ORFs are sequentially numbered (21, 169). The MCMV genome contains short terminal direct repeats as well as short internal direct repeats and inverted repeats throughout the genome that do not isomerize to generate additional sequence arrangements (38, 107, 143). MCMV ORFs are numbered sequentially from 1 to 170 and are designated by an uppercase M where the ORF has sequence similarity to an HCMV ORF or by a lowercase m for ORFs not conserved (143).

HCMV life cycle

As shown in Fig. 2, the HCMV life cycle begins when the virus attaches to the cell surface. Initial attachment is accomplished by tethering of viral glycoproteins, gM, gN, and gB to heparin sulfate proteoglycans expressed ubiquitiously on the surface of cells (13, 30, 83). Tethering is followed by more stable interactions between viral glycoproteins and one or more cell surface receptors leading to fusion and internalization of the viral capsid and tegument proteins (13, 114). Integrins (43, 74, 192), platelet-

derived growth factor receptor (167), and epidermal growth factor receptor (193) have all been implicated as cellular entry receptors with utilization likely dependent on the host cell. Post-entry capsids are then transported to the nuclear pores where the viral genome is released (114).

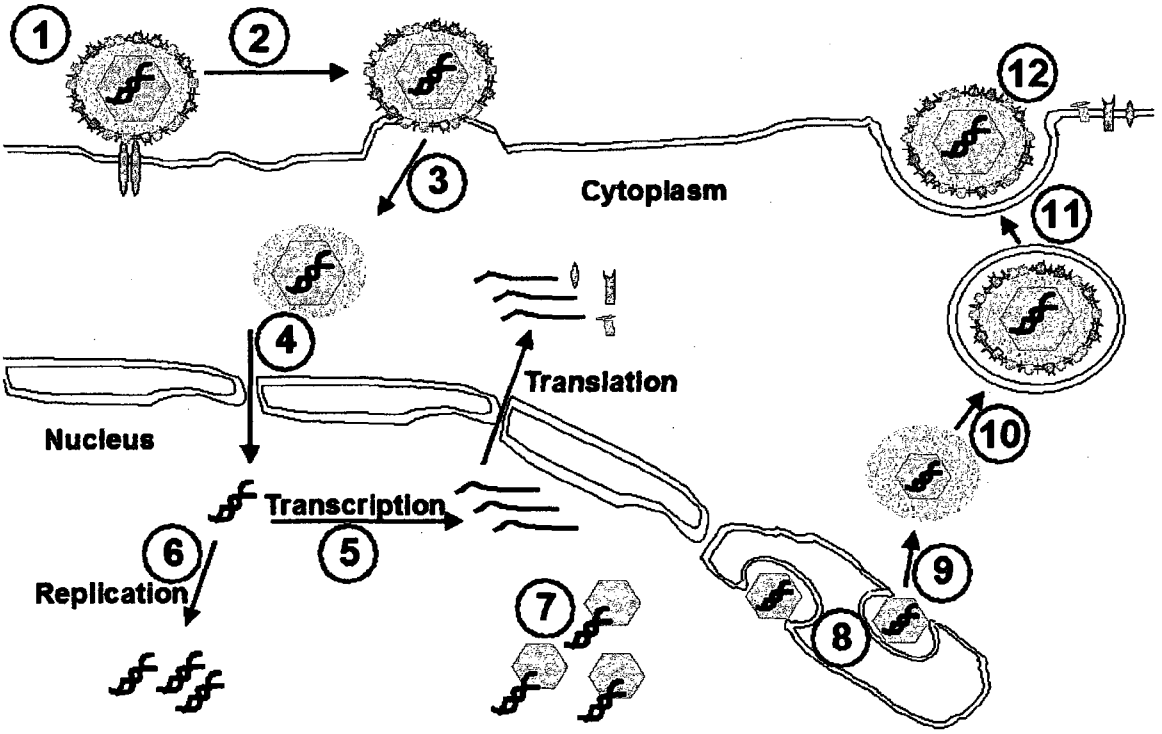

FIG. 2. Life cycle of HCMV. The life cycle begins when the virus attaches to receptors at the cell surface (1). Virus fuses with cell membrane (2). Capsid and tegument are released into the cytoplasm (3) and then the capsid travels to the nucleus (4). Viral genes are transcribed and translated (5) some of which enter the nucleus for capsid formation (not shown). Viral DNA is replicated (6), nucleocapsids are formed (7), and bud through the dual membrane of the nucleus (8). Some tegumentation is thought to occur in the nucleus (not shown) and cytoplasm (9). Viral glycoproteins are transported to the cell surface (not shown). Tegumented capsids acquire a double membrane along with viral glycoproteins from cytoplasmic vesicles (10). The viral envelope fuses with the cell membrane (11) and budding results in virions with a single membrane (12).

Replication of DNA proceeds with three temporal waves of viral gene expression termed immediate early, early, and late, where each phase of expression controls progression to the next (114, 164). Immediate early gene expression follows entry, is independent of expression of viral genes, and occurs via cellular transcription factors and viral transcriptional transactivators found in the tegument (114, 164). Generally, expression of immediate early genes yields non-structural products that inhibit apoptosis, inhibit anti-viral host protein shutoff, modulate expression of MHC class I expression, and are transcriptional transactivators required for expression of viral early and late genes (23, 114). Expression of many early genes results in products required for replication of viral DNA (164). HCMV encodes numerous enzymes and proteins involved in transcription and DNA replication, for example, the DNA polymerase and associated processivity factor, the single-stranded DNA binding protein, and among others, enzymes involved in nucleotide metabolism (114). Late gene expression follows genome replication and mainly yields structural proteins including glycoproteins, tegument proteins, and proteins required for capsid formation (164).

Viral DNA replication and capsid formation occur in the nucleus of infected cells. Viral capsid proteins and other viral proteins required for capsid formation form some interactions in the cytoplasm, but are ultimately transported to the nucleus for final procapsid assembly and formation (48). Maturation of procapsids occurs with a series of cleavages of the scaffolding elements mediated by a viral protease (48). DNA-containing nucleocapsids are formed when the viral terminase recognizes signals on the concatameric DNA and interacts with the procapsid to position the DNA for packaging (48). Mechanics of packaging are not fully understood, but result in cleavage of the

concatameric DNA leading to deposition of single, full-length genome in the nucleocapsid (48).

Mature virions are formed after tegumentation of nucleocapsids and envelopment at the cell surface (40). A temporary envelope is formed when nucleocapsids bud from the inner nuclear membrane and is shed after budding through the outer nuclear membrane. Addition of some tegument proteins may occur during nuclear egress, but tegumentation is thought to occur largely in the cytoplasm in distinct compartments (40, 68, 154, 155). Viral glycoproteins are processed via cellular machinery and are transported to the plasma membrane (40). Presently, tegumented capsids are thought to acquire a double membrane along with the processed viral glycoproteins from cytoplasmic vesicles which then fuse with the plasma membrane during exocytosis resulting in release of mature virions with a single envelope (40).

HCMV pathogenesis and epidemiology

HCMV is transmitted through urine, saliva, tears, semen, cervical secretions, and breast milk (130). As a consequence of primary infection shedding can occur for prolonged periods of months to years (130). Naïve individuals are thought to contact virus at mucosal surfaces in the respiratory tract, upper alimentary tract, or genitourinary tract under natural conditions (130). Transmission from mother to baby can occur transplacentally, intrapartum, or during breast feeding. Additionally, primary infection can be transmitted to naïve people in blood products or transplanted tissues (130). After acute infection, lifelong latency is established giving rise to periodic reactivations (130, 159).

The virus infects a variety of different cell types including endothelial cells, epithelial cells, stromal cells, fibroblasts, hepatocytes, smooth muscle cells, neuronal cells, neutrophils, and monocytes/macrophages (71, 117, 160). As a consequence of this broad cell tropism disease manifestations are observed in most tissues/organs of the immunocompromised host including salivary glands, lung, liver, pancreas, kidney, eye, ear, placenta, alimentary tract, heart, ovaries, pituitary, adrenals, thyroid, brain, and skin (130). Monocytes of the peripheral blood and their $CD34^+$ progenitors in bone marrow are believed to be sites of viral latency (96, 106, 159, 181).

HCMV infection is rather ubiquitous worldwide and prevalence increases with age although the age of initial infection and overall prevalence correlates with socioeconomic status (130). Generally, higher prevalence and lower age at acquisition of infection is observed within developing countries and in groups with lower socioeconomic status in developed countries (130). In the United States it is estimated that 1.5 per 100 adults (age 12-49) are infected each year in high income classes whereas that number increases to 3.5/100 people in low income classes (29).

Generally, infection of immune competent people is asymptomatic, but can result in mononucleosis and symptoms ranging from the more common malaise, headache, fatigue, and fever, to the less common lymphadenopathy, pharyngitis, splenomegaly, hepatomegaly, and rash (130).

HCMV infection is the leading viral cause of birth defects and symptomatic congenital infections present with multisystem involvement (130). Symptoms such as jaundice, hepatitis, hepatosplenomegaly, petechiae, and thrombocytopenia can lead to severe disease, but typically clear within a few weeks after birth (130). However,

symptomatic infections involving the central nervous system (CNS) can result in permanent damage including hearing loss, impaired vision, cerebral palsy, and mental retardation (130). Approximately 5% to 10% of congenital infections result in symptoms, but 7-25% of asymptomatic infants are prone to CNS sequelae (130).

Immunocompromised individuals such as bone marrow and solid organ transplant patients, chemotherapy patients, and acquired immunodeficiency syndrome (AIDS) patients can suffer from minor symptoms such as self-limited fevers to major multisytem disease (130). Severity of infection correlates with degree of immunosuppresion (66, 130). Morbidity of transplant recipients can vary depending on type of transplantation and the most common symptoms are fever, leukopenia, malaise, arthralgias, and macular rash although more serious disease including pneumonitis, gastrointenstinal ulceration, severe hepatic dysfunction, opportunistic fungal infection, and impaired graft function can also occur (130). Within one year of transplantation 75% of organ recipients are affected by some form of HCMV disease (66). The source of infection is reactivation of latent virus either within the recipient or in donor organ, cells, or blood products with the latter resulting in more severe disease for seronegative recipients (130). For AIDS patients the introduction of highly active antiretroviral therapy has significantly decreased HCMV disease by preventing severe immunodeficiency (66). However, symptoms still occur with the most common being retinitis with associated vision loss and less common CNS diseases including polyradiculopathy and encephalitis (66).

The murine model of CMV infection and disease

Due to the strict species specificity of Cytomegaloviruses, numerous animal

models have emerged for the study of HCMV pathogenesis. The MCMV model is an appropriate model due to the similarities between the two viruses in virion structure, genome content, and pathogenesis. In addition to conservation in virion structure and morphology, the protein content of the virions is very similar. Recently, proteomic approaches were utilized to analyze the viron proteome of both HCMV and MCMV (85, 176). Except for glycoproteins, the number of structural proteins isolated from the virions was strikingly similar including five HCMV capsid proteins compared to four for MCMV and fourteen HCMV tegument proteins compared to ten for MCMV (85, 176). Furthermore, of the 58 MCMV proteins identified (38 with known function) and the 59 total proteins isolated from HCMV, 32 of these are homologous (85, 176).

The genomes also have numerous properties in common. First, the genomes are nearly identical in size at approximately 230 kbp and of these 180 kbp are essentially collinear with similar gene organization (21, 143). The G + C content is also similar at many points across the two genomes (21, 143). Furthermore, 78 ORFs of MCMV are generally homologous to HCMV ORFs and the viruses share various conserved gene families (21, 143). The viruses share many functional homologs some with little or no sequence homology (18) and like HCMV, MCMV displays a temporal wave of gene expression (95, 114).

Importantly, the viruses exhibit similarities in pathogenesis making MCMV an appropriate model for HCMV. As with HCMV, infection of adult MCMV-resistant mice with virulent virus is usually asymptomatic, acute infection is followed by latency, and the virus can be reactivated upon immune suppression of the infected host (18, 95). Infection of MCMV-susceptible mouse strains results in morbidity and mortality.

Genetic comparisons between resistant and susceptible strains of mice have determined that resistance correlates with an ability to control early infection via natural killer (NK) cells (18, 95). Similarly, severe HCMV disease is observed in humans with NK cell-deficiency (95). As with HCMV, MCMV infection in immunocompromised adult mice is severe. The viruses exhibit similar cell and organ tropism and, as with HCMV, multiple organ damage is observed with severe morbidity and high mortality in MCMV-infected immunocompromised mice (95). Similar to HCMV congenital infection, experimental infection of mouse neonates results in CNS damage and developmental abnormalities (95). However, MCMV is not a model for transplacentally acquired infection as the murine virus does not cross the placenta.

Macrophages as determinants of CMV pathogenesis

Macrophages and their precursors, monocytes, are considered a critical cell type for HCMV and MCMV pathogenesis. These cells are involved in all stages of infection as they are important in acute infection, as well as in persistence and latency. Contact with HCMV-infected bodily fluids results in virus replication in epithelial cells and endothelial cells at initial sites of infection which then spreads to the peripheral blood (PB) where monocytes become infected (160). HCMV and MCMV encode chemokine homologs that attract leukocytes to initial sites of infection and promote a monocyte-associated viremia (133, 152). This may be a strategy for viral dissemination as monocytes are believed to be responsible for viral spread from the PB to host tissues (52, 162, 174, 203).

Although monocytes are the prominent cell type infected in the PB and harbor

CMV genomes, they are not productively infected (35, 98, 108, 166, 180, 181, 188, 189). In some cases viral gene expression has been detected, but is limited to early events and virus is not released from cultured monocytes or in the PB of infected individuals (41, 49, 113, 148, 181, 182). Instead, monocytes and hematopoietic precursor cells have been shown to be sites of viral latency (78). Virus can be reactivated in these cells and productive infection is related to the degree of differentiation of monocytes into macrophages (45, 71, 78, 165, 182). Yurochko and Huang (203) demonstrated that HCMV binding to peripheral blood monocytes initiates signal transduction events resulting in production of inflammatory cytokines. Further studies showed that even in the absence of viral gene expression, HCMV induces differentiation of these cells into macrophages which display transendothelial migration and increased cell motility (162, 163). A model was proposed from these studies suggesting that HCMV induces monocyte differentiation to allow spread of infectious virus to host tissues (162).

Macrophages as deterrents of CMV pathogenesis

In addition to their role as determinants of CMV pathogenesis, macrophages also have a role as mediators of the innate immune response against CMV. For example, macrophages are induced by the type II interferon, interferon gamma (IFN-γ), to produce nitric oxide (156), which can inhibit CMV replication in several human cell lines and in infected mice (12, 97, 122, 126). Type I interferons (IFNα/β) produced by macrophages and dendritic cells can also limit viral replication (36, 197) and appear to modulate the innate and adaptive immune response during MCMV infection (34). Two antiviral agents, tumor necrosis factor alpha (TNFα) and virus inhibitory protein, endoplasmic

reticulum-associated, interferon-inducible (viperin), produced by macrophages are induced by CMV infection (25, 57, 198, 206). Both proteins inhibit viral replication and have been shown to block late gene expression (25, 65). Certain antiviral effects appear to be macrophage-specific. For example, Presti et al. (140) demonstrated that IFN-γ inhibits the growth of MCMV more efficiently in macrophages than fibroblasts. Genes regulated in response to IFN-γ were different in macrophages and the antiviral effects were independent of known mechanisms (140). Thus, while differentiation of monocytes into macrophages favors virus production, activation of macrophages by inflammatory mediators leads to an antiviral state (57).

CMV has evolved to counteract many of these macrophage-induced antiviral effects. For example, HCMV inhibits gene expression of IFNα-induced antiviral effectors by blocking signal transduction (112). In HCMV infected cells viperin distribution is dramatically altered, perhaps as a means for the virus to evade the harmful effects of the protein (25). MCMV disrupts TNFα autocrine responses in macrophages by reducing levels of TNF receptor on the cell surface (138). Given their importance in infection it is not surprising that CMV has developed numerous strategies for avoidance of immune recognition in macrophages. For example, HCMV and MCMV inhibit antigen presentation to CD4+ T lymphocytes by down-regulating major histocompatibility complex (MHC) class II molecules (63, 124, 145). Specific MCMV products also prevent expression of MHC class I molecules on the surface of macrophages, thus preventing antigen presentation to cytotoxic T lymphocytes (100). In addition, HCMV infection of activated macrophages results in up-regulation of HLA-G, which likely provides protection of the infected cell from immune killing (127).

M140 and M141 are determinants of macrophage tropism

Presently, despite the crucial role of monocytes/macrophages in CMV immunity and pathogenesis, only a limited number of MCMV genes have been identified that are important for optimal growth in these cells (57). We have demonstrated the importance of the M140 and M141 genes in macrophage tropism. Compared to wild type (WT) MCMV, a mutant virus (RV10) disrupted of M140, M141, and adjacent gene M139, shows nearly 3 $\log_{10}$ lower growth in the differentiated macrophage cell line, IC-21, but not in fibroblast cells (62). A growth defect of over 2 $\log_{10}$ was also found at peak titers in primary, differentiated macrophages obtained by peritoneal lavage (62). Importantly, we found a similar growth defect in the macrophage-dense spleens of infected BALB/c mice. Although WT virus replicated to as high as 10^4 plaque forming units (PFU)/ml on day 3 postinfection, RV10 displayed little to no growth in this organ (62). We also tested the virulence of RV10 in SCID mice which lack functional T and B lymphocytes. Although virulence of tissue culture-passaged virus is attenuated in BALB/c mice, SCID mice are exquisitely sensitive. We found that infection with 10^4 PFU of WT virus was 100% lethal in these mice by 28 days postinfection, but mice infected with RV10 survived at least 90 days postinfection (62).

Our current model predicts that replication in macrophages is an important factor in MCMV virulence and therefore, the virus has evolved strategies to ensure growth in this cell type. We further characterized the growth of viruses individually disrupted of expression of the M139 (RVΔ139), M140 (RVΔ140) and M141 (RVΔ141) genes. Although RVΔ139 had no growth defect in IC-21 macrophages or the spleens of BALB/c

mice (61), our collaborators have shown that a transposon insertion mutant of M139 is defective for growth in IC-21 macrophages (105). We found that RVΔ140 displayed a nearly identical growth defect to that of RV10 in IC-21 macrophages and in the spleens of BALB/c mice (61). However, RVΔ141 displayed an intermediate phenotype, both *in vitro* and *in vivo*. While RV10 and RVΔ140 have a nearly 3 $\log_{10}$ lower growth than WT virus in IC-21 macrophages, RVΔ141 replication is at most 2 $\log_{10}$ lower than WT (61). Likewise, replication of RV10 and RVΔ140 in the spleen is nearly undetectable, but RVΔ141 replicated as high as 10^3 PFU/ml in this tissue (61). Thus, pM140 and pM141 are determinants of macrophage tropism and given the importance of monocytes/macrophages in viral spread and dissemination, are important for viral pathogenesis.

Characterization of pM140 and pM141

We previously characterized expression of M140 and M141 at the level of mRNA and protein. The transcripts of M140 and M141 are expressed with early kinetics, and are 3' coterminal with each other and with transcripts of an adjacent gene, M139 (59). The protein products of the M140 and M141 genes are expressed at early and late times with similar kinetics and correspond to proteins of 56 kDa and 52 kDa, respectively (61). Steady-state levels of the proteins increase over the course of infection, beginning at three hours post-infection in fibroblasts and at six hours post-infection in IC-21 macrophages (61). Both proteins are members of the US22 gene family (see below) and contain all four motifs characteristic of the family and pM140 also contains an acidic domain (Fig.

3A, B) (59, 143). Currently, a function for the US22 motifs or the acidic domain has not been demonstrated.

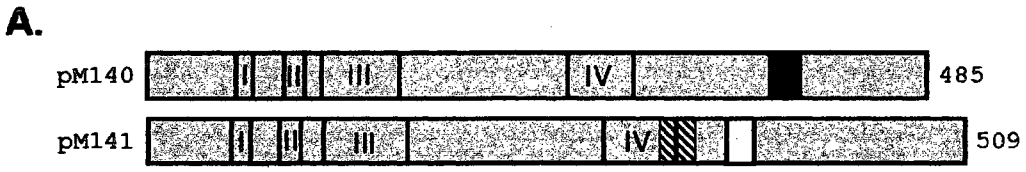

Motif I: Consensus - OXOXXPXXW
pM140 - 57 LPLGIPHNW
pM141 - 54 IPLGFPQDW

Motif II: Consensus - OOCCX-XLXXOG
pM140 - 86 IVCCDEPLTVVG
pM141 - 82 LLCCEEALIPLG

Motif III:
pM140 - 109 EDAGAALCLGAWTRVFVYEIQEDAMILVAPDLDKLARFGLLHCETLYRR
pM141 - 111 GYGVSLVLSGEYGRVYVYTASDDTLHLVARNLEELGRFGISRRSFAYKE

Motif IV:
pM140 - 261 FSIHHLLVIDTFGAIYTLDMQREKFYRVADGITMLLRAGMAK
pM141 - 284 FRADHVIVADKFGAVYSLLVYSRAGLTRRVADSVAEFFQMGMLK

B.
pM140 Acidic Domain: 386 TNEEEDWTDTNEWEQEDDDN

C.
pM141 Putative NLS: 317 KRVFSSSFEFRQRERRK

D.
pM141 PEST domain: 360 RFDSPTDDEDYVPADCMAE

FIG. 3. Known or predicted motifs in the amino acid sequence of pM140 and pM141. Numbers represent amino acids corresponding to the position of the motifs in the protein sequence. A. Diagram of full length pM140 and pM141 showing the location of protein domains (top). The location of US22 motifs is represented in each protein as open boxes. In pM140 the location of an acidic domain is represented by a black box. In pM141 the location of a putative NLS (nuclear localization signal) is represented by a hatched box and a PEST motif is represented by a white box. M140 and M141 belong to the US22 gene family which can contain up to four conserved motifs with unknown function. Both proteins contain all four motifs as shown. The consensus sequence of Motifs I and II are shown. Motifs III and IV are less well defined, but are characterized by stretches of nonpolar residues. Hydrophobic residues are denoted by O, any amino acid by X, and nonpolar residues are underlined. B. M140 contains an acidic domain. Acidic residues are underlined. C. M141 is predicted to contain a NLS. Basic residues are underlined. D. M141 is predicted to contain a PEST motif rich in proline (P), glutamic acid (E), serine (S), threonine (T).

The proteins exist in at least two stable complexes in infected macrophages and fibroblasts as determined by immunoprecipitation analysis using high stringency salt and detergent washes (82). One complex is composed of pM140, pM141, pM139, and an unidentified protein of approximately 98 kDa (82). Sucrose gradient purification of these proteins predicts that the four proteins exist as one or more large complexes, estimated to be as large as 669 kDa (82). A second complex found in infected cells is composed of pM140 and pM141 formed in the absence of pM139 (82). This complex is predicted to be 158 kDa and thus may be composed of, for example, two pM140 molecules and one pM141 molecule (82). Although the stoichiometry of the pM140 and pM141 complex has not been determined, this predicted ratio is supported by the relative intensities of the co-immunoprecipitated pM140 and pM141 bands (82). Alternatively, a third unidentified protein of approximately 50 kDa could be a component of this complex. We have also demonstrated complex formation between pM140 and pM141 expressed from transiently-transfected cells and from *in vitro* translation (82). Thus, pM140 and pM141 complexing may take on various forms and may include other viral or cellular proteins. In addition, the composition of the complexes may vary with cell type.

The M140 and M141 proteins have differential patterns of localization when expressed individually or together. We have demonstrated, using cell fractionation techniques, that both proteins can be isolated from the nucleus and the cytoplasm of infected fibroblasts and IC-21 macrophages (61). The M140 protein is found almost exclusively in the nucleus of transiently-transfected fibroblasts or macrophages while pM141 is distributed diffusely throughout the cytoplasm and to a lesser extent, the nucleus (82). Interestingly, the only localization signal predicted by bioinformatics

analysis is a putative nuclear localization signal in pM141 (Fig. 3C). Confocal microscopy analysis of fibroblasts and IC-21 macrophages transiently expressing both proteins demonstrates that the proteins predominantly co-localize to a perinuclear region (82). The proteins co-localize with *cis*-Golgi markers, but not with a marker directed against the *trans*-Golgi compartment (82). Further analysis of the localization of pM140 revealed that this perinuclear region is adjacent to enlarged microtubule organizing centers observed specifically in infected macrophages and not in fibroblasts (60). These centers were found to have characteristics of aggresomes which are concentrated sites of proteasomes, mitochondria, and chaperone proteins for the degradation of aggregated proteins that have traveled to the microtubule organizing center (31, 196). If the aggresomes are unable to degrade the protein aggregates, degradation may occur through autophagy (31, 196).

Further characterization of RVΔ140 demonstrates an indirect function of pM140 in stabilizing viral capsids. The number of viral particles is reduced in RVΔ140-infected cells and steady-state levels of two virion proteins, the major capsid protein (MCP) and a tegument protein, M25, were reduced specifically in RVΔ140-infected macrophages and not fibroblasts (60). Although we did not determine the half-life of M25, the half-life of the MCP was found to be 9 hours in WT-infected cells compared to 6 hours in RVΔ140-infected cells (60). The localization of pM140 adjacent to aggresome-like structures formed in macrophages, the reduction in levels of virion proteins, and the reduction in viral capsids suggests that capsid stability is affected by pM140 indirectly through the more general role of regulating viral protein stability in macrophage cells.

Although the functionality of the domain has not been investigated, pM141 contains a PEST domain and these domains are found on rapidly degraded proteins (Fig. 3D (144, 149)). We have observed a reduction in the steady-state levels of pM141 and the half-life of the protein is reduced from 2 hours in WT-infected cells to 1 hour in RVΔ140-infected cells (61). However, this effect of pM140 is observed in both macrophages and fibroblasts and thus, may reflect regulation of pM141 by pM140 in all cell types.

US22 Gene Family

M140 and M141 are members of the US22 gene family found in all beta-herpesviruses (59, 143). Members of this gene family contain up to four conserved motifs with unknown function (94, 120). US22 motifs I and II have consensus sequences while motifs III and IV are defined by stretches of nonpolar amino acids (94). The M140 and M141 proteins contain all four US22 motifs as shown in Fig. 3A.

M140 and M141 are homologs of HCMV genes US23 and US24, respectively, neither of which are essential genes (21, 143, 201). Unlike their murine counterparts, US23 and US24 are required for efficient viral growth in fibroblasts and have been isolated from virion particles (37, 201). Presently, US23 has not been studied in greater detail. However, US24-deficient mutants have a replication defect in fibroblasts after viral DNA travels to the nucleus, but prior to expression of immediate-early genes (44). Thus, although US23 and US24 are homologous to M140 and M141 based on similarities in sequence, there is no apparent functional homology between these human and mouse US22 genes.

In addition to US23 and US24, HCMV has 10 other US22 family member genes including UL23, UL24, UL28, UL29, UL36, UL43, IRS1, TRS1, US22, and US26 (21). Of these only UL28, UL29, TRS1, US23, US24, and US26 have been shown to enhance replication of the virus in fibroblasts while the remaining six are dispensable for growth in this cell type (201). Of the genes where functional mechanisms have been investigated, the UL36 protein has been shown to inhibit Fas-mediated apoptosis by preventing activation of caspase-8 (161), the TRS1 protein is required for efficient assembly of DNA-containing capsids (1), the IRS1 and TRS1 proteins are transcriptional transactivators of numerous viral genes (86, 151, 171), and the IRS1 and TRS1 proteins inhibit anti-viral host protein shutoff likely by preventing activation of protein kinase R (23, 55). Restriction of primary HCMV replication to fibroblasts and a very limited number of other cell types *in vitro* has hindered studies on the role of these US22 family genes in cell type-specific replication.

Ten additional US22 genes are also found in MCMV including M23, M24, m25.1, m25.2, M36, M43, M128, M139, m142, and m143 (143). Of these, only m142 and m143 are essential genes and function similar to IRS1/TRS1 in blocking activation of protein kinase R (16, 22, 24, 58, 105, 185). Interestingly, m142 and m143 also form a complex; in fact, complexing is required to bind double-stranded RNA and PKR (22). M136, a sequence and positional homolog to HCMV UL36, has similarly been found to inhibit Fas-mediated apoptosis by binding to caspase-8 (105). Comprehensive mutational analysis of MCMV US22 genes demonstrated the requirement of M43 for optimal viral replication in numerous cell types and of M36 for optimal replication in macrophages (105).

Protein/protein interactions

The M140 and M141 proteins form a complex in infected cells (82). We hypothesized that the proteins function as a complex to optimize replication in macrophages. Proper functioning of many proteins requires that they interact with regulatory proteins or form complexes that confer functional properties. These protein/protein interactions are involved in every aspect of cell biology and disruption of protein complexing may lead to disease (131). Furthermore, viruses have numerous ways to co-opt cellular protein/protein interactions for their benefit or to disrupt these interactions when they are inhibitory to viral pathogenesis (114). Proteins rarely function as isolated entities and may either function in complex with one or a small number of other proteins or, in some cases, as large multi-protein complexes (3, 87, 115). In fact, complexes of ten or more proteins mediate most of the major cellular processes (3). Multi-protein complexes function in replication, transcription, splicing, translation, and protein degradation (3, 205).

In addition to large protein machines, myriad regulatory interactions occur between protein pairs that are strictly required for protein function and may be transient in nature or more stable (205). Transient protein/protein interactions are required for signaling cascades, post-translational modifications, enzyme reactions, and translocation of proteins to distinct subcellular locations (87, 115, 131, 205). More stable interactions are required to regulate temporally-controlled proteins such as transcription factors (87). Complexing of transcription factors with regulatory proteins inhibits function of the transcription factor until the expression of the target genes is required (118).

Interactome mapping has become possible with the advent of *in silico* methods and high-throughput proteomic techniques. Experiments involving the interactome have demonstrated that most proteins only interact with a few other proteins while a much smaller proportion of proteins can interact with a large number of partners (56). Surface areas of proteins are limiting and some interaction domains are specific to bind to single proteins (87). In other cases where proteins are able to bind to numerous partners, the binding site of these proteins contains critical amino acid residues that make conserved interactions with multiple partners (87).

Protein/protein interactions occur through interaction domains in the proteins and these domains may be conformation-dependent or -independent (87). Complex formation between proteins is mediated by shape, chemical complementarity, and flexibility of proteins and occurs at the surface of the proteins through weak, noncovalent interactions (87). Complexing among proteins may be constitutive, as in the case of the proteasome, or may be transient and induced, as is the case with cell signaling cascades. The amino acids residues located at the protein interface vary with the type of interaction (87, 131, 132). This is likely due to the strength of interaction as constitutive complexing generally is formed from hydrophobic interactions and transient interactions are more reliant on salt bridges and hydrogen bonds (87).

An excellent example of the myriad protein/protein interactions that are required to regulate a single protein is that of the transcription factor, nuclear factor-κB (NF-κB). The first level of regulation relates to function and is within the protein molecule. NF-κB is a dimeric molecule composed of members of the Rel family of proteins (103). Since each subunit makes contacts with DNA, different combinations of complexed subunits

have an ability to regulate transcription of different genes (103). Furthermore, different dimers can alternately activate or repress transcription of genes (103).

Another layer of complexity is that NF-κB activation of target genes is not constitutive and thus must be regulated. This regulation occurs by complexing between NF-κB and another protein, IκBα. Despite the fact that NF-κB has a NLS that is required for entry into the nucleus the protein remains localized to cytoplasm in most cell types due to protein/protein interactions with IκBα that mask the NLS (103). Yet another level of complexity is that IκBα not in complex is a rapidly degraded protein (104). NF-κB complexing masks the degradation signal of IκBα preventing rapid degradation (104).

Activation of NF-κB requires numerous transient protein/protein interactions. Activation begins at the cell surface where complexing between inflammatory cytokines or pattern recognition molecules and their respective receptors leads to several possible signaling cascades. These cascades encompass numerous transient interactions between proteins whereby upstream effectors are activated and phosphorylate downstream effectors ultimately leading to phosphorylation of IκBα (103). Phosphorylation of the protein allows it to be recognized by a ubiquitin ligase that adds ubiquitin moieties through transient interactions causing degradation of the protein, release of NF-κB, unmasking of the NLS, and allowing NF-κB to interact with transport proteins that carry it into the nucleus (84, 103, 183). Once in the nucleus NF-κB regulates expression of numerous genes involved in immune responses (103).

Nucleocytoplasmic transport

The M140 protein is localized predominantly in the nucleus while pM141 is localized diffusely throughout the cytoplasm and, to a lesser extent, the nucleus (82). However, co-expression alters the localization of either protein and they are found co-localized in a perinuclear region adjacent to aggresomes (82). Transport of most proteins from the cytoplasm to the nucleus is regulated and occurs through large nuclear pore complexes (Fig. 4A), up to 125 MDa in size, embedded in the dual membrane of the nuclear envelope (33, 146). These complexes are composed of 500-1000 total proteins called nucleoporins that are mostly soluble (32, 33). The nucleoporins form a symmetrical scaffold embedded in the nuclear envelope that surrounds a channel bounded by a cytoplasmic and nuclear ring. Each ring has filaments attached with the cytoplasmic side having loose ends and the nuclear filaments forming a distal ring called the nuclear basket. Ions and some proteins up to approximately 60 kDa in size can traverse the nuclear pore by passive diffusion (102, 137, 168, 190). However, larger proteins must be actively transported into the nucleus. In addition, transport of many small proteins is also regulated. Presently, the nature of the permeability barrier is still under debate, but the channel is lined with the nucleoporins that contain multiple repeats of phenylalanine (F) and glycine (G), the so-called FG-nups, necessary for directed transport of proteins (7-10, 147, 175, 183).

Nuclear import or export of proteins (Fig. 4B) is typically controlled by specific signals, nuclear localization signals (NLSs) or nuclear export signals (NESs), respectively, found in the primary sequence of the protein or formed from secondary or tertiary structural elements (183). Soluble transport receptors bind the signal-containing

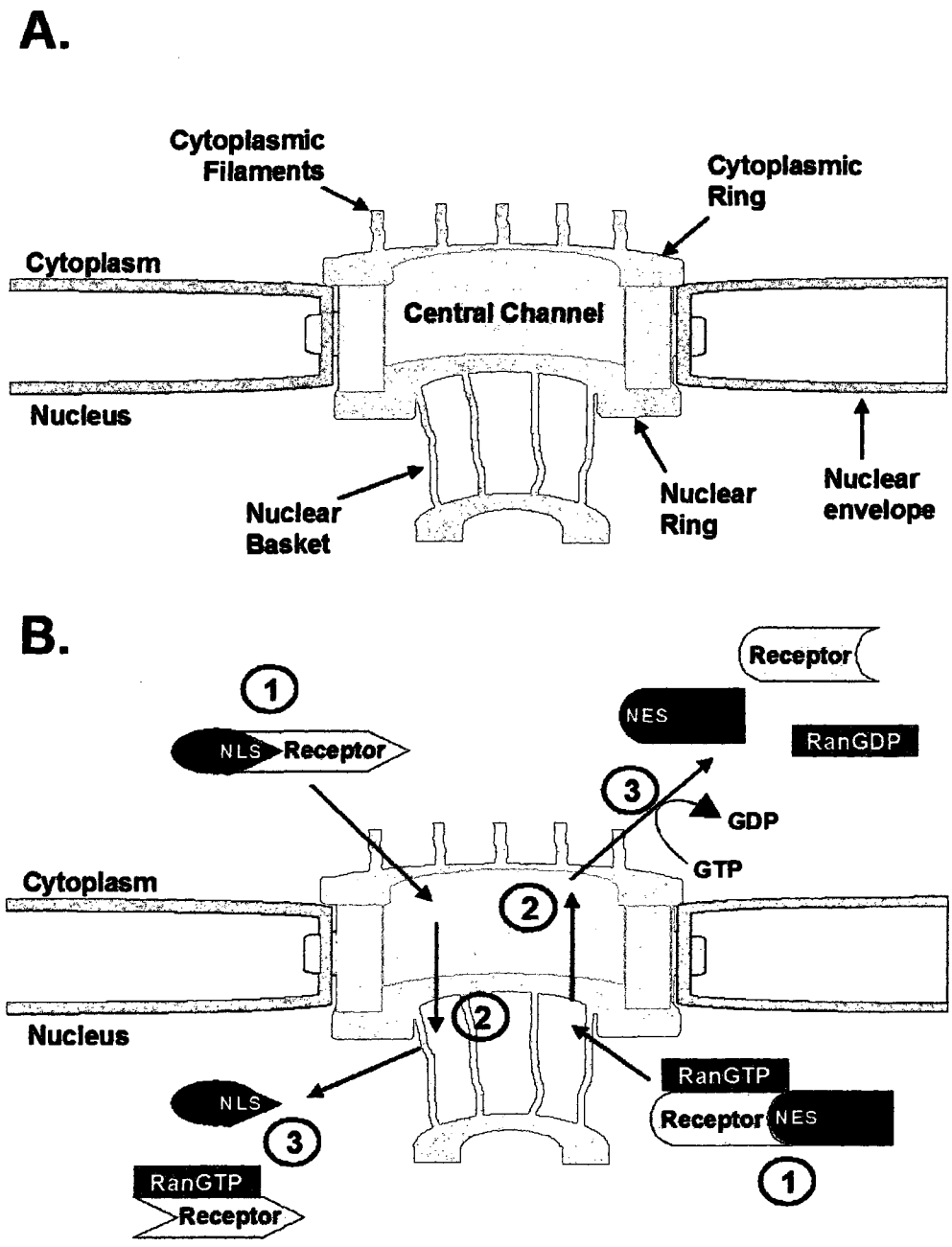

FIG. 4. Structure of the nuclear pore and nucleocytoplasmic shuttling. A. Representation of the nuclear pore with arrows pointing to the location of the cytoplasmic and nuclear rings, nuclear basket, cytoplasmic filaments, and nuclear membrane. B. Schematic representation of nuclear import (left) and nuclear export (right). The first step of nuclear import occurs when an import receptor binds to a NLS-containing target protein (1). The target protein/receptor complex enters the nucleus (2) by interacting with nucleoporins of the nuclear pore (not shown). In the nucleus, binding of RanGTP to the receptor causes release of the target protein (3) and the RanGTP/receptor complex is recycled back to the cytoplasm (not shown). The first step of nuclear export is complex formation of a RanGTP-bound export receptor with a NES-containing target protein (1). The complex crosses the nuclear pore (2) via interactions with the receptor and nucleoporins (not shown). Upon entering the cytoplasm, GTP is hydrolyzed causing the complex to dissociate (3) after which the receptor is recycled back to the nucleus (not shown).

cargo proteins and are thought to interact with the FG repeats of the FG-nups through multiple, low-affinity binding reactions during nuclear translocation (183). In other cases adaptor molecules bind to the signal sequences and are themselves bound by the transport receptors (199). Directionality of transport is controlled by the gradient of small guanine triphosphatase (GTPase), Ran, and its associated factors (75, 199, 200). Export receptors bind cargo in complex with RanGTP in the nucleus where the RanGTP levels are highest. Cargo is released in the cytoplasm upon hydrolysis of RanGTP after which the receptor and RanGDP are recycled back to the nucleus. On the other hand, import receptors bind cytoplasmic cargo in the absence of RanGTP and release cargo upon binding to RanGTP in the nucleus. The RanGTP/import receptor complex is recycled back to the cytoplasm where hydrolysis of RanGTP results in release of the import receptor for re-use.

The first NLS identified, PKKKRKV (single letter amino acid code), was that of the simian virus 40 (SV40) large T antigen (80). This and other so-called classical NLSs, or basic type NLSs, are monopartite or bipartite clusters of basic amino acids (200). Different classes of NLS have been identified with no known homology to the basic type NLS and are imported through distinct transport receptors, but import of basic NLS-containing proteins has been more extensively studied (172, 200). Nuclear import of these proteins requires a nuclear pore targeting complex composed of importin α and importin β (73, 141). The NLS is recognized and bound by the importin α adaptor protein (51). The importin β receptor transports the NLS-containing cargo protein/importin α complex into the nucleus (50, 72).

Presently, the most well characterized NESs are the leucine-rich NESs which are rich in hydrophobic amino acids and require leucine residues for function (200). The leucine-rich NESs are recognized and bound by the CRM1 receptor and are transported to the cytoplasm by CRM1 in complex with RanGTP (46, 47, 170).

Proteasome-mediated protein degradation

In the absence of pM140, steady-state levels of pM141 are reduced and pM141 is degraded at a faster rate (61). The most common mechanism of protein degradation is via the proteasome which is a 2.5 MDa multisubunit complex with three proteolytic activities including chymotrypsin-like, trypsin-like, and caspase-like activities (77, 92, 128). Proteasomes are fairly evenly distributed throughout the nucleus and cytoplasm, but are concentrated at distinct subcellular sites (135). For example, the microtubule organizing center is enriched in proteasomes and serves as a major site for the degradation of aggregated proteins (196).

The proteolytic core or 20S proteasome (Fig. 5A) is cylindrical in shape and consists of four stacked rings (77, 92). Each ring is composed of seven different, related subunits with the two identical outer rings containing α subunits (α1 - α7) and the two identical inner rings composed of β subunits (β1 - β7). The catalytic sites are contained in the inner subunits while the outer subunits interact with the 19S regulatory complex and a variety of other regulatory complexes. Each 19S regulatory complex is composed of at least 18 different subunits arranged as a base and lid (77). The lid contains a ring of ATPases and directly interacts with the 20S core particle. The 20S proteasome along with two 19S complexes composes the 26S proteasome (128).

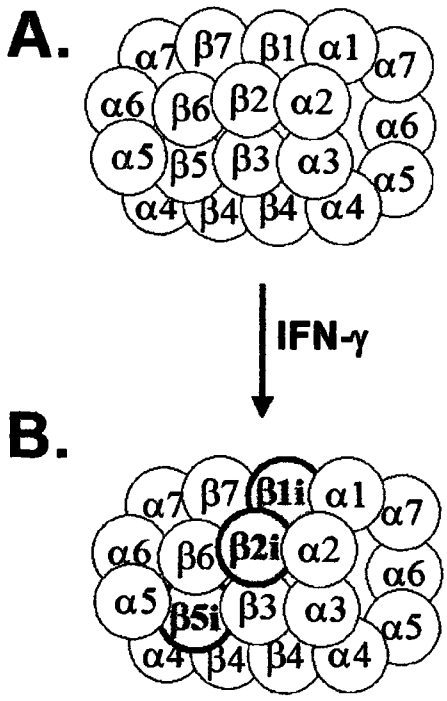

FIG. 5. Structure of the 20S constitutive proteasome (A) and immunoproteasome (B). The constitutive 20S proteasome (A) consists of four stacked rings containing 14 different subunits (represented as circles). The outer rings are composed of seven different α subunits (α1-α7) and the inner rings are composed of seven different β subunits (β1-β7) that contain the proteolytic machinery (not shown). Upon IFN-γ stimulation, biogenesis of the immunoproteasome (B) occurs with incorporation of β1i, β2i, and β5i in place of the β1, β2, and β5 subunits.

Both 26S and 20S proteasomes can be isolated from mammalian cells (77, 92, 128). Access to the catalytic sites of the 20S proteasome is gated by the α subunits thereby limiting access to the closed chamber (53, 54, 101, 194). Association of the 19S regulatory complex or one of two additional regulatory complexes, proteasome activator (PA) 28 and 200, results in opening of the chamber and thus, the regulatory complexes control translocation into the chamber (77, 93, 195). In addition, the regulatory subunit recognizes the targeted proteins and, through the action of the ATPases, is responsible for

their unfolding and transfer into the catalytic chamber (77, 93, 195). Thus, it was long believed that only the 26S proteasome was capable of proteolysis. However, the core 20S proteasome has been implicated in the degradation of numerous proteins (4, 128).

The 20S core contains six active sites with proteolytic activity categorized by similarities in substrate specificity rather than by catalytic mechanism (92). Cleavage by the two chymotrypsin-like or two trypsin-like sites occurs preferentially after hydrophobic or basic residues, respectively. The two remaining sites, once referred to as peptidyl glutamyl peptide hydrolase sites, cleave preferentially after acidic amino acids and are currently referred to as post-acidic or caspase-like sites. Degradation of proteins is processive generating peptides between three to twenty-two residues long (2, 91, 123).

In addition to the 20S proteasome described above formed from subunits that are constitutively expressed, a so-called immunoproteasome (Fig. 5B) can also be formed from IFN-γ-inducible subunits in response to viral infection (177). In the immunoproteasome each of the three catalytic subunits in both of the β rings is replaced by the IFN-γ-inducible catalytic subunits, β1i, β2i, and β5i, during biogenesis of new proteasomes (177). Furthermore, the rate of biogenesis of immunoproteasomes is enhanced compared to that of the constitutive proteasomes (177). In addition to the formation of immunoproteasomes, IFN-γ upregulates expression of the two subunits that form the PA28 regulatory complex (177). Ultimately, these IFN-γ-induced changes in the proteasome serve as an antiviral response, leading to altered substrate cleavage, enhanced generation of specific peptides, and increased variability in antigenic peptides that can be displayed for immune recognition of infected cells (14, 177). The cyotmegaloviruses have developed mechanisms to counteract this antiviral response.

Although MCMV induces immunoproteasome formation *in vivo*, this induction is blocked in IFN-γ-induced mouse embryonic fibroblasts in culture (88). HCMV also inhibits immunoproteasome formation in cultured cells exposed to IFN-γ, including fibroblasts and endothelial cells (88, 111). These effects are most likely due to the ability of CMV to interfere with IFN-γ signal transduction (110, 111, 207).

A wide variety of reversible and irreversible proteasome inhibitors have been identified and are currently being used as tools of cellular and molecular biology (92). Many of these are peptide-based compounds attached to a pharmacophore which occupies the catalytic site of the protease while the short peptide associates with the substrate binding pocket (92). Most of the natural and synthetic compounds inhibit the chymotrypsin-like activity of the proteasome because these compounds are more cell permeable than inhibitors of the other two proteolytic activities (92). For example, MG132 is an irreversible, peptide aldehyde inhibitor of the proteasome which can also inhibit cellular calpains and cathepsins at a 10-fold higher concentration to that required to inhibit the proteasome (92). Epoxomicin is an example of a peptide epoxyketone inhibitor that is irreversible, but is a more specific inhibitor with no known intracellular targets (92). Additional classes of peptide inhibitors exist including peptide boronates and peptide vinyl sulfones as well as the non-peptide inhibitors, lactacystin and β-lactone. Thus, various inhibitors are available to study the role of proteasomes in degradation of proteins of interest.

Routes to the proteasome

The majority of proteins currently studied are targeted to the proteasome by covalent attachment of polyubiquitin chains (92). Protein ubiquitination occurs by the action of two or three enzymes (Fig. 6) (77). First, the E1 ubiquitin activating enzyme activates ubiquitin by the formation of a high energy thioester bond. The activated ubiquitin is then transferred to a thiol group of an ubiquitin-conjugating enzyme (E2) which, in some cases, can directly transfer the ubiquitin moiety to protein targets. However, most protein targets receive ubiquitin from an E3 ubiquitin ligase enzyme which acts by either facilitating the transfer of ubiquitin from E2 or by direct transfer after binding to the ubiquitin molecule (77).

Ubiquitin, a small amino acid of 76 residues, is most commonly added to internal lysine residues of target proteins via an isopeptide bond between the ε-amino group of the protein substrate and the C-terminal carboxy group of ubiquitin, but cysteine, serine, and threonine linkages have also been observed (17, 77, 179, 191). Multiple additions of the ubiquitin moiety result in the formation of polyubiquitin chains with additions to lysine 48 of ubiquitin being the most common and most commonly associated with proteasomal degradation of the tagged protein (77). However, ubiquitin contains 7 internal lysine residues and polyubiquitination of other lysine residues as well as monoubiquitination of some proteasomal substrates have also been demonstrated to target proteins for proteasomal degradation (6, 15, 67, 90). Furthermore, the density of ubiquitin on protein substrates is proposed to be as important as the type of ubiquitin linkage or the formation of long polyubiquitin chains (77, 90). Nonetheless, for proteins degraded in this

pathway, addition of the required ubiquitin moieties targets proteins to the proteasomes where the lid of the regulatory complex is thought to recognize the ubiquitinated molecules and initiate processing into the proteasome (77). During processing the protein substrates are de-ubiquitinated by deubiquitinases and ubiquitin is recycled (77).

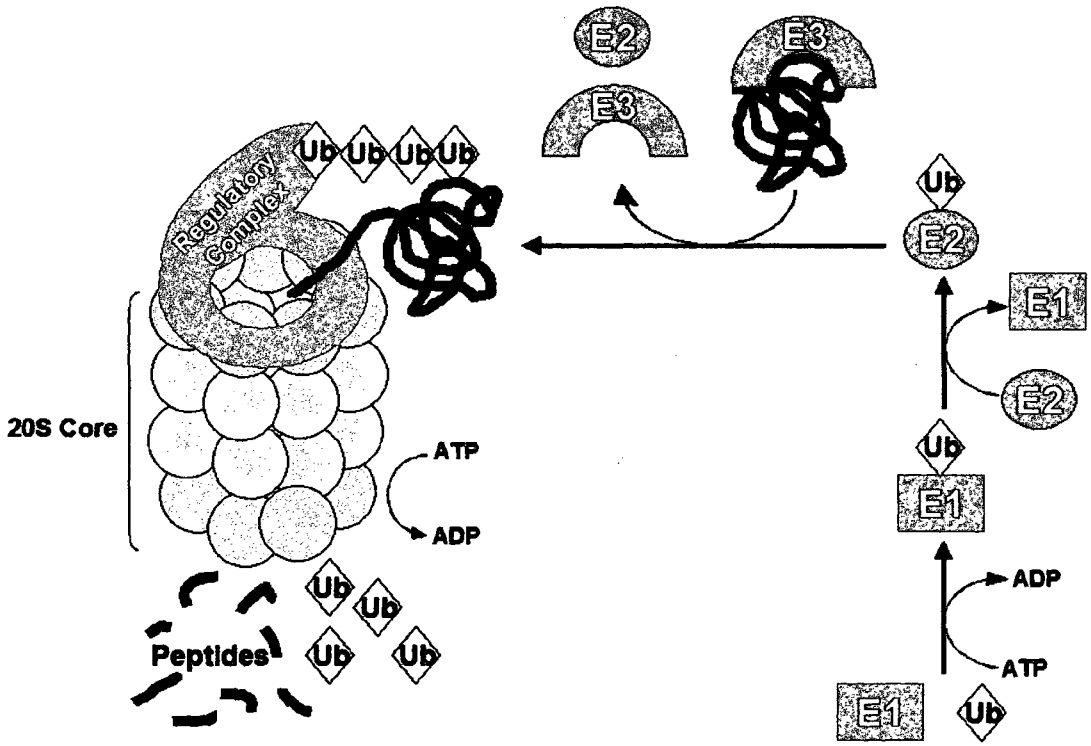

FIG. 6. The ubiquitin-proteasome system of protein degradation. Addition of ubiquitin (Ub) to a target protein occurs via the action of three enzymes. First a high energy bond is formed between the E1 activating enzyme (E1) and ubiquitin and requires hydrolysis of adenosine triphosphate (ATP) to adenosine diphosphate (ADP). In the second step, a bond is formed between the E2 ubiquitin-conjugating enzyme (E2) and ubiquitin and in some cases E2 can directly transfer the ubiquitin molecule to the target protein (not shown). In the final step an E3 ubiquitin ligase (E3) recognizes the target protein (represented by the black line) and facilitates transfer of the ubiquitin molecule. Multiple ubiquitin moieties can be added by the successive action of E1, E2, and E3 and the ubiquitin moieties are recognized by the regulatory complex that is associated with the 20S core proteasome. In reactions requiring ATP, the regulatory complex causes protein unfolding and transfer into the catalytic core (not shown) after which the target protein is degraded to smaller peptides and the ubiquitin molecules are hydrolyzed for recycling.

Proteasomal degradation of proteins can also occur independent of ubiquitin. Presently, the mechanisms for this type of degradation are incompletely understood and relatively few proteins have been identified that undergo ubiquitin-independent degradation. Asher, Reuven, and Shaul (4) proposed a model for ubiquitin-independent degradation involving the 20S proteasomes and degradation "by default". Given that unstructured regions are common in proteins degraded by the 20S proteasome in an ubiquitin-independent fashion, the model predicts that these proteins are inherently unstable and will be degraded in a passive process "by default" (4). In fact, some proteins with unstructured regions are degraded by the 20S proteasome by affecting structure of the cylinder and causing opening of the orifice without the need of regulatory complexes (77, 128).

Nevertheless, both the 20S and 26S proteasomes have been shown to be involved in ubiquitin-independent degradation (4, 77, 128). In fact, single proteins can exhibit complex degradation involving both forms of the proteasome. For example, ornithine decarboxylase (ODC), an enzyme in the polyamine synthesis pathway, is active as a homodimer, but the association between dimers is weak and monomers are subject to ubiquitin-independent degradation by the 20S proteasome (4, 77). However, when polyamine levels are high the antizyme-1 protein is induced, which complexes with the ODC, disrupts the homodimer, and directs ubiquitin-independent degradation of ODC monomers via the 26S proteasome (4, 77). Notably, despite the fact that ODC appears to be an inherently unstable protein due to 20S degradation, accelerated turnover occurs upon antizyme-mediated 26S degradation (4, 77).

Individual proteins can exhibit degradation by ubiquitin-dependent and -independent means. For example, ubiquitin-dependent degradation of the tumor suppressor protein, p53, has been extensively studied. The E3 ubiquitin ligase, Mdm2, binds to p53 and ubiquitinates the protein thereby targeting it for 26S proteasomal degradation (5). Several other ubiquitin ligases target p53 for degradation by ubiquitination (5). However, p53 is also subject to degradation via the 20S proteasome independent of interactions with ubiquitin ligases and may represent ubiquitin-independent degradation "by default" (4, 5).

In addition to the growing number of cellular proteins that are degraded by ubiquitin-independent pathways, numerous viral proteins also appear to be degraded in this fashion (89, 109, 178, 187, 202). For example, MCMV IE pp89 protein is degraded by the 20S proteasome independent of ubiquitination (187). In other cases viruses target key antiviral cellular proteins for degradation using ubiquitin-independent pathways (20, 70, 81, 134). For instance, the HCMV pp71 tegument protein can target several cellular proteins for ubiquitin-independent degradation (70, 81). Targets include Daxx which has the capacity to repress viral gene expression as well as members of the retinoblastoma family of tumor suppressors which regulate cell cycle (70, 81).

Various signals have emerged that target proteins for degradation. For example, the PEST domain is observed in the primary sequence of numerous short-lived proteins (144, 149). Although there is no consensus sequence the domains are enriched in proline, serine, glutamic acid, threonine, and, to a lesser extent, aspartic acid (144, 149). The domains are frequently flanked by positively charged amino acids, are uninterrupted by positively charged residues, are highly variable in length, and can be found anywhere in

the protein sequence (144). The domains serve as either constitutive or conditional degradation signals and numerous studies have demonstrated that removal of the motif results in increased protein stability while transfer to stable proteins confers instability (144). PEST motifs commonly target proteins for degradation by the ubiquitin-proteasome system (11, 144). However, the motifs also target proteins for degradation by proteasome-independent mechanisms and for ubiquitin-independent proteasomal degradation (11, 144). For example, IκBα exists in two forms; as a free molecule and in complex with NFκB (104, 157). Unbound IκBα is degraded by the proteasome in an ubiquitin-independent manner that requires the PEST domain located within the C terminus of the protein (104). Complexing masks the PEST domain and prevents intrinsic degradation (104).

CHAPTER II

SPECIFIC AIMS

The overall objective of this project was to characterize regulation of pM141 by pM140, at the molecular level. The M140 and M141 proteins structurally and functionally interact to optimize replication of MCMV in macrophages (61, 62, 105), a critical cell type for pathogenesis that supports productive and latent infection (64, 136). Structural interaction is evident by formation of a stable pM140/pM141 complex that localizes to a perinuclear region proximal to the microtubule organizing center (60, 82). Functional interactions are evident in that pM140 stabilizes pM141, increasing its half-life two-fold (61). Furthermore, co-expression of the proteins results in redistribution of pM140 from a diffuse nuclear pattern and pM141 from a diffuse localization in the cytoplasm and, to a lesser extent, the nucleus to the perinuclear locale (82). Thus, the importance of this project is in understanding to what extent the proteins cooperate to function in macrophage tropism and how the proteins are regulated. An understanding of how CMV proteins are regulated is fundamental to developing anti-viral therapies that are effective, specific, and non-toxic to the host.

The specific aims of the project were:

1) To map the interaction domains of pM140 and pM141. Mapping the interaction domains within pM140 and pM141 is a prerequisite to generating interaction-defective alleles within MCMV to assess the role of complex formation in the pathogenesis of the virus. Towards this goal, plasmid constructs were generated to express N- or C-terminal truncation mutants of pM140 or pM141. Each truncation mutant or full-length protein was radiolabeled in *in vitro* translation reactions. In some

cases the mutant proteins were co-expressed with the full-length binding partner and then immunoprecipitations were performed to assess which mutant retained an ability to form a complex. In other cases the mutant protein was mixed with the full-length binding partner expressed as a glutathione S transferase (GST) fusion protein after which GST pulldown assays were performed to assess complexing.

2) To map the localization domain(s) of pM141. It is possible that in addition to complexing, proper localization of pM140 and pM141 is important for the function of these US22 proteins. The M141 protein is found localized diffusely throughout the cytoplasm and, to a lesser extent, the nucleus when expressed individually (82). Interestingly, when pM140 and pM141 are co-expressed, pM141 is relocalized to a perinuclear region and exhibits a punctate staining pattern (82). Mapping the localization domain within pM141 was therefore undertaken as in Aim 1. Truncation mutants or full-length pM141 were expressed transiently in NIH3T3 fibroblast cells after which the cells were fluorescently stained to detect pM141 or distinct subcellular compartments. Localization of each mutant protein was examined by confocal microscopy and compared to the localization of the full-length protein.

3) To determine the method of pM141 degradation and assess the contribution of pM140 in protecting pM141 from degradation. It is possible that appropriate levels of pM141 are required for proper protein function of pM141, pM140, or both proteins. Thus, we sought to determine the mechanisms governing pM141 stability. To assess whether the proteasome is required for the degradation of pM141, RVΔ140- or WT-infected cells were treated with proteasome inhibitors and then steady-state levels of pM141 in the presence or absence of inhibitor were compared. To assess the contribution

of ubiquitination to pM141 degradation we immunoprecipitated pM141 in the presence or absence of proteasome inhibitor and looked for polyubiquitinated forms of the protein. Furthermore, we examined the steady-state levels of pM141 in cells containing a temperature-sensitive defect in the E1 ubiquitin-activating enzyme. To determine if pM140 can stabilize pM141 in a concentration-dependent manner we titrated increasing amounts of a M140-expression plasmid into RVΔ140-infected fibroblasts and compared the relative amount of pM141 levels. To assess whether complexing with pM140 is required for protecting pM141 from degradation we tested a panel of pM140 truncation mutants for their ability to complex with pM141 and then tested the ability of the mutants to stabilize pM141.

CHAPTER III

INTERACTION DOMAIN MAPPING OF pM140 AND pM141

Introduction

Protein/protein interactions are involved in every aspect of cellular biology. These interactions may be transient or stable depending on the proteins involved and their function (87). Proteins rarely act in isolation and may function in small or large complexes or may form complexes as a means of regulation (3, 115). The binding sites of proteins may be specific for a single protein or may contain amino acids that make conserved interactions with numerous other proteins (87). Interaction domains may be dependent on conformation of the protein or may a linear within the sequence of the protein and rely on shape, chemical complementarity, and flexibility of the proteins involved (87).

The M140 and M141 genes each express a single protein of 56 kDa and 52 kDa, respectively, and the transcripts and protein products are expressed with similar kinetics (59, 61). We have demonstrated that pM140 and pM141 are members of a stable complex also containing the products of an adjacent gene, pM139, and an unidentified protein of approximately 98 kDa (82). In addition to this larger complex, we have also demonstrated that a pM140/pM141 complex exists and can be isolated in the absence of pM139 (82). Given the importance of pM140 and pM141 in macrophage tropism, it is important to understand the extent to which the proteins function individually or in complex. We hypothesized that pM140 and pM141 complexing is required for function. To address this hypothesis we generated plasmid constructs with large deletions in each

of the genes that express N- and C-terminally deleted proteins. For each gene, each mutant construct was expressed *in vitro* and assayed for an ability to complex with the full-length binding partner. Mapping the interaction domains will allow us to generate mutant MCMV with interaction-defective alleles to assess the contribution of complexing in protein function.

Materials and Methods

Generation of plasmids. We generated plasmid constructs to express either full-length or N- or C-terminally truncated pM140 for the purpose of expressing the proteins in *in vitro* transcription/translation reactions. A full-length (FL) construct of the M140 gene that expresses the protein with an N-terminal polyhistidine (His) and Xpress-epitope tag, His140FL, was generated as previously described (82). The C-terminal truncation mutant, pHis140ApaSTOP, was generated via linker insertion mutagenesis. Briefly, the palindromic Bsu36ISTOP primer (Table 1) which contains a stop codon in all three frames was annealed to form double-stranded DNA. Specifically, 100 μg of primer was annealed in 1X annealing buffer (200 mM Tris, pH 7.5, 500 mM sodium chloride, 100 mM magnesium chloride) by incubating the mixture at 70°C for 10 minutes after which the primers were allowed to slowly equilibrate to room temperature. The linker DNA was then precipitated with 1/10 volume of sodium acetate and 2 volumes of ethanol. For the purpose of phosphorylating the linker DNA, approximately 10 μg of the precipitated DNA was reacted with 5 units of T4 Polynucleotide Kinase (New England Biolabs) according to manufacturer's instructions. The phosphorylated linkers were ligated to ApaI-digested His140FL after the ApaI site had been blunted by reacting the digested

DNA with 1 unit of T4 DNA polymerase (Invitrogen) in the presence of 0.1 mM dNTPs. The excess primer was removed and the DNA was religated to form the His140ApaSTOP construct which expresses an N- terminally His/Xpress-tagged M140 protein deleted of 62 C-terminal amino acids.

TABLE 1. List of primers utilized in generating M140 and M141 plasmid constructs. Contents include the primer name, the DNA sequence of the primer, and the restriction endonuclease enzyme site introduced in the DNA sequence after amplication (where applicable). Not applicable (N/A).

Primer Name	Primer Sequence (5' TO 3')	Site Introduced
ForwHis140forCTermMapping	TAGGGAGACCCAAGCTGGCTAGCG	N/A
140ForUpstreamM1	GCGTTCCGCGGATCCTACCGCCACCAGTCGAAC	BamHI
140ForUpstreamM2	GACCCCCGCGAGCGGATCCGAGGAACTGAAAGG	BamHI
140ForUpstreamM3	CATCCGCAACAACGACGGATCCGAGGATGCGGG	BamHI
140ForDownstreamM3	GGACGATCTCGACCGGGGATCCGATTACTGCC	BamHI
Bsu36ISTOP	CTAACTAATTACCTCAGGTAATTAGTTAG	Bsu36I
140RevUpstreamAcidic	CGTGTACATCGCGGCCGCCTATCTCTTCATGG	NotI
140RevDownstreamMotif4	TCGAAGCGGCCGCCTTACGCGATGGCCTTG	NotI
140RevUpstreamMotif4	CTTCAGGTTCGGCGGCCGCTAGATATCCAG	NotI
140RevDownstreamMotif3	AGTAATCGGGCGGCCGCTCGAGTTAGTCCTGGC	NotI
Rev140FLNotIforMapping	TTCTCTCTCTCTGTCTGCGGCCGCTGGCGC	NotI
ForFLAG141forCTermMapping	ACGCAAATGGGCGGTAGGCGTGTACGG	N/A
141ForUpstreamMotif1	CGCGATCGAGAAGCTTGACGGGAAGG	HindIII
141ForUpstreamMotif2	CGGATCGGGCAAGCTTTGCTGGTCC	HindIII
141ForDownstreamMotif3	CGGACCTGGTGAAGCTTAGGTACATCGC	HindIII
141ForUpstreamMotif4	CGACCCCGAGTTCAAGCTTTGCTGG	HindIII
141RevMostCTerm	ACACGTAGGGATCCTCGCCCTACCGACC	BamHI
141RevNextCTerm	TCGTCCAGGATCCAGGGTCAGCAGGAGTG	BamHI
141RevDownstreamMotif4	ATGCTCTCCGGATCCTCTTAGCGGCGCTC	BamHI
141RevUpstreamMotif4	TAGCCCAGGATCCCGATCTACGACCACG	BamHI
141RevUpstreamNLS	CATCTGGAAGGATCCGGCCTAGCTGTCGG	BamHI
141RevFL28fromTAG	AGGTGGAGATGAGGATCCCGCTGGTGG	BamHI
For141FLwSmaI	TTGGTGTGTGTGTGCCCGGGGGTGGCGAGATG	SmaI
Rev141FLwBamHI	ACTGGGGAGGGATCCCAGGGATGCCAC	BamHI

The remaining four M140 3' truncation mutants, 140USAcidic/TOPO, 140DSM4/TOPO, 140USM4/TOPO, and 140DSM3/TOPO, were generated by PCR amplification of distinct regions within the M140 gene using the primer pairs listed in Table 2 with His140FL (82) as template DNA. After amplication each PCR product was ligated into the TA cloning vector, pCR4-TOPO, (Invitrogen) as per manufacturer's directions and the resultant 140USAcidic/TOPO, 140DSM4/TOPO, 140USM4/TOPO, and 140DSM3/TOPO constructs are designed to express N-terminal His/Xpress epitope-tagged fusion proteins deleted of 105, 179, 259, 305 amino acids, respectively. The sequence of each truncated gene was verified. The orientation of each gene in the cloning vector was verified to assess which of the flanking promoters would drive *in vitro* expression (T3 for 140USAcidic/TOPO and 140USM4/TOPO; T7 for 140DSM4/TOPO and 140DSM3/TOPO).

M140 gene constructs truncated at the 5' end of the gene were generated similarly except that the pCR4-TOPO vector was used as an intermediate vector prior to subcloning. Distinct regions of the M140 gene from the His140FL (82) template were amplified by PCR (Table 2), the amplified products were ligated into pCR4-TOPO as instructed by the manufacturer, and the M140 gene sequence was verified to be correct. The truncated M140 gene products were digested out of the intermediate vector using the BamHI and NotI sites introduced by the primer sets (Table 1) and the fragments were resolved by electrophoresis on a 1% agarose gel. Each fragment was purified using the QIAquick Gel Extraction Kit (Qiagen) according to manufacturer's instructions and was ligated into BamHI/NotI-digested His140FL so that each mutant will be expressed as a fusion protein with an N-terminal His/Xpress epitope tag. The resulting

140ForUSM1/His, 140ForUSM2/His, 140ForUSM3/His, and 140ForDSM3/His constructs express M140 proteins deleted of 36, 76, 108, and 184 N-terminal amino acids, respectively.

TABLE 2. Primer pairs used to generate 3' truncations of M141 and 5' or 3' truncations of M140 in the pCR4-TOPO background. Contents include the primer set (see Table 1) used to generate the plasmids listed in the Table and the full-length and abbreviated names of the plasmids that appear throughout the text and Figures.

Plasmid Name	Abbreviation	Primer Set
140UpstreamAcidic/TOPO	140USAcidic/TOPO	ForwHis140forCTermMapping
		140RevUpstreamAcidic
140DownstreamMotif4/TOPO	140DSM4/TOPO	ForwHis140forCTermMapping
		140RevDownstreamMotif4
140UpstreamMotif4/TOPO	140USM4/TOPO	ForwHis140forCTermMapping
		140RevUpstreamMotif4
140DownstreamMotif3/TOPO	140DSM3/TOPO	ForwHis140forCTermMapping
		140RevDownstreamMotif3
140ForUpstreamMotif1/TOPO	140ForUSM2/TOPO	140ForUpstreamM1
		Rev140FLNotIforMapping
140ForUpstreamMotif2/TOPO/	140ForUSM1/TOPO	140ForUpstreamM2
		Rev140FLNotIforMapping
140ForUpstreamMotif3/TOPO	140ForUSM3/TOPO	140ForUpstreamM3
		Rev140FLNotIforMapping
140ForDownstreamMotif3/TOPO	140ForDSM3/ TOPO	140ForDownstreamM3
		Rev140FLNotIforMapping
141FL28fromTAG/TOPO	FLAG141FL-T7	ForFLAG141forCTermMapping
		141RevFL28fromTAG
141MostCTerm/TOPO	141MostCT/TOPO	ForFLAG141forCTermMapping
		141RevMostCTerm
141NextCTerm/TOPO	141NextCT/TOPO	ForFLAG141forCTermMapping
		141RevNextCTerm
141DownstreamMotif4/TOPO	141DSM4/TOPO	ForFLAG141forCTermMapping
		141RevDownstreamMotif4
141UpstreamNLS/TOPO	141USNLS/TOPO	ForFLAG141forCTermMapping
		141RevUpstreamNLS
141UpstreamMotif4/TOPO	141USM4/TOPO	ForFLAG141forCTermMapping
		141RevUpstreamMotif4

We also generated plasmid constructs of the M141 gene that express C-terminally truncated proteins under control of a promoter to drive expression in *in vitro* transcription/translation reactions. A construct that expresses full-length pM141 as a FLAG-epitope N-terminal fusion protein under control of a mammalian expression promoter, FLAG-M141, was generated as previously described (82). Five 3' truncation mutants were generated using PCR to amplify regions of the M141 gene using the F141 (82) construct as a template (see Table 2 for the list of primers used in PCR reactions). Each PCR product was ligated into pCR4-TOPO as per manufacturer's instructions and the sequence of the M141 gene was verified. Each gene was determined to be under control of the T7 promoter. Each of the constructs is designed to be expressed as an N-terminally-tagged FLAG epitope fusion protein. The FLAG141FL-T7 construct expresses full-length pM141 while the C-terminal truncation constructs, 141MostCTerm/TOPO, 141NextCTerm/TOPO, 141DSM4/TOPO, 141USNLS/TOPO, and 141USM4/TOPO, express pM141 deleted of 59, 115, 176, 202, 251 amino acids, respectively.

To generate a plasmid to express full-length pM140 as a GST fusion protein a BamHI to NotI fragment from His140FL (82) was inserted into BamHI/NotI-digested pGEX-6P-2 (GE Healthcare) after the fragment was electrophoresed on 1% agarose and purifed using the QIAquick Gel Extraction Kit (Qiagen) according to manufacturer's instructions. This construct, GST140FL, expresses pM140 as an N-terminally tagged GST fusion.

A plasmid was also constructed to express full-length pM141 as a glutathione S-transferase (GST) fusion protein. The entire M141 gene was amplified by PCR using

F141 (82) as a template with the For141FLwSmaI and For141FLwBamHI primers (Table 1). The PCR product was ligated into pCR4-TOPO (as per manufacturer's instructions) as an intermediate vector. The sequence was verified and a SmaI to BamHI fragment from the intermediate vector was inserted into SmaI/BamHI-digested pGEX-6P-2 after the fragment was electrophoresed on a 1% agarose gel and purifed, according to manufacturer's directions, using the QIAquick Gel Extraction Kit (Qiagen). This construct, GST141FL, expresses full-length pM141 as an N-terminally tagged GST fusion protein.

Two plasmids that express non-related proteins as GST fusions were used as negative controls for the GST pulldowns. A plasmid that expresses the human cytomegalovirus IE86 protein as an N-terminal GST fusion protein was a kind gift from Julie Kerry (Eastern Virginia Medical School, Norfolk, VA). A plasmid that expresses the interferon-inducible gene, IFI16, was a kind gift from Joseph Trapani (The Austin Research Institute, Victoria, Australia).

Restriction Enzyme Digestion. All restriction enzymes (New England Biolabs) were used according to manufacturer's directions. Typically, between 5-15 units of enzyme per μg of DNA was used in digestions which were reacted at the appropriate temperature for 3 to 5 hours.

Ligations. Wherever PCR products were ligated into the pCR4-TOPO vector using the TOPO TA Cloning Kit the ligations were performed as directed by the manufacturer. All other ligations were conducted using a minimum of a three fold molar ratio of insert to vector in the presence of 0.5 units of T4 DNA Ligase (Invitrogen) according to the manufacturer's instructions with an overnight incubation at 4°C. In the

case of linker insertation mutagenesis, approximately 1 μg of vector DNA was reacted with approximately 2.5 μg of phosphorylated linker in the presence of 5 units of T4 DNA Ligase and 1X Blunt End Buffer (0.066 M Tris-Cl, pH 7.6, 5 mM magnesium chloride, 5 mM dithiothreitol, 1 mM hexamminecobalt chloride, 0.2 mM ATP, 0.5 mM spermidine HCl) for 24 hours at 4°C.

Transformations. All transformations were performed with chemically-competent cells as described below. All transformations involving the pCR4-TOPO vector (Invitrogen) were performed in TOP10 cells using the TOPO TA Cloning Kit for Sequencing (Invitrogen) as per manufacturer's instructions. The 5' M140 truncation mutants and GST140FL were transformed into XL-1 blue cells with 1 to 2 μl of ligated DNA after a 30 minute incubation on ice. The transformation was performed with a heat shock at 42°C for 1.5 minutes. After an incubation on ice for 2 more minutes 800 μl of SOC Medium (153) was added to cells for a 1 hour recovery at 37°C with agitation. Competent cells were prepared as per Sambrook (153). GST141FL was transformed into NovaBlue cells (Novagen) according to manufacturer's instructions.

Polymerase chain reaction. PCR reactions were carried out with 20 pmol of forward and reverse primers and with 1 ng of template DNA using the Titanium Taq PCR Kit (Clontech) as per manufacturer's instructions except that 0.5 μl of DNA polymerase was used. Standard cycling conditions were as follows: 1 cycle of 95°C for 5 minutes; 30 to 35 cycles of 95°C for 30 seconds, 60°C for 30 seconds, 72°C for between 2 and 2.5 minutes; and 1 cycle of 72°C for 10 minutes on the MyCycler Thermal Gradient (Bio-Rad). In generating the 5' truncation mutants of M140 it was necessary to alter the standard conditions as follows: 1 cycle of 95°C for 1 minute; 35 cycles of 95°C for 30

seconds, 68°C for 2 minutes; and 1 cycle of 72°C for 10 minutes. In certain cases it was necessary to perform gradient PCR using the standard conditions above except that instead of 60°C for 30 seconds a gradient of 50-65°C was used.

Sequencing. Sequencing reactions were performed using the BigDye Terminator v3.1 Cycle Sequencing Kit (Applied Biosystems) according to manufacturer's instructions except that the ready reaction premix was diluted 1:16 before use. M140 or M141 gene inserts ligated into the pCR4-TOPO vector (see above) were sequenced using 1 pmol of M13 forward or reverse primers contained in the TOPO TA Cloning Kit (M13 primer sites flank the multiple cloning site of the vector) and, in some cases, the primers used to generate the PCR product ligated into the vector. In most cases the thermocycling conditions were as follows: 95°C for 30 seconds, 47° for 10 seconds, and 60°C for 4 minutes for 34 cycles on a MyCycler Thermal Cycler. In other cases the following conditions were used to generate longer extensions: 15 cycles of 95°C for 10 seconds, 47°C for 5 seconds, 60°C for 1 minute and 15 seconds; 5 cycles at 95°C for 10 seconds, 47°C for 5 seconds, 60°C for 1 minutes and 30 seconds; 5 cycles at 95°C for 10 seconds, 47°C for 5 seconds, 60°C for 2 minutes. Sequencing was performed on an ABI Prism 3130 Genetic Analyzer from Applied Biosystems.

Amplification of plasmids. When plasmids were required for the purpose of screening cloned DNA by restriction enzyme digestion the plasmids were amplified by growing a single colony of transformed bacteria (see above) overnight at 37°C with agitation in 3 ml of Luria-Bertani Medium (LB (153)) containing either 0.2 mg/ml ampicillin (Sigma) or 50 μg/ml kanamycin (Sigma) where appropriate. Approximately 1.5 ml of overnight culture was pelleted by centrifugation at 14,000X g for 1 minute after

which the resulting pellet was resuspended in 100 µl of Solution I (50 mM Tris, pH 8.0, 50 mM glucose, 10 mM EDTA). After a 5 minute incubation on ice 200 µl of Solution II (0.2 M sodium hydroxide, 1% Trition X-100) was added to the sample. Cell lysis was allowed to proceed on ice until the cloudy solution began to clear (approximately 2-3 minutes). The solutions were neutralized by addition of 150 µl of Solution III (3 M sodium acetate, pH 4.8). After a 5 minute incubation on ice the solutions were centrifuged for 5 minutes at 14,000X g. Supernatant was collected and incubated with 1 volume of isopropanol for 5-10 minutes at room temperature. Plasmids were harvested by centrifugation at 14,000X g for 5-10 minutes. The plasmid-containing pellet was washed with 500 µl of 70% ethanol and pelleted as before. The dried pellet was resuspended in 50 µl of sterile water and then 10 µl was used per restriction digest.

To generate large scale plasmid preparations the plasmids were first amplified in 5 ml of starter culture of LB with 0.2 mg/ml ampicillin or 50 µg/ml kanamycin (where appropriate) overnight at 37°C with agitation. The starter culture was used to inoculate 250 ml of LB containing the appropriate antibiotic which was incubated at 37°C with agitation for between 14-18 hours. Plasmids were purified using the Plasmid Maxi Kit (Qiagen) according to manufacturer's instructions. In some cases the Quantum Prep Plasmid Maxiprep Kit (Bio-Rad) was used to purify DNA.

***In vitro* transcription/translations.** Reactions were conducted using the TnT Coupled Reticulocyte Lysate System (Promega) with 30 µCi (Specific Activity >1000Ci/mM) of [^{35}S] methionine or [^{35}S] methionine/cysteine (GE Healthcare) according to manufacturer's directions in the presence of 40 units RNasin ribonuclease inhibitor (Promega). T3 or T7 RNA polymerase was used where indicated (see above).

To test expression of translated proteins, aliquots (2-5 µl) from each reaction were resolved on a 10-20% Gradient Tris-HCL Ready Gel (Bio-Rad) after boiling proteins for 5 minutes in the presence of SDS-PAGE loading dye (5% glycerol, 1% SDS, 80 mM Tris-HCl, pH 6.8, 0.1% bromophenol blue) and 2 µl of ß-mercaptoethanol to denature the proteins. After electrophoresis the gel was fixed with three 20 minutes washes in 50% methanol/10% acetic acid solution, dessicated, and exposed to autoradiography film overnight. Films were developed using a SRX-101A Processor (Konica Minolta).

Antibodies. Numerous antibodies were used to immunoprecipitate protein complexes. The generation of rabbit polyclonal antibodies raised against pM140 or pM141 has been previously described (61) and 5 µl of antibody or preimmune serum was utilized. We utilized 2 µg of anti-HisG antibody (Invitrogen) or mouse IgG2a (Biodesign International, Saco, ME) as a negative control. In other experiments we utilized 2 µg of anti-FLAG M2 monoclonal antibody (Sigma) or mouse IgG1κ (Sigma) as a negative control.

Immunoprecipitations. Aliquots (between 2.5-40 µl) of *in vitro* translated proteins were diluted to 250 µl total volume in 10S Buffer (50 mM HEPES, pH 7.2, 250 mM sodium chloride, 0.3% NP-40, 0.1% Triton-X-100, 0.005% SDS, 10 mM sodium phosphate, pH 7.0, 1 mM sodium fluoride, 0.1 mM phenylmethylsulfonyl fluoride (PMSF), 0.5 mM DTT) before being incubated with appropriate antibodies for 2 hours at 4°C with rocking. The protein/antibody complexes were then incubated with 30 µl Protein A/G Plus Agarose (Santa Cruz) overnight at 4°C with rotation. Immune complexes were washed three times in SNNTE Buffer (50 mM Tris, pH 7.4, 5 mM EDTA, 0.5 M sodium chloride, 5% sucrose, 1% NP-40) and three times in RIPA buffer

(50 mM Tris, pH 7.4, 0.15 M sodium chloride, 1% Triton-X-100, 0.1% SDS, 1% deoxycholic acid) with centrifugations of 500X g at 4°C for 5 minutes between each wash. Protein complexes were denatured with 5 minutes of boiling in the presence of SDS-PAGE loading dye and 2 µl ß-mercaptoethanol prior to SDS-PAGE on 12.5% acrylamide gels. Detection of radiolabeled proteins was accomplished in one of two ways. In some cases, the gel was fixed with three 20 minutes washes in 50% methanol/10% acetic acid solution, dessicated, and exposed to autoradiography film for 4-8 weeks after which films were developed using a SRX-101A Processor. In other cases, the dessicated gel was exposed to a phosphor screen for 1-3 weeks without fixation and then the phosphor screen was visualized on a Typhoon 9410 Variable Mode Imager (GE Healthcare). Protein analysis was performed using the ImageQuant TL Software.

His pulldown assay with immobilized cobalt chelate. The ProFound Pull-Down PolyHis Protein:Protein Interaction Kit from Pierce was utilized for these assays under two different experimental conditions. Under condition one the immobilized cobalt chelate was equilibrated as per manufacturer's instructions except that washes were performed with 250 µl buffer and subsequent centrifugations at 500X g at 1 minute each. Twenty microliters of each *in vitro* translated protein (see above) was mixed together for 2 hours at 4°C with rotation to allow complexing after the sample volume was brought to 250 µl total volume with BupH Tris buffered saline contained in the kit with 40 mM imidazole added. After this incubation 50 µl of equilibrated cobalt chelate was incubated with the samples overnight at 4° with rotation. Samples were pelleted by centrifugation at 500X g for 5 minutes at 4°C and pellets were subjected to three washes in SNNTE buffer containing 40 mM Imidazole followed by three washes in RIPA buffer

containing 40 mM Imidazole. After pelleting, the protein complexes were denatured with 5 minutes of boiling in the presence of SDS-PAGE loading dye and 2 µl ß-mercaptoethanol prior to SDS-PAGE on 12.5% acrylamide gels.

In other cases, experiments were conducted under the same conditions with the exception that 10S Buffer was used to equilibrate the cobalt chelate and was used to bring the mixed proteins up to volume to allow complexing. Furthermore, all post-pulldown washes were performed with the buffers described above except that imidazole was not added.

Detection of radiolabeled proteins was accomplished by exposing the dessicated gel to a phosphor screen for 1-3 weeks following visualization of the screen on a Typhoon 9410 Variable Mode Imager.

Preparation of GST and GST Fusion Proteins. One hundred nanongrams of plasmid expressing GST alone (pGEX-6P-2) or GST fusion proteins was transformed into chemically-competent BL21 cells via a heat shock of 42°C for 2.5 minutes after an incubation of 30-40 minutes on ice. Subsequent to heat shock the cells were incubated in 1 ml of LB (153) for 1 hr at 37°C with agitation. Single colonies, isolated after plating between 100 to 150 µl of the transformed cells on LB/agar plates containing 0.2 mg/ml ampicillin (Sigma), were used to inoculate a 5 ml starter culture of LB with 02.mg/ml ampicillin which was incubated overnight at 37°C with agitation. The following day the entire starter culture was used to inoculate 250 ml of LB with 0.2mg/ml ampicillin which was incubated at 37°C with agitation until the optical density at 550 nm reached 0.8-1.0. The cells were incubated as before for an additional 4 hrs in the presence or absence of 1mM isopropyl ß-D-1-thiogalactopyranoside (Fisher Scientific) after which the bacterial

cells were pelleted. Each pellet was resuspended in 25 ml of Buffer A (20 mM HEPES, pH 7.5, 0.1 M potassium chloride, 0.2 mM EDTA, pH 8.0, 20% glycerol, 1% Triton X-100, 1 mM DTT, 1 mM PMSF) and was then sonicated to lyse the cells. Sonications were performed with a Fisher Scientific Sonic Dismembrator Model 100 using a 1/8 inch tip with four 13 watt pulses for 30 seconds each. Cellular debris was separated by centrifugation at 19,837X g for 10 minutes at 4°C. The supernatant, containing proteins of interest, was reserved for use in GST pulldown assays.

Purification of GST-tagged Proteins and GST Pulldown Assays. GST fusion proteins were precipitated using Glutathione Sepharose (GE Healthcare) according to manufacturer's instructions. Specifically, 400 µl of glutathione sepharose was mixed with each aliquot of the prepared GST protein samples (see above) for 2 hours at 4°C with rotation. The GST protein/Glutathione Sepharose complexes were washed five times in NETN Buffer (0.5% NP-40, 20 mM Tris, pH 8.0, 100 mM sodium chloride, 1 mM EDTA) after pelleting for 5 minutes at 500X g. After the final wash the pellet was resuspended in 150 µl of NETN. A 20 µl aliquot of each precipitated protein was resolved on a 10-20% Gradient Tris-HCL Ready Gel (Bio-Rad) after pelleting and denaturing by boiling for 5 minutes in the presence of SDS-PAGE loading dye and 2 µl of ß-mercaptoethanol. The gel was fixed with two 15 minutes washes in 50% methanol/10% acetic acid solution. After overnight staining with SYPRO Ruby Protein Gel Stain (Invitrogen, 1:1 SYPRO Ruby/water) the gel was visualized on the Kodak Gel Logic 200 Imaging System and the amount of pGST140FL or pGST141FL was quantitated relative to that of each negative control proteins (GST, GSTIE86, GSTIFI16) using ImageQuant TL Software.

In order to precipitate *in vitro* translated proteins (see above) the purified GST fusion protein/glutathione sepharose complexes were mixed with 20 µl of lysate containing radiolabeled protein for 2 hours at 4°C with rotation. Before mixing, volumes containing relative quantities of purified pGST140FL or pGST141FL to that of negative control proteins (no more than 50 µl total volume) were first equilibrated with 500 µl Binding Buffer (25 mM HEPES, pH 7.5, 12.5 mM magnesium chloride, 20% glycerol, 0.1% NP-40, 150 mM potassium chloride, 0.15mg/ml bovine serum albumin, 1 mM DTT) by centrifugation of 500X g for 5 minutes at 4°C and then the pellet was resuspended in 200 µl fresh binding buffer. After mixing, the complexes were washed three times in either NETN, SNNTE, or RIPA buffer or were washed three times in SNNTE followed by three RIPA washes (as indicated in results) with centrifugations of 500X g at 4°C for 5 minutes between each wash. Protein complexes were denatured and resolved by SDS-PAGE on 12.5% acrylamide gels. Detection of radiolabeled proteins was accomplished by exposing the dessicated gel to a phosphor screen for 1-3 weeks following visualization of the screen on a Typhoon 9410 Variable Mode Imager. Protein analysis was performed using the ImageQuant TL Software.

Results

Interaction domain mapping of pM141. We had previously demonstrated that pM140 and pM141 form a stable complex (82) and we wanted to determine which region(s) of pM141 were required for binding. M141 is a member of the US22 family found in all beta-herpesviruses and is characterized by having up to four conserved motifs (21, 39, 59, 94, 119, 120, 143). The M141 protein contains all four motifs (Fig. 3

(59)). Although a function for the motifs has not been identified the conserved nature of the motifs implies that they impart an important property for the proteins. Thus, we targeted these motifs in our deletional analysis (Fig. 7). For this purpose we generated large scale deletions at the 5' and 3'ends of the gene. Full-length and each of the deletion mutants were expressed as epitope tag fusion proteins so that we could capture the proteins via the epitope tag without the concern of deleting the epitope(s) recognized by rabbit polyclonal antibodies (61).

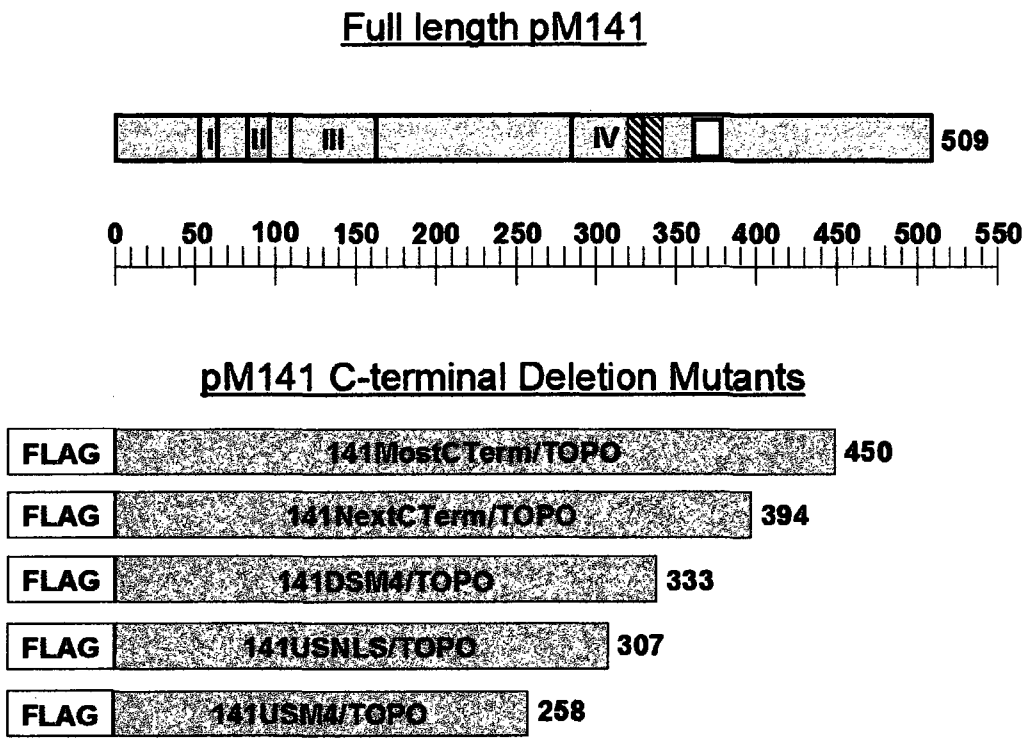

FIG. 7. Diagram showing the panel of pM141 C-terminal deletion mutants generated to map the interaction domain of the protein. Full-length pM141 is shown at the top along with the location of the US22 Motifs (open boxes), the NLS (hatched box) which shares some overlap with motif IV, and the PEST motif (white box). The ruler is shown for reference with each tick mark corresponding to 10 amino acids. Each pM141 deletion mutant is shown drawn to scale with the location of the FLAG epitope tag (not drawn to scale).

Specifically, we generated a construct that expresses full-length pM141 as an N-terminally tagged FLAG epitope fusion protein, FLAG141FL-T7. We have previously shown that a pM141/FLAG epitope fusion protein retained the ability to complex with pM140 when the proteins were transiently expressed in fibroblasts (82).

Constructs were also generated with deletions in M141 from the 3' end of the gene that express each deletion mutant protein as a fusion protein with an N terminal FLAG tag (Fig. 7). The p141MostCTerm/TOPO and p141NextCTerm/TOPO mutants retain all four US22 Motifs and are deleted of 59 and 115 amino acids, respectively. The p141DSM4/TOPO mutant is deleted of 176 amino acids downstream of the putative NLS. The mutant, p141USNLS/TOPO, is deleted of the putative NLS and 202 C-terminal amino acids. The p141USM4/TOPO mutant, deleted of the NLS and Motif IV, is missing 251 amino acids.

We first sought to determine if pFLAG141FL-T7 and the deletion mutants could be expressed *in vitro*. Each of the protein products was expressed from coupled transcription/translation reactions as [^{35}S] methionine labeled products. The full-length and C-terminally truncated products were efficiently expressed and predominantly two protein products were translated (Fig. 8). The native start codon of M141 is present in each of the plasmid constructs. Therefore, the higher molecular weight and predominant product most likely represents the FLAG epitope fusion protein generated from the start codon upstream of the FLAG tag while the lower molecular weight product most likely represents protein generated from the native M141 start codon that does not contain the epitope tag (Fig. 8).

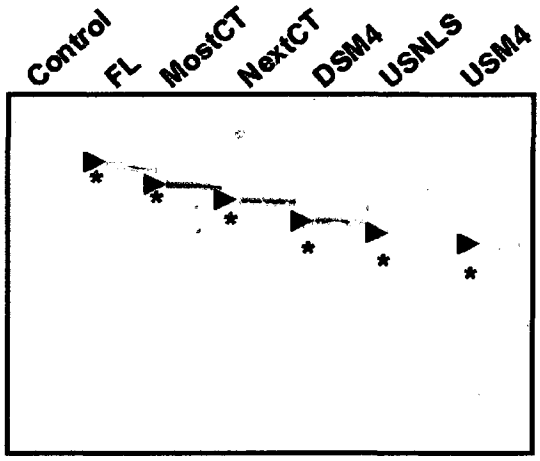

FIG. 8. Expression of *in vitro* translated full-length and C-terminally truncated pM141 mutants. Plasmids that express FLAG141FL-T7 (FL) M141, 141MostCT/TOPO (MostCT), 141NextCT/TOPO (NextCT), 141DSM4/TOPO (DSM4), 141USNLS/TOPO (USNLS), or 141USM4/TOPO (USM4) were expressed from coupled transcription/translation reactions using rabbit reticulocyte lysates in the presence of [^{35}S] methionine/cysteine. A negative control (Control) reaction was performed without addition of plasmids. A fraction from each of the reactions was loaded onto a SDS-PAGE gel, electrophoresed, and exposed to x-ray film for an overnight exposure. Asterisk (*) shows proteins expressed without the FLAG epitope tag while arrows (►) is indicates proteins expressed with the FLAG epitope fusion.

We next sought to determine if an *in vitro* translated, His epitope-tagged, full-length pM140 construct, pHis140FL, could be immunoprecipitated with pFLAG141FL-T7 or the C-terminally truncated pM141 mutants using an anti-FLAG antibody to capture the FLAG epitope fused to each of the pM141 constructs. We have previously demonstrated that the His epitope tag in His140FL does not interfere with complex formation (82). We tested a panel of the pM141 mutants including pFLAG141-T7, p141DSM4/TOPO, and p141USM4/TOPO where each of them was co-expressed with pHis140FL the co-translated proteins were subjected to immunoprecipitation with either the anti-FLAG antibody or IgG1 which is the isotype-matched control. Each construct was efficiently co-expressed with pHis140FL (Fig. 9, input). Two predominant products

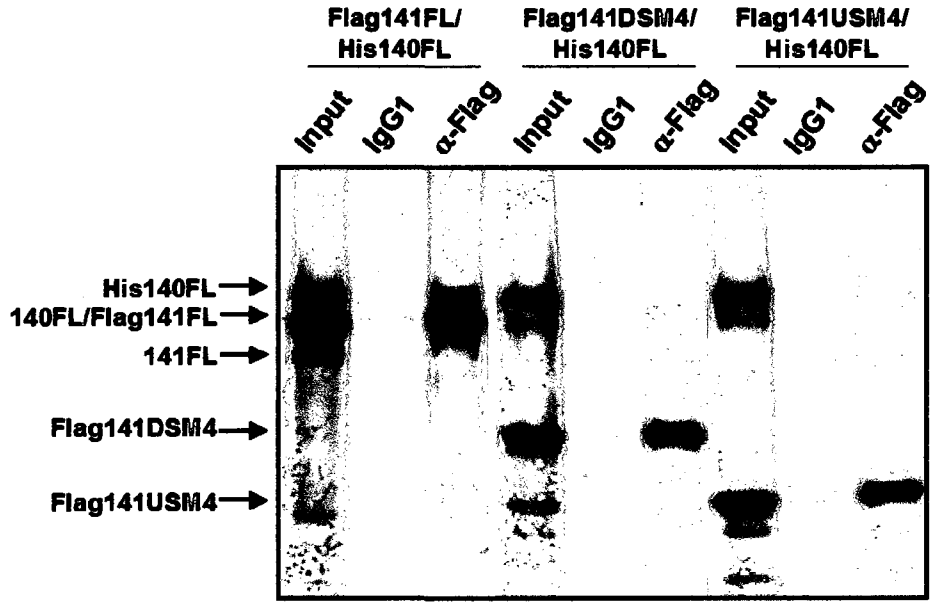

FIG. 9. Anti-FLAG antibody immunoprecipitations of co-translated pHis140FL and either pFLAG141FL-T7 (FLAG141FL), p141DSM4/TOPO (FLAG141DSM4), or p141USM4/TOPO (FLAG141USM4). The His140FL protein was co-expressed with each of the pM141 mutants shown above using coupled transcription/translation reactions with rabbit reticulocyte lysates in the presence of [^{35}S] methionine. The resulting proteins were loaded directly onto SDS-PAGE for analysis (input) or were first subjected to immunoprecipitations with either anti-FLAG antibody or isotype-matched control antibody (IgG1) as indicated. Arrows point to the location of each of the epitope-tagged proteins as indicated as well as pM140 expressed without the His tag fusion (140FL) and pM141 expressed without the FLAG tag fusion (141FL).

were consistently produced from pHis140FL. The higher molecular weight product represents His-tagged pM140 while the lower molecular weight product most likely represents pM140 without the His epitope fusion tag as expressed from the native start codon that is still present in the construct. Similarly, and as seen in Fig. 8, the predominant and higher molecular weight product of each of the pM141 constructs represents the FLAG epitope- tagged protein and a lower molecular weight product was also seen representing each construct minus the tag. We also observed some additional lower molecular weight products expressed from each construct and they most likely

represent breakdown products of pHis140FL, the pM141 mutants, or both. As expected, we were able to precipitate significant amounts of each of the FLAG-tagged pM141 mutants with the anti-FLAG antibody. However, IgG1 also precipitated a significant amount of each of the pM141 mutants and to a lesser extent, pHis140FL. Thus, we were unable to confirm complexing between even full-length pM141 and pM140 because the level of binding with the isotype-matched control is too high.

The results from Fig. 9 implied that there was a significant amount of binding of our proteins with the IgG1 control and that, as a consequence, the anti-FLAG antibody may be able to non-specifically precipitate native pM141 and pHis140FL. This led us to test the extent to which protein was brought down non-specifically with the anti-FLAG antibody. Thus, we performed immunoprecipitations of the native, non-tagged pM141 and of pHis140FL in the presence or absence of pM141. We found that the anti-FLAG antibody precipitated a comparable amount of pHis140FL regardless of whether pFLAG141FL-T7 was expressed (Fig. 10, left panel). We were also able to precipitate native pM141 with the anti-FLAG antibody despite the fact that the protein does not contain the FLAG epitope (Fig. 10, right panel). The combined results from Fig. 9 and Fig. 10 demonstrated that background binding of pM140 to the anti-FLAG antibody is too high to allow us to use anti-FLAG immunoprecipitations of the FLAG-tagged constructs for mapping interaction domains of pM141.

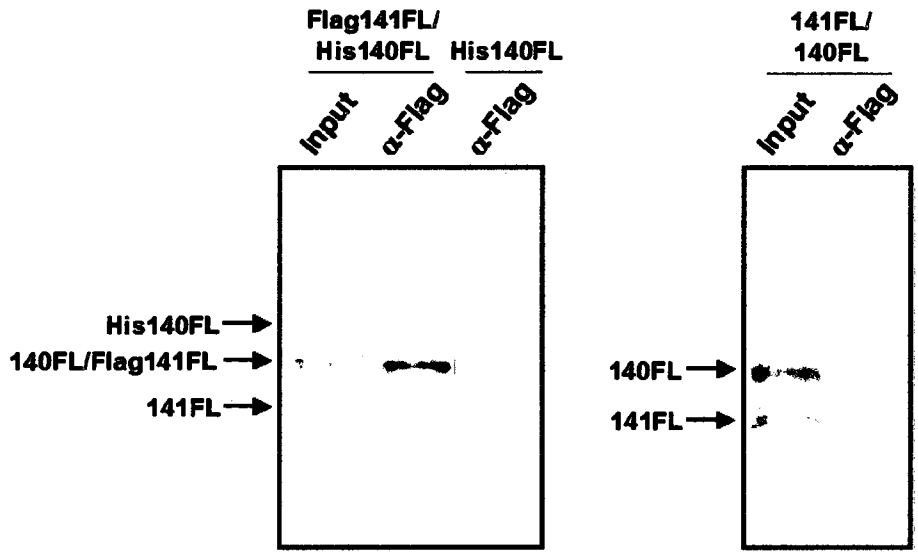

FIG. 10. Anti-FLAG immunoprecipitations of tagged and non-tagged pM140 in the presence or absence of pM141. In the left panel pHis140FL was expressed individually or with pFLAG141FL-T7 (FLAG141FL) while in the right panel native pM140 (140FL) was co-expressed with native pM141 (141FL) using coupled transcription/translation reactions with rabbit reticulocyte lysates in the presence of [^{35}S] methionine. The resulting proteins were loaded directly onto SDS-PAGE for analysis (input) or were first subjected to immunoprecipitations with anti-FLAG antibody.

Thus, we next sought to determine if the pM141 deletion mutants could be precipitated with the anti-His antibody when the proteins were co-expressed with pHis140FL. The mutant proteins, FLAG141FL-T7, 141DSM4/TOPO, 141USNLS/TOPO, and 141USM4/TOPO, were co-expressed with pHis140FL and the products were subjected to immunoprecipitations with anti-His antibody. As shown in Fig. 11, each of the constructs was efficiently expressed in the assay and the anti-His antibody was able to specifically precipitate the pHis140FL. Unfortunately, the control antibody, IgG2a, non-specifically bound to and precipitated significant amounts of pFLAG141FL-T7 as well as each of the pM141 deletion mutants. Furthermore, the quantity of each pM141 mutant protein that was brought down with anti-His was

comparable to that of the quantity precipitated with IgG2a so that the results cannot be accurately interpreted.

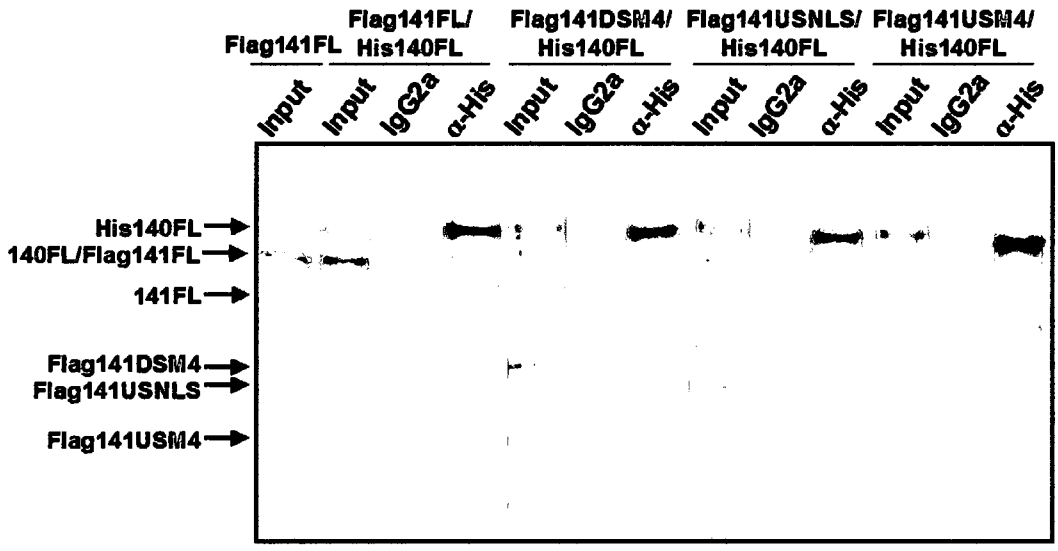

FIG. 11. Anti-His immunoprecipitations of pHis140FL co-expressed with pFLAG141FL-T7 (FLAG141FL), p141DSM4/TOPO (FLAG141DSM4), p141USNLS/TOPO (FLAG141USNLS), or p141USM4/TOPO (FLAG141USM4). The His140FL protein was co-expressed with each of the pM141 mutants shown above using coupled transcription/translation reactions with rabbit reticulocyte lysates in the presence of [^{35}S] methionine. The resulting proteins were loaded directly onto SDS-PAGE for analysis (input) or were first subjected to immunoprecipitations with either anti-His antibody or isotype-matched control antibody (IgG2a) as indicated. Arrows point to the location of each of the epitope-tagged proteins as indicated as well as pM140 expressed without the His tag fusion (140FL) and pM141 expressed without the FLAG tag fusion (141FL).

Given that the isotype-matched control to the anti-His antibody was able to non-specifically precipitate the FLAG-tagged pM141 constructs, we next assessed the extent to which pFLAG141FL-T7 could be brought down non-specifically with the anti-His antibody in the absence of pHis140FL. We also tested native pM141 in the assay in the

event that anti-His was binding non-specifically to the FLAG epitope of the pM141constructs rather than binding to a pM141 epitope. We found that even in the absence of pHis140FL anti-His antibody precipitated clearly detectable levels of pM141 expressed with or without the FLAG epitope tag (Fig. 12). The combined results of Fig. 11 and Fig. 12 demonstrated that background binding of the pM141 deletion mutants to the anti-His antibody was too high to use the antibody in immunoprecipitations assays with pHis140FL as a means of mapping the interaction domain of pM141.

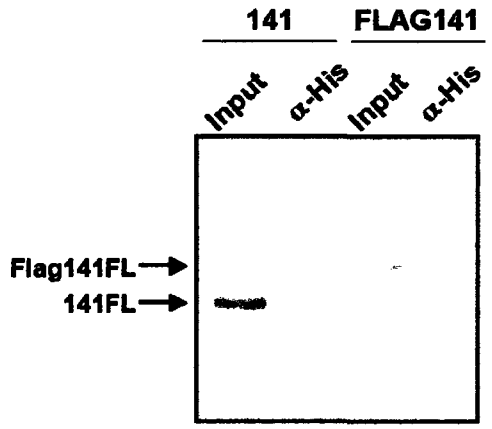

FIG. 12. Immunoprecipitations of native pM141 (141) or pFLAG141FL-T7 (FLAG141) with anti-His antibody. Native pM141 or pFLAG141 were expressed as indicated from coupled transcription/translation reactions with rabbit reticulocyte lysates in the presence of [^{35}S] methionine/cysteine. The resulting proteins were loaded directly onto SDS-PAGE (input) or were first subjected to immunoprecipitations with anti-His antibody.

Given the degree of non-specific binding of the antibodies in immunoprecipitations we next turned to pulldown assays with the ProFound Pull-down PolyHis Protein:Protein Interaction Kit from Pierce in an attempt to pulldown pM141 co-

expressed with pHis140FL. The Profound system relies on a cobalt chelated affinity gel to recognize His-tagged proteins rather than anti-His antibodies. We first performed the assay with native, full-length pM141 with the long-term goal of mapping the pM141 interaction domain(s) using our FLAG-tagged pM141 deletion mutants. As seen in Fig. 13 and as expected, pHis140FL was brought down in the assay regardless of the presence of pM141. Unfortunately, even in the absence of pHis140FL, pM141 was pulled down non-specifically in quantities at least as great as that of pM141 co-expressed with pHis140FL. This was true regardless of whether imidazole was added to the wash buffers to reduce non-specific binding. In fact, addition of imidazole actually enhanced binding of pM141 regardless of the presence of pHis140FL. This result demonstrated that background binding of pM141 to the cobalt chelate was too high to use in a His tag pulldown of pHis140FL for the purpose of mapping the pM141 interaction domain(s).

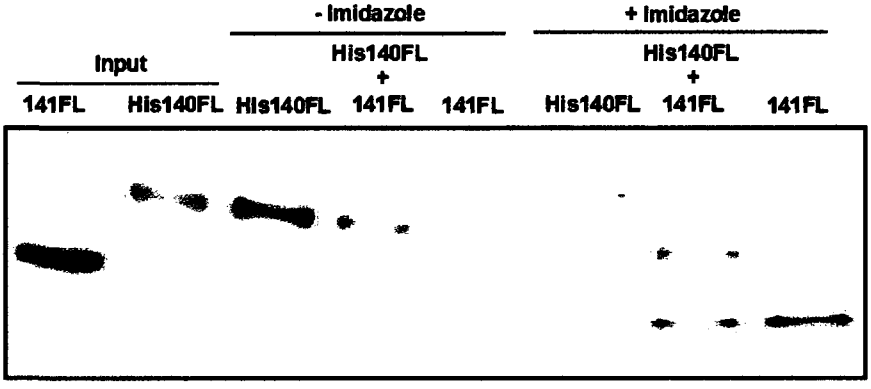

FIG. 13. Pierce ProFound pulldown assay of full-length, native pM141 (141FL) in the presence or absence of pHis140FL. The His140FL protein was co-expressed with p141FL or where indicated the proteins were expressed individually. Proteins were generated using coupled transcription/translation reactions with rabbit reticulocyte lysates in the presence of [^{35}S] methionine/cysteine. The labeled proteins were loaded directly onto SDS-PAGE for analysis (input) or were first subjected to the pulldown assay and were washed in buffers in the presence or absence of imidazole as indicated.

Thus, we next sought to determine if the pM141 interaction domain(s) could be mapped by utilizing GST pulldowns assays with GST-tagged pM140 construct (pGST140FL). These assays were performed by reacting *in vitro* translated pFLAG141FL-T7 with pGST140FL amplified in and harvested from *E. coli*. As seen in Fig. 14A, pFLAG140FL-T7 was brought down with pGST140FL. Unfortunately,

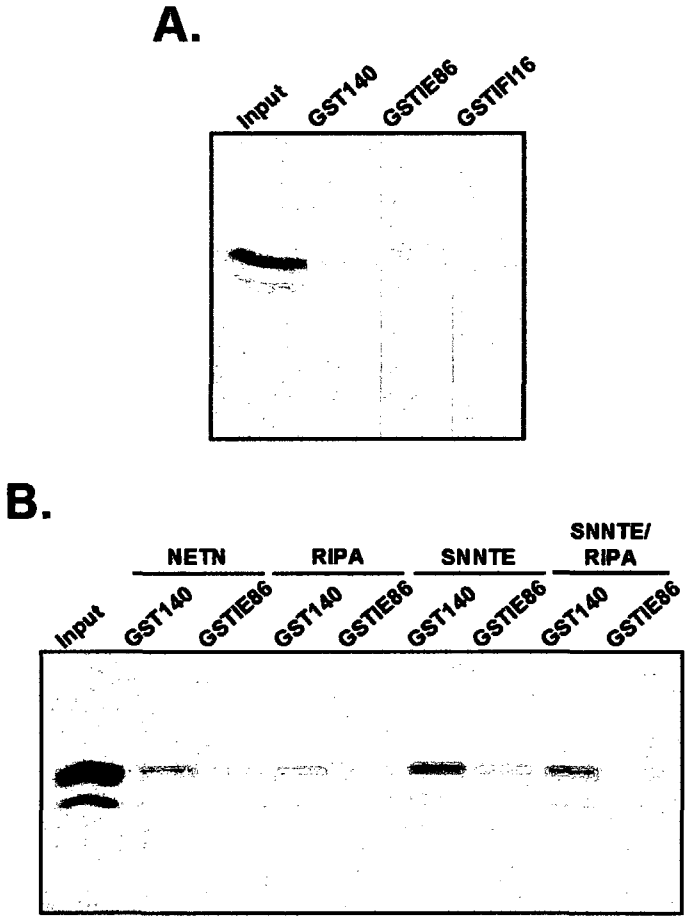

FIG. 14. GST pulldown assays of pGST140FL (GST140) and pFLAG141FL-T7. The GST140, GSTIE86, and GSTIFI16 proteins were amplified in *E. coli*, harvested, and subjected to pulldown with glutathione sepharose. The FLAG140FL-T7 protein was generated using coupled transcription/translation reactions with rabbit reticulocyte lysates in the presence of [^{35}S] methionine/cysteine. The labeled protein was loaded directly onto SDS-PAGE for analysis (input) or was first subjected to pulldown with purified GST fusion proteins as indicated. A. Pulldown assays were performed using NETN to wash the samples. B. Pulldown assays were performed as in A, but also using the indicated buffers (RIPA, SNNTE, or both) for washing.

equivalent amounts of the protein were also brought down with two negative control proteins expressed as GST fusions, GSTIE86 and GSTIFI16. We also tested different wash buffers in conjunction with our pulldown assays to see if we could reduce the amount of non-specific binding of pFLAG141FL-T7. We found that there was a large degree of non-specific pFLAG141FL-T7 binding regardless of whether washes were performed with NETN, RIPA, SNNTE, or SNNTE followed by RIPA (Fig. 14B). These results demonstrated that background binding of pFLAG141FL-T7 to our negative control proteins was too high to use GST pulldown assays with pGST140FL to map pM141 interaction domain(s).

Interaction domain mapping of the pM140 protein. Simultaneous to our experiments with pM141, we performed experiments to map the interaction domain of pM140. For this purpose we generated large scale 5' and 3' deletions in the M140. We also generated a mutant, His140ApaSTOP, which has a stop codon introduced at the 3' end of the gene. The full-length and deletion mutants were expressed as an N-terminally tagged, His epitope fusion proteins (Fig. 15). M140 is also a member of the US22 family (59) and contains all four motifs characteristic of the family (Fig. 3). As with pM141, we targeted these motifs in our deletional analysis (Fig. 15). In addition, pM140 contains a region rich in acidic amino acids (Fig. 3) and this acidic domain was also targeted. The 140ForUSM1/TOPO construct expresses a mutant protein that retains all four US22 motifs, but is missing the first 36 N-terminal amino acids. The 140ForUSM2/TOPO mutant is deleted of 76 N-terminal amino acids including US22 Motif I and the 140ForUSM3/TOPO is deleted of 108 N-terminal amino

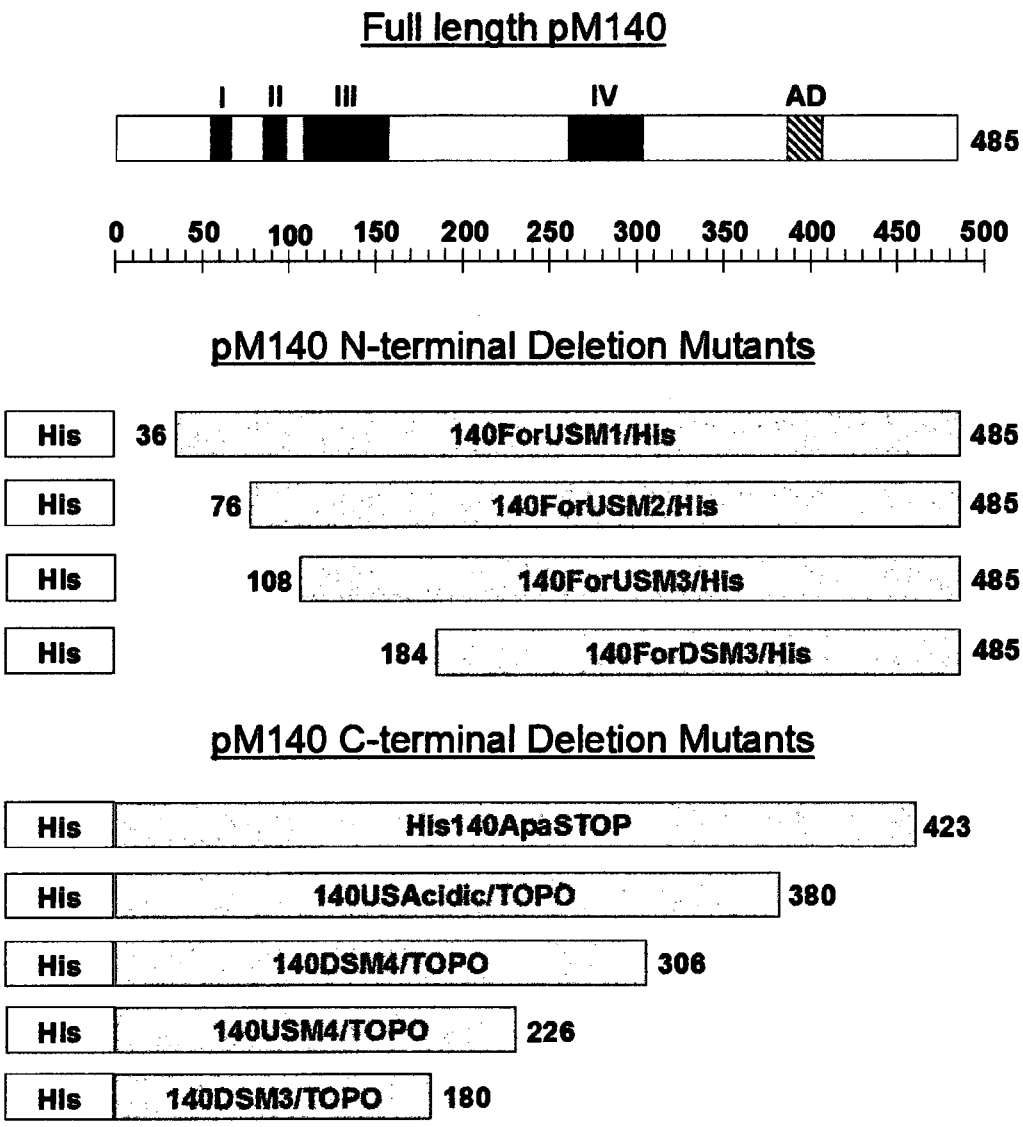

FIG. 15. Diagram of the panel of pM140 N- and C-terminal deletion mutants screened for an ability to interact with pM141. Full-length pM140 is shown at the top along with the location of the US22 motifs (filled blocks) and the acidic domain (AD). The ruler is shown for reference with each tick mark corresponding to 10 amino acids. Each pM140 deletion mutant is shown drawn to scale with the location of the His epitope tag (not drawn to scale).

acids including Motifs I and II. The 140ForDSM3 mutant is deleted of Motifs I, II, and III and 184 N-terminal amino acids. The His140ApaSTOP construct expresses a mutant protein deleted of 62 C-terminal amino acids adjacent to the acidic domain while the 140USAcidic/TOPO mutant is missing 105 amino acids including the acidic domain. The 140DSM4/TOPO construct is missing 179 C-terminal amino acids adjacent to Motif IV while this motif is deleted of 259 amino acids along with Motif IV. The 140DSM3/TOPO mutant is missing 305 C-terminal amino acids adjacent to Motif III.

We first asked if the pM140 mutants could be efficiently expressed *in vitro*. For this purpose each of the plasmid constructs was added to coupled *in vitro* transcription/translation reactions in the presence of [^{35}S] methionine/cysteine and the resultant proteins were analyzed by SDS-PAGE. The His140FL protein and each of the N-terminal deletion mutants were expressed efficiently (Fig. 16, left panel). Each of the C-terminal deletion mutants was expressed to levels that were clearly detectable (Fig. 16, right panel). In general, the C-terminal deletion mutants are deleted of more methionines and cysteines than the N-terminal deletion mutants and thus, are not labeled to an equivalent extent. This fact is reflected in the levels of C-terminal deletion mutants detectable relative to that of the N-terminal deletion mutants.

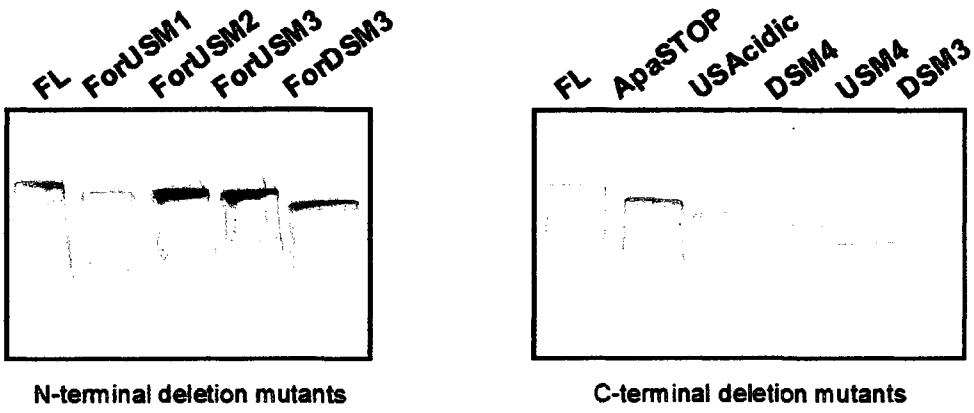

FIG. 16. Expression of *in vitro* translated full-length and either N-terminally truncated (left panel) or C-terminally truncated (right panel) pM140 mutants. Plasmids that express His140FL (FL), 140ForUSM1/TOPO (ForUSM1), 140ForUSM2/TOPO (ForUSM2), 140ForUSM3/TOPO (ForUSM3), 140ForDSM3/TOPO (ForDSM3), His140ApaSTOP (ApaSTOP), 140USAcidic/TOPO (USAcidic), 140DSM4/TOPO (DSM4), 140USM4/TOPO (USM4), and 140DSM3/TOPO (DSM3) were expressed from coupled transcription/translation reactions using rabbit reticulocyte lysates in the presence of [^{35}S] methionine/cysteine. A fraction from each of the reactions was loaded onto a SDS-PAGE gel, electrophoresed, and exposed to x-ray film for an overnight exposure.

Next, we performed GST pulldown assays to determine which of the pM140 deletion mutants retained an ability to complex with full-length, GST-tagged pM141, pGST141FL. We first examined the binding of full-length pM140 and found that pHis140FL was able to bind efficiently to pGST141FL (Fig. 17). Although we did observe background binding of pHis140FL to the negative control protein (GSTIE86), when the amount of GST141FL-bound His140FL was quantitated and compared to that of GSTIE86-bound pHis140FL we observed a small, but consistent increase. These results demonstrate that there is specific binding of pHis140FL to pGST141FL. When we tested the N-terminal mutants in our assay we found that each of the mutants was expressed efficiently and exhibited similar levels of binding to pGST141FL as to that of GSTIE86 (Fig. 17A). When background binding was subtracted and binding levels were

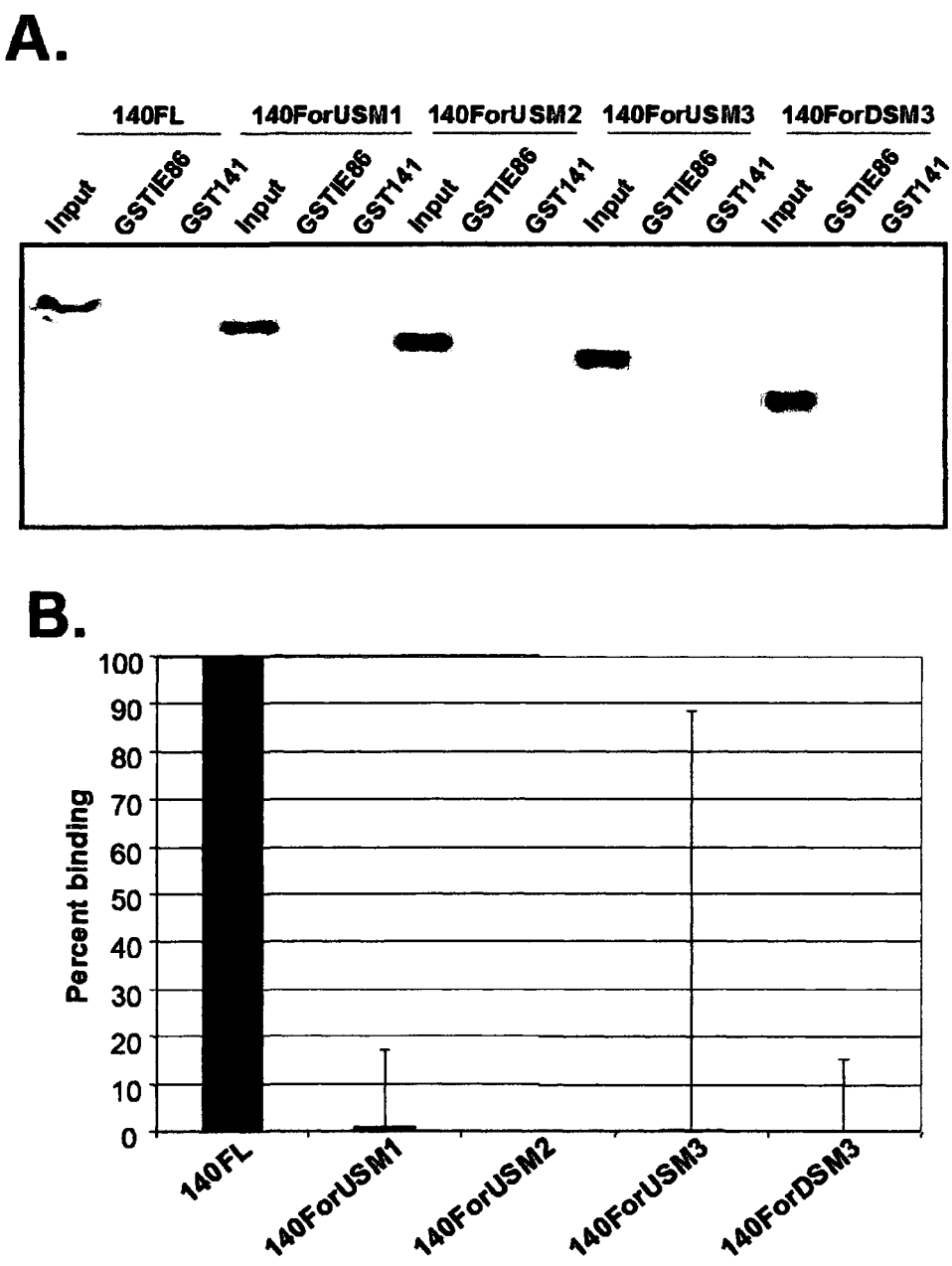

FIG. 17. GST pulldown assays of pGST141FL (GST141) and the pM140 N-terminal deletion mutants. The GST141 and GSTIE86 proteins were amplified in *E. coli*, harvested, and subjected to pulldown with glutathione sepharose. The His140FL and M140 deletion mutant proteins were generated using coupled transcription/translation reactions with rabbit reticulocyte lysates in the presence of [^{35}S] methionine/cysteine. The labeled proteins were loaded directly onto SDS-PAGE for analysis (input) or were first subjected to pulldown with purified GST fusion proteins as indicated. A. Radiographs of pHis140FL (140FL), p140ForUSM1/TOPO (140ForUSM1), p140ForUSM2/TOPO (140ForUSM2), p140ForUSM3/TOPO (140ForUSM3), and p140ForDSM3/TOPO (140ForDSM3). B. Quantitation of pulldown assays of the mutants are shown after background binding to GSTIE86 was subtracted. Quantitation is shown as percent binding where pHis140FL is set to 100%.

quantitated and compared to levels of pHis140FL binding, we found that binding was nearly or completely abolished with each of the N-terminal deletion mutants (Fig. 17B). These results demonstrate that the 36 most N-terminal amino acids of pM140 contain an interaction domain. When we tested the C-terminal mutants in our assay we found that pHis140ApaSTOP and p140USAcidic/TOPO had binding at least as comparable as pHis140FL, but that each mutant deleted of further C-terminal amino acids had significantly reduced binding to pGST141FL (Fig. 18A). In fact, upon quantitation, we found that pHis140ApaSTOP and p140USAcidic/TOPO exhibited increased binding relative to pHis140FL while p140DSM4/TOPO and p140DSM3/TOPO only bound to 18% or 5% of pHis140FL levels, respectively (Fig. 18B). The 140USM4/TOPO protein retained some binding ability relative to the flanking mutants at 67% binding of pHis140FL (Fig. 18B). These results demonstrate that the internal amino acids 180-306 of pM140 are required for optimal binding to pM141.

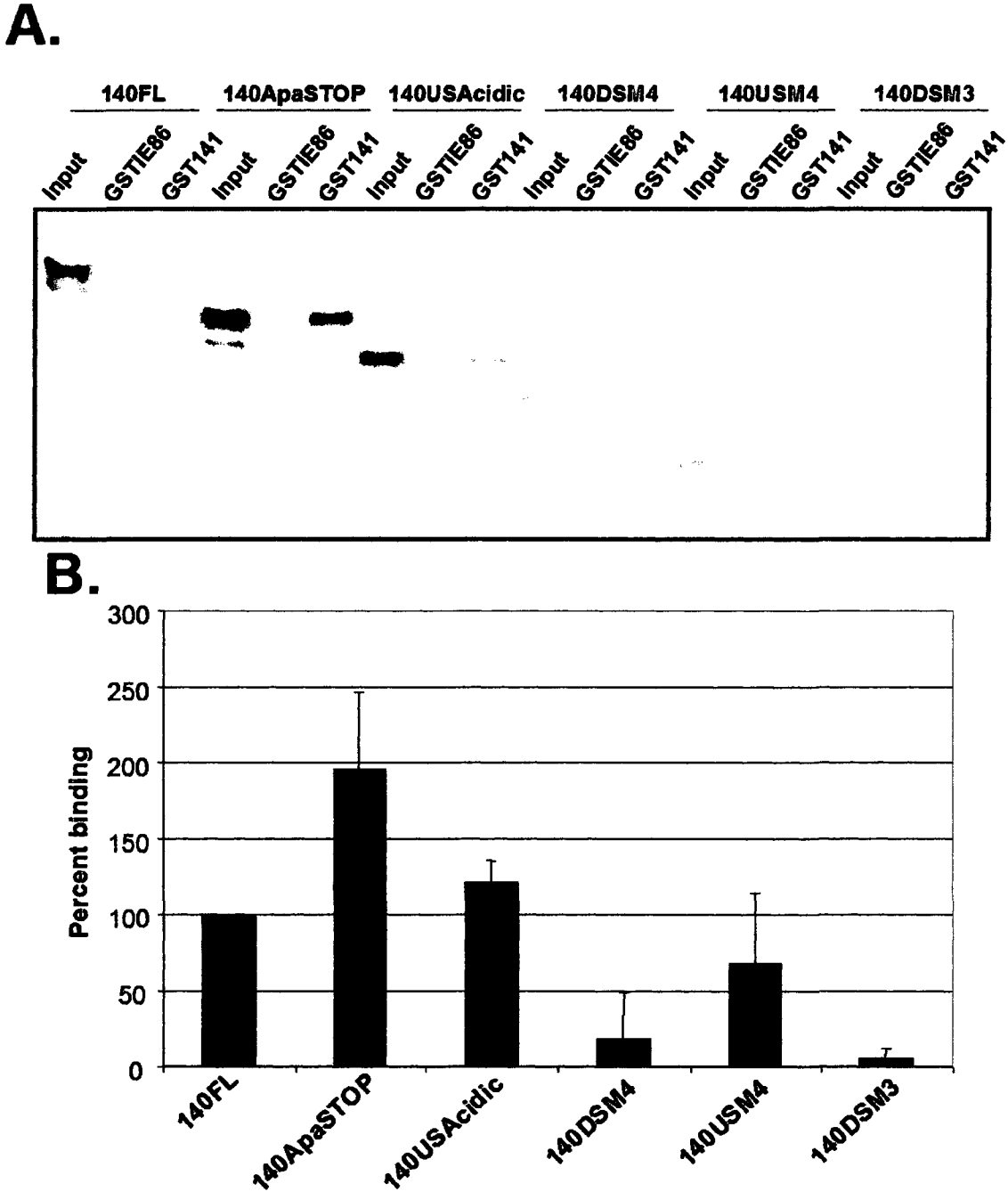

FIG. 18. GST pulldown assays of pGST141FL (GST141) and the pM140 C-terminal deletion mutants. The GST141 and GSTIE86 proteins were amplified in *E. coli*, harvested, and subjected to pulldown with glutathione sepharose. The His140FL and M140 deletion mutant proteins were generated using coupled transcription/translation reactions with rabbit reticulocyte lysates in the presence of [^{35}S] methionine/cysteine. The labeled proteins were loaded directly onto SDS-PAGE for analysis (input) or were first subjected to pulldown with purified GST fusion proteins as indicated. A. Radiographs of pHis140FL (140FL), pHis140ApaSTOP (140ApaSTOP), p140USAcidic/TOPO (140USAcidic), p140DSM4/TOPO (140DSM4), p140USM4/TOPO (140USM4), and p140DSM3/TOPO (140DSM3). B. Quantitation of pulldown assays of the mutants are shown after background binding to GSTIE86 was subtracted. Quantitation is shown as percent binding where pHis140FL is set to 100%.

Discussion

The M140 and M141 proteins are members of at least two complexes inside infected cells (82) suggesting that the proteins may function in complex. We sought to map the interaction domains of the proteins. This would provide us with the tools to generate MCMV with an interaction-defective allele so that we can determine the extent to which complexing affects the function of the proteins in macrophage tropism.

pM141 Interaction Domain Mapping. We were unable to map the domain of pM141 that confers binding to pM140. In each of the assays we tested and under each experimental condition we observed non-specific binding in quantities that made us unable to accurately interpret our results.

Immunoprecipitations were not a viable option to pull down our proteins of interest for interaction domain mapping. We observed non-specific binding between pM140 and the anti-FLAG antibody and between pM141 with the anti-His antibody. This was true regardless of whether the target proteins were fused to epitope tags.

We were not able to utilize a His pulldown assay in conjunction with an immobilized cobalt chelate to map the interaction domains. We found that more pM141 was pulled down in the absence of His-tagged pM140 than in the protein's presence. This was true even in the presence of elution compound added to reduce non-specific binding.

We were unable to map the interaction domains of pM141 using GST pulldown assays with GST-tagged pM140. We found that pM141 bound non-specifically to our negative control proteins, GST-tagged IE86 and GST-tagged IFI16, to levels comparable

to that seen with binding to GST-tagged pM140. IE86 is a non-related HCMV viral protein that is a transcriptional activator of the HCMV DNA polymerase gene, UL54, as well as other viral and cellular promoters (173). IFI16 is a cellular protein that inhibits cell cycle progression, regulates the DNA damage response, and represses transcription of UL54 (79, 129). Binding of pM141 or pM140 to IE86 or IFI16 is not predicted since microarray analysis of cells infected with a mutant virus deleted of M139, M140, and M141 did not reveal differences in viral gene expression compared to WT-infected cells (unpublished observation). Furthermore, we have shown that pM140 functions indirectly to stabilize viral capsids (60). Thus, binding of pM141 or pM140 to IE86 or IFI16 is most likely truly nonspecific.

Our combined results indicate that pM141 expressed *in vitro*, rather than achieving the proper conformation, is a globular protein that can bind non-specifically with at least moderate affinity to non-interacting protein partners including antibodies. Given this assumption, *in vitro*-expressed pM141 would bind non-specifically to additional antibodies and proteins. However, we have previously demonstrated that pM141 expressed from *in vitro* coupled transcription/translation reactions did not crossreact with our polyclonal antibodies, anti-M139 or anti-M140 (61). Thus, although we did not pursue these experiments, it may be possible to map the interaction domain(s) using immunoprecipitation assays with anti-M140 to pull down pM141 with native pM140.

We have previously immunoprecipitated the larger complex of His-tagged/pM139, pM140, and pM141 from fibroblasts transiently expressing the proteins using an anti-His antibody (82). Under these conditions, we did not observe non-specific

binding of the proteins to the anti-His antibody. In addition, we do not observe significant binding of transiently expressed FLAG-M141 to our anti-M140 antibody in the absence of pM140 (82). Thus, another feasible approach may be to map the interaction domain from pM141/pM140 constructs expressed transiently in cultured cells in conjunction with immunoprecipitations assays.

pM140 Interaction Domain Mapping. We identified two distinct regions of pM140 that are essential for optimal binding to pM141 *in vitro*. One of the regions is at the extreme N terminus of the protein and the second comprises 126 internal amino acids in the C-terminal half of the protein. Our results demonstrate that the pM140 interaction domain is non-contiguous and that pM140 can only complex with pM141 if the protein is in the proper conformation so that pM141 can make contact with both interaction domains.

An alternative explanation is that only one interaction domain exists in the protein at the extreme N terminus and that the 126 internal amino acids are required for proper pM140 folding. We found that if we removed the 36 most N-terminal amino acids of pM140 the protein could not bind to pM141. If any further N-terminal amino acids were removed the results were identical. However, our results with the C-terminal mutants were more variable. We observed binding with two deletion mutants missing fewer C-terminal amino acids (up to 105 amino acids removed). When further internal amino acids were removed, resulting in a total of 179 amino acids removed from the C terminus, binding was abolished. Interestingly, we recovered some binding with the adjacent mutant deleted of 259 amino acids, but binding was abolished again with a mutant

deleted of 305 amino acids. These results may indicate that the internal amino acids are required for proper protein folding. Under this assumption, deletion of 179 or 305 total amino acids results in a conformation that does not allow access of the N-terminal interaction domain to pM141. Deletion of 259 amino acids allows the truncation mutant to fold in a conformation that allows the N terminus to be exposed to pM141.

We performed our interaction domain mapping using screens of proteins generated from *in vitro* translations. These results should be confirmed in cells expressing the proteins from transient transfections and infections so that the proteins are translated and expressed under native conditions. Presently, we have not tested the N-terminal mutants for their ability to bind pM141 in cultured cells. However, these experiments have been performed with the relevant C-terminal mutants (see Chapter V) and the results support the hypothesis that the C terminus may confer conformation rather than binding to pM141.

CHAPTER IV

LOCALIZATION DOMAIN MAPPING OF pM141

Introduction

The majority of nucleocytoplasmic shuttling of proteins is regulated as a means for functional compartmentalization in the cell (199). The shuttling occurs through nuclear pore complexes embedded in the dual membrane of the nuclear envelope. Directed transport of proteins in and out of the nucleus is typically controlled by specific signals, NLSs and NESs, in the primary sequence of the protein (199). Soluble transport receptors bind directly to the signal sequences and then interact with the nuclear pore complexes to import or export the cargo proteins (199). In other cases adaptor molecules bind to the signal sequences and are themselves bound by the transport receptors (199). Directionality of transport is controlled by a small guanine triphosphatase (GTPase), Ran, and its associated factors (75, 199, 200). Export receptors bind cargo in complex with RanGTP in the nucleus where the RanGTP levels are highest. Their cargo is released in the cytoplasm upon hydrolysis of RanGTP to RanGDP. The receptor and RanGDP are recycled to the nucleus. On the other hand, import receptors bind cytoplasmic cargo in the absence of RanGTP and release cargo upon binding to RanGTP in the nucleus. The RanGTP/import receptor complex is recycled back to the cytoplasm where RanGTP is again hydrolyzed to RanGDP.

The classical NLSs, or basic type NLSs, are monopartite or bipartite clusters of basic amino acids (200). Nuclear import of proteins containing the basic type NLSs requires a nuclear pore targeting complex composed of importin α and importin β (73,

141). The NLS is recognized and bound by the importin α adaptor protein (51). The importin β receptor transports the NLS-containing cargo protein/importin α complex into the nucleus (50, 72). Other types of NLSs have been identified with no known homology to the basic type NLS (200). The most well characterized NESs are the leucine-rich NESs which are rich in hydrophobic amino acids and require leucine residues for function (200). The leucine-rich NESs are recognized and bound by the CRM1 receptor and are transported to the cytoplasm by CRM1 in complex with RanGTP (46, 47, 170).

In the absence of other viral proteins, pM141 is predominantly localized diffusely throughout the cytoplasm with significantly less nuclear staining and pM140 is localized almost entirely to the nucleus (82). Interestingly, when the proteins are co-expressed the localization of either protein is altered and they can be found co-localized in a perinuclear region with a punctate staining pattern (82). Thus, pM141 may retrieve pM140 from the nucleus. The complex localization pattern of the proteins suggests that the proteins may function in multiple subcellular locations and that proper regulation of localization may be required for function. As a prerequisite for understanding to what extent proper localization affects protein function we sought to map the localization domains of pM141. We hypothesized that pM141 can traverse the nuclear compartment and contains distinct signals for nuclear export and import since pM141 can be isolated from both compartments (61), may retrieve pM140 from the nucleus to the perinuclear locale, and since only pM141 is predicted to contain a NLS. Our approach to mapping the NES and NLS was to systematically cover the M141 gene with 5' or 3' deletions of increasing size. Then the localization of each mutated gene product, expressed transiently as an epitope tagged fusion, was assessed by immunofluorescence with confocal microscopy.

Mapping the localization domains would allow us to eventually generate mutant MCMV with altered trafficking of pM141, thus providing a means to assess this function in MCMV pathogenesis.

Materials and Methods

Generation of plasmids. We generated plasmid constructs designed to express either full-length or N- or C-terminally truncated pM141 proteins in transiently transfected cells. A construct that expresses full-length pM141 as a FLAG-epitope N-terminal fusion protein under control of a mammalian expression promoter, FLAG-M141, was generated as previously described (82). To generate N-terminal truncation mutants, distinct regions of the M141 gene were amplified by PCR using the primer pairs shown in Table 3 with FLAG-M141 (82) as template. The amplified products were ligated into pCR4-TOPO as an intermediate vector according to manufacturer's instructions and the M141 gene sequence was verified. The truncated M141 gene products were digested out of the intermediate vector using the HindIII and BamHI sites introduced by the primer sets (see Table 1 for the sites introduced) and the fragments were resolved by electrophoresis on a 1% agarose gel. Each fragment was purified using the QIAquick Gel Extraction Kit (Qiagen) according to manufacturer's instructions and was ligated into HindIII/BamHI-digested pEGFP-C3 (BD Biosciences) so that each mutant was expressed as a fusion protein with an N-terminal EGFP epitope tag. The resulting GFP141ForUSM1, GFP141ForUSM2, GFP141ForDSM3, and GFP141ForUSM4 constructs express pM141 deleted of 39, 62, 162, and 243 amino acids, respectively. A construct designed to express full-length pM141 with an N-

terminal EGFP tag, GFP141FL, was also generated. A SalI to SmaI fragment of FLAG-M141 (82) was resolved on a 1% agarose gel, purifed with the Qiaquick Gel Extraction Kit according to manufacturer's instructions, and then ligated into SalI/SmaI-digested pEGFP-C1 (BD Biosciences).

TABLE 3. Primer pairs used to generate 5' truncations of M141 in the pCR4-TOPO background. Contents include the primer set (see Table 1) used to generate the plasmids listed in the Table and the full-length and abbreviated names of the plasmids that appear throughout the text and Figures.

Plasmid Name	Abbreviation	Primer Set
GFP141ForUpstreamMotif1/TOPO	GFP141ForUSM1/TOPO	141ForUpstreamMotif1
		141RevFL28fromTAG
GFP141ForUpstreamMotif2/TOPO	GFP141ForUSM2/TOPO	141ForUpstreamMotif2
		141RevFL28fromTAG
GFP141ForDownstreamMotif3/TOPO	GFP141ForDSM3/TOPO	141ForDownstreamMotif3
		141RevFL28fromTAG
GFP141ForUpstreamMotif4/TOPO	GFP141ForUSM4/TOPO	141ForUpstreamMotif4
		141RevFL28fromTAG

Constructs to express pM141 C-terminal mutants in transiently transfected cells were generated by subcloning the C-terminal truncation mutants from the pCR4-TOPO background (see Chapter III) into p3XFLAG-CMV-7 (Sigma). HindIII to BamHI fragments from 141MostCTerm/TOPO, 141NextCTerm/TOPO, 141DSM4/TOPO, 141USNLS/TOPO, or 141USM4/TOPO were resolved on 1% agarose gels by electrophoresis and the DNA inserts were purified according to manufacturer's directions using the Qiaquick Gel Extraction Kit. Each purified fragment was subsequently ligated into HindIII/BamHI-digested p3XFLAG-CMV-7 generating constructs, 141MostCTerm/FLAG7, 141NextCTerm/FLAG7, 141DSM4/FLAG7,

141USNLS/FLAG7, and 141USM4/FLAG7, that express pM141 fused N-terminally with the FLAG epitope tag and deleted of 59, 115, 176, 202, and 251 N-terminal amino acids, respectively.

We also generated plasmid constructs of the M141 gene that express C-terminally truncated proteins fused at the N terminus with the EGFP tag. The 141MostCTerm/FLAG7, 141NextCTerm/FLAG7, 141DSM4/FLAG7, 141USNLS/FLAG7, and 141USM4/FLAG7 plasmids were digested HindIII to BamHI and each purifed fragment was ligated into pEGFP-C3. Each mutant, GFP141MostCTerm, GFP141NextCTerm, GFP141DSM4, GFP141USNLS, and GFP141USM4 expresses pM141 deleted of 59, 115, 176, 202, or 251 amino acids, respectively.

Restriction Enzyme Digestion. All restriction enzymes (New England Biolabs) were used according to manufacturer's directions. Typically, between 5-15 units of enzyme per ug of DNA was used in digestions which were reacted at the appropriate temperature for 3 to 5 hours.

Ligations. Except where PCR products were ligated into the pCR4-TOPO vector using the TOPO TA Cloning Kit as per directed by the manufacturer, ligations were conducted using a minimum of a three fold molar ratio of insert to vector in the presence of 0.5 units of T4 DNA ligase (Invitrogen) according to the manufacturer's instructions with an overnight incubation at 4°C.

Transformations. All transformations were performed with chemically-competent cells as described. All transformations involving the pCR4-TOPO vector were performed in TOP10 cells using the TOPO TA Cloning Kit for sequencing as per

manufacturer's instructions. All of the 5' M141 truncation mutants and the FLAG epitope fused C-terminal M141 mutants were transformed into XL-1 blue cells with 1 to 2 µl of DNA after a 30 minute incubation on ice. The transformation was performed with a heat shock at 42°C for 1.5 minutes. After an incubation on ice for 2 more minutes 800µl of SOC Medium (153) was added to cells for a 1 hour recovery at 37°C with agitation. Competent cells were prepared as per Sambrook (153). GFP141FL was transformed into NovaBlue cells (Novagen) according to manufacturer's instructions.

All of the EGFP fused 3' M141 truncation mutants were transformed into TOP10 cells with at least 1.5 µl of ligated DNA after a 30 minute incubation on ice. The transformation was performed with a heat shock at 42°C for 1 minute. After a 3 minute incubation on ice 1 ml of LB was added to cells for a 1 hour recovery at 37°C with agitation. Competent cells were prepared as per Sambrook (153).

Polymerase chain reaction. PCR reactions were carried out with 20 pmol of forward and reverse primers and with 1 ng of template DNA using the Titanium Taq PCR Kit (Clontech) as per manufacturer's instructions except that 0.5 µl of DNA polymerase was used. Standard cycling conditions were as follows: 1 cycle of 95°C for 5 minutes; 35 cycles of 95°C for 30 seconds, 65°C for 30 seconds, 72°C for 2.5 minutes; and 1 cycle of 72°C for 10 minutes on the MyCycler Thermal Gradient.

Amplification of plasmids. When plasmids were required for the purpose of screening cloned DNA by restriction enzyme digestion the plasmids were amplified by growing a single colony of transformed bacteria (see above) overnight at 37°C with agitation in 3 ml of LB containing either 0.2 mg/ml ampicillin or 50 µg/ml kanamycin where appropriate. Approximately 1.5 ml of overnight culture was pelleted by

centrifugation at 14,000X g for 1 minute after which the resulting pellet was resuspended in 100 µl of Solution I (50 mM Tris, pH 8.0, 50 mM glucose, 10 mM EDTA). After a 5 minute incubation on ice 200 µl of Solution II (0.2 M sodium hydroxide, 1% Trition X-100) was added to the sample. Cell lysis was allowed to proceed on ice until the cloudy solution began to clear (approximately 2-3 minutes). The solutions were neutralized by addition of 150 µl of Solution III (3 M sodium acetate, pH 4.8). After a 5 minute incubation on ice the solutions were centrifuged for 5 minutes at 14,000X g. Supernatant was collected and incubated with 1 volume of isopropanol for 5-10 minutes at room temperature. Plasmids were harvested by centrifugation at 14,000X g for 5-10 minutes. The plasmid-containing pellet was washed with 500 ml of 70% ethanol and pelleted as before. The dried pellet was resuspended in 50 µl of sterile water and then 10 µl was used per restriction digest.

To generate large scale plasmid preparations the plasmids were first amplified in 5 ml of starter culture of LB with 0.2 mg/ml ampicillin or 50 µg/ml kanamycin (where appropriate) overnight at 37°C with agitation. The starter culture was used to inoculate 250 ml of LB containing the appropriate antibiotic which was incubated at 37°C with agitation for between 14-18 hours. Plasmids were purified using the Plasmid Maxi Kit (Qiagen) according to manufacturer's instructions. In some cases the Quantum Prep Plasmid Maxiprep Kit (Bio-Rad) was used to purify DNA.

Sequencing. Sequencing reactions were performed using the BigDye Terminator v3.1 Cycle Sequencing Kit according to manufacturer's instructions except that the ready reaction premix was diluted 1:16 before use. Reactions were conducted using 1 pmol of M13 Forward or Reverse primers contained in the TOPO TA Cloning Kit (M13 primer

sites flank the multiple cloning site of the vector) and, in some cases, the 141RevDownstreamMotif4, 141RevMostCTerm, and 141Rev28fromTAG primers (Table 1). In some cases the thermocycling conditions were as follows: 95°C for 30 seconds, 47° for 10 seconds, and 60°C for 4 minutes for 34 cycles on a MyCycler Thermal Cycler. In other cases the following conditions were used to obtain longer sequence reads: 15 cycles of 95°C for 10 seconds, 47°C for 5 seconds, 60°C for 1 minute and 15 seconds; 5 cycles at 95°C for 10 seconds, 47°C for 5 seconds, 60°C for 1 minutes and 30 seconds; 5 cycles at 95°C for 10 seconds, 47°C for 5 seconds, 60°C for 2 minutes. Sequencing was performed on an ABI Prism 3130 Genetic Analyzer from Applied Biosystems.

Cells. NIH3T3 cells (CRL-1658; American Type Culture Collection), a mouse fibroblast line, were propagated in Dulbecco's Modified Eagle's Media (Mediatech) supplemented with 1% L-glutamine (Mediatech) and 10% heat-inactivated bovine calf serum (HyClone, Logan, UT). NIH3T3 cells were maintained in a humidified incubator at 37°C with 5% carbon dioxide.

Transient Transfections. NIH3T3 cells were transfected using either TransFectin (Bio-Rad) or Metafectene (Biontex, Germany). When transfections were performed using Transfectin, cells were seeded into 25 cm^2 culture flasks 24 hours prior at a density of 6×10^5 cells in 4 mls of propagation media. Cells were transfected with a total of 18 µl of Transfectin and a total of 9 µg of plasmid DNA. Plasmid DNA and Transfectin were added to 500 µl aliquots of Dulbecco's Modified Eagle's Media, mixed together, vortexed for 5 seconds, incubated at room temperature for 20 minutes, and added directly to the cells. Twenty four hours post-transfection approximately 1×10^5 cells/4.2cm^2 well were propagated into Two-Well Lab-Tek Chamber Slides (Nalge Nunc

International, Rochester, NY) which were processed 48 hours later.

When using Metafectene, cells were seeded 18 hrs prior to transfection in 25 cm^2 culture flasks at a density of 3 x 10^5 cells. Six micrograms of plasmid DNA and 9 µl of Metafectene were added to 100 µl aliquots of Dulbecco's Modified Eagle's Media, mixed together, vortexed for 5 seconds, and incubated at room temperature for 20 minutes. Media used to seed the cells was removed, two milliliters of propagation media was added to the transfection mixes, and this was added to the cells. Twenty four hours post-transfection approximately 1 x 10^5 cells/4.2cm^2 well were propagated into Two-Well Lab-Tek Chamber Slides which were processed 48 hours later.

Confocal microscopy. Cells propagated in chambered slides were washed three times in 1 ml of cold phosphate-buffered saline. Cells were fixed and permeablized by adding 1 ml of cold 100% methanol for a 10 minute incubation at -20°C after which the cells were washed three more times in phosphate-buffered saline. Cells were blocked in phosphate-buffered saline with 5% Sterile Goat Serum (Rockland Immunochemicals Inc., Gilbertsville, PA) (blocking solution) for 45 minutes at 37°C. Primary antibodies were diluted in blocking solution and applied for 45 minutes at 37°C. After three washes in phosphate-buffered saline, secondary antibody was diluted in blocking solution and incubated with the cells for 45 minutes at 37°C. Cells were washed again as before and in some cases the DNA-binding dye, TO-PRO-3 (Invitrogen), was diluted in blocking solution before adding to the cells for a 20 minute incubation at 37°C. After a final wash in phosphate-buffered saline, chambers were removed and approximately 10 µl of Component A from the SlowFade Antifade Kit (Invitrogen) was applied before adding glass coverslips. A Zeiss LSM510 laser scanning confocal microscope (Jena, Germany)

equipped with argon (488nm), HeNe1 (543nm), and HeNe2 (633nm) lasers was utilized for visualizing fluorescently-labeled cells and image analysis was performed using MetaMorph Offline 6.3 Meta Imagining Software (Molecular Devices Corporation, Sunnyvale, CA).

Antibodies and Dyes. The following primary antibodies were used: Anti-FLAG M2 monoclonal antibody (Sigma) and mouse IgG1κ (Sigma) at 20 μg/ml or monoclonal anti-α-tubulin (Sigma) and mouse IgG1κ (Sigma) at 1 μg/ml. Secondary antibodies were either whole molecule goat anti-mouse IgG TRITC Conjugate (Sigma) diluted 1:128 or Fc specific goat anti-mouse IgG FITC Conjugate (Sigma) diluted 1:200. When the nucleic acid stain TO-PRO-3 (Invitrogen) was used, the dye was diluted 1:1000.

Results

The M140 and M141 proteins exhibit an altered localization depending on whether the proteins are co-expressed or expressed individually suggesting that the proteins may function in more than one subcellular location. As a prerequisite to understand the extent to which proper localization affects the function of the proteins we sought to map the interaction domain of pM141. For this purpose we generated 5' or 3' truncations in the M141 gene so that we could examine the localization of the truncated protein products. M141 is a member of the US22 gene family and contains all four conserved motifs characteristic of the family (Fig. 3) (21, 39, 59, 94, 119, 120, 143). The function of the motifs has not been identified. However, the conserved nature of the motifs suggests that they confer an important property to the proteins. Therefore,

identical to our approach for mapping interaction domains, we targeted the motifs in our deletion mapping. Additionally, we targeted the putative NLS of the protein. The N-terminal truncation mutants are expressed as EGFP fusion proteins with an N-terminal tag (Fig. 19). The pGFP141ForUSM1 mutant retains all four motifs and is deleted of 39 N-terminal amino acids adjacent to Motif I. The pGFP141ForUSM2 mutant, missing 62 N-terminal amino acids, is deleted of Motif I. The pGFP141ForDSM3 mutant is deleted of Motif II and III and is missing 162 amino acids at the N terminus. The pGFP141ForUSM4 mutant is deleted of 243 N-terminal amino acids adjacent to Motif IV.

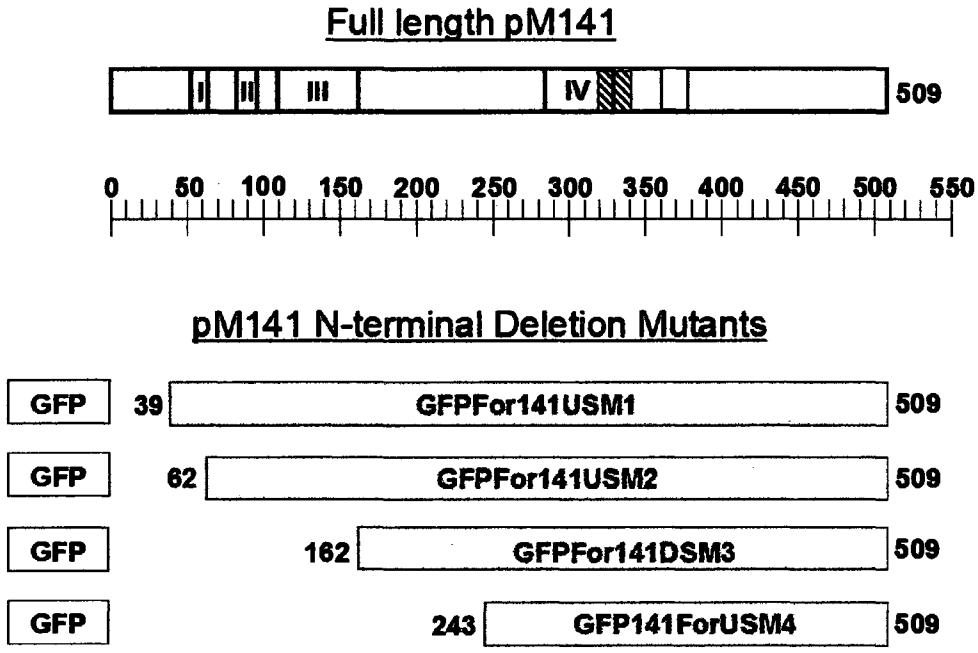

FIG. 19. Map of the panel of pM141 N-terminal deletion mutants analyzed for localization domain mapping. Full-length pM141 is shown at the top along with the location of the US22 Motifs (open boxes), the putative NLS (hatched box) which shares some overlap with Motif IV, and the PEST motif (white box). The ruler is shown for reference with each tick mark corresponding to 10 amino acids. Each pM141 deletion mutant is shown drawn to scale with the location of the GFP tag (not drawn to scale).

For these experiments we transiently-transfected fibroblast cells with plasmid constructs that express each of the deletion mutants or a construct expressing a full-length M141/EGFP fusion, GFP141FL. The EGFP tag in each protein was visualized directly by confocal microscopy. The nuclear compartment was delineated using TO-PRO-3 while the cytoplasmic compartment was stained for α-tubulin. We found that each of the N-terminal deletion mutants exhibited a localization pattern identical to that of the full-length protein (Fig. 20) suggesting that the N terminus of the protein does not contain a localization domain.

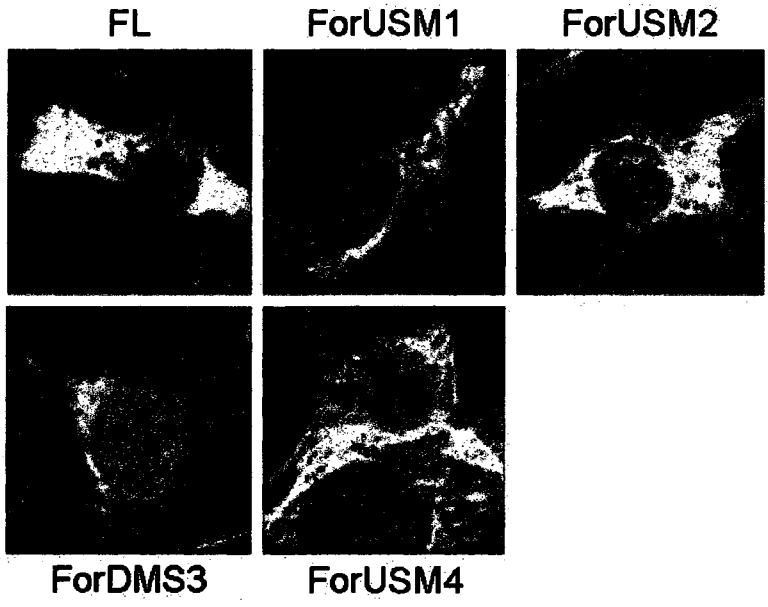

FIG. 20. Localization of the EGFP-tagged pM141 N-terminal deletion mutants. NIH3T3 fibroblast cells were transfected with GFP141FL (FL), GFP141ForUSM1 (ForUSM1), GFP141ForUSM2 (ForUSM2), GFP141ForDSM3 (ForDSM3), or GFP141ForUSM4 (ForUSM4). Approximately 72 hours post-transfection the cells were stained to detect either the nucleus (TO-PRO-3; blue) or cytoplasm (anti-α-tubulin primary and TRITC-conjugated secondary; red). The M141 protein was detected via the EGFP tag shown in green. Confocal images are shown with an original magnification of x40.

Therefore, we similarly screened the panel of C-terminal deletion mutants except that these mutants contained an N-terminal FLAG epitope tag (Fig. 21). The p141MostCTerm/FLAG7 and p141NextCTerm/FLAG7 mutants retain all four US22 Motifs and are deleted of 59 and 115 amino acids, respectively. The p141DSM4/FLAG7 mutant is deleted of 176 amino acids adjacent to the putative NLS. The p141USNLS/FLAG7 mutant is deleted of the putative NLS and 202 C-terminal amino acids. The p141USM4/FLAG7 mutant, deleted of the NLS and Motif IV, is missing 251 amino acids. Fibroblasts were transiently-transfected with each of the mutant constructs

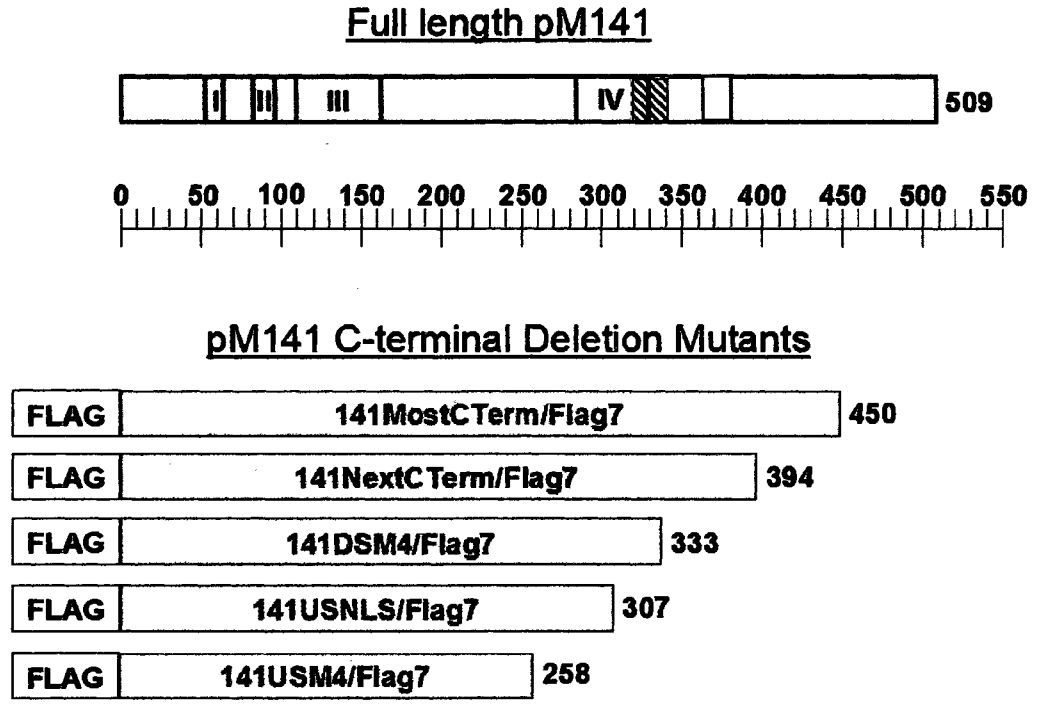

FIG. 21. Map of the panel of pM141 C-terminal deletion mutants analyzed for localization domain mapping. Full-length pM141 is shown at the top along with the location of the US22 Motifs (open boxes), the putative NLS (hatched box) which has some overlap with Motif IV, and the PEST motif (white box). The ruler is shown for reference with each tick mark corresponding to 10 amino acids. Each pM141 deletion mutant is shown drawn to scale with the location of the FLAG epitope tag (not drawn to scale).

and pM141 was detected via staining for the FLAG epitope tag. Cells were counterstained with TO-PRO-3. We found that p141MostCTerm/FLAG7 and p141NextCTerm/FLAG7 displayed a localization identical to the full-length pM141 (Fig. 22). However, p141DSM4/FLAG7, p141USNLS/FLAG7, and p141USM4/FLAG7 displayed an alternative localization. Some cells had a localization similar to the full-length protein (not shown), but we observed significantly more nuclear staining in over half of the cells examined (Fig. 22).

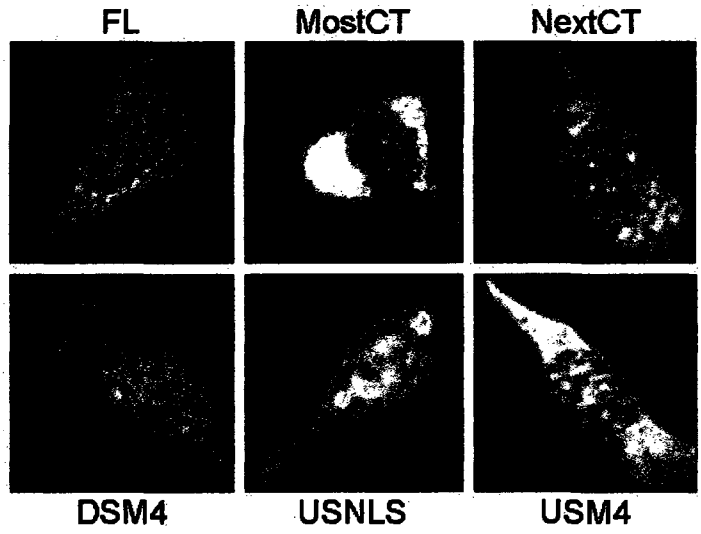

FIG. 22. Localization of FLAG epitope tagged pM141 C-terminal deletion mutants. NIH3T3 fibroblasts cells were transfected with either FLAG-M141 (FL), 141MostCTerm/FLAG7 (MostCT), 141NextCTerm/FLAG7 (NextCT), 141DSM4/FLAG7 (DSM4), 141USNLS/FLAG7 (USNLS), or 141USM4/FLAG7 (USM4). Approximately 72 hours post-transfection the cells were stained with anti-FLAG primary antibody and secondary antibody conjugated to TRITC (red). Nuclei were stained with TO-PRO-3 (blue). Shown are confocal microscopy images with an original magnification of x40.

We considered that the mutants displaying significantly more nuclear protein may be small enough to traverse the nucleus by passive diffusion. Therefore, each of the mutants was subcloned into a plasmid vector that confers expression as N-terminal EGFP fusion proteins, adding an additional 29 kDa to each of the mutant proteins. We found that the localization pattern was shifted (Fig. 23). As with the FLAG epitope tagged mutants, pGFP141MostCTerm and pGFP141NextCTerm had a localization pattern identical to full-length pM141. However, pGFP141DSM4 mutant also exhibited localization like full-length pM141 while the FLAG-tagged version of this mutant was observed to have significantly more nuclear protein (Fig. 22). Furthermore, although we observed that pGFP141USNLS and pGFP141USM4 have more nuclear protein compared to full-length protein (Fig. 23), we observed less accumulation compared to the FLAG-tagged mutant proteins (Fig. 22) and only a fourth of the cells examined exhibited nuclear accumulation. These results suggest that the FLAG-tagged p141DSM4, p141USNLS, and p141USM4 traversed the nucleus by passive diffusion.

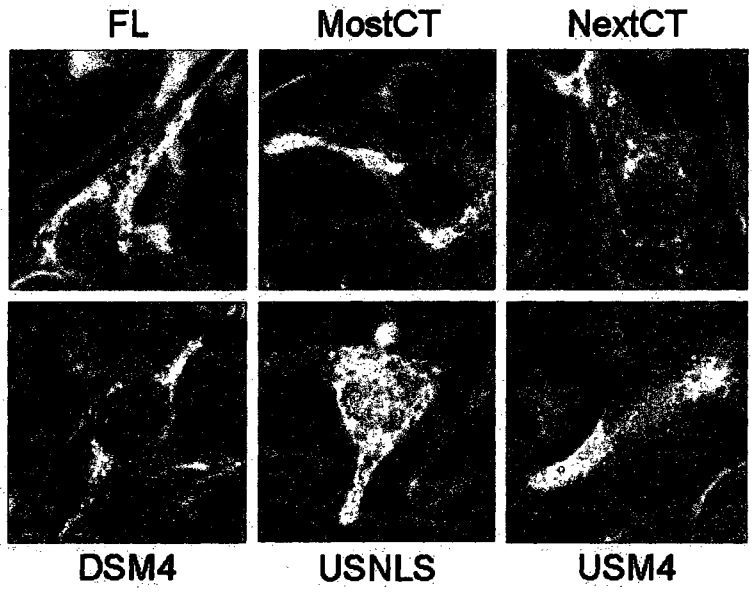

FIG. 23. Localization of EGFP-tagged pM141 C-terminal mutants. NIH3T3 fibroblasts were transfected with either GFP141MostCTerm (MostCT), GFP141NextCTerm (NextCT), GFP141DSM4 (DSM4), GFP141USNLS (USNLS), GFP141USM4 (USM4), or GFP141FL (FL). Cells were fixed and stained approximately 72 hours later with an anti-α-tubulin primary antibody and TRITC-conjugated (red) secondary antibody. Nuclei were stained with TO-PRO-3 dye (blue) and pM141 was detected via the EGFP tag (green). Confocal microscopy images are shown. Original magnification is x40.

Discussion

The M141 protein can be found in both cytoplasm (predominantly) and nucleus of infected cells while pM140 is localized mainly to the nucleus (82). However, when the proteins are co-expressed they co-localize to a perinuclear region (82). These results suggest that the proteins may function in multiple locations inside the cell. We hypothesized that pM141 contained a NES and NLS and sought to map the localization domains of the proteins as a prerequisite to better understand how proper localization is related to the function of the proteins. However, we were unable to detect either signal despite using a strategy that included deletion mapping with complete gene coverage.

Two main possibilities exist to explain our results: 1) the protein does contain signals for nuclear shuttling that were not uncovered by our strategy, or 2) the protein enters the nucleus via passive diffusion, but is shuttled back to the cytoplasm by a NES.

Hypothesis: pM141 contains signals for nuclear shuttling not uncovered by our strategy. One strategy for mapping localization domains is to generate mutant proteins deleted of increasing N- and C-terminal amino acids (99, 125, 158). Using this strategy a localization domain is mapped by a process of elimination whereby a small deletion mutant retains localization like full-length protein and a mutant deleted of adjacent larger amino acids is excluded from a subcellular compartment of interest. We chose this strategy beacause of the availability of large scale deletion mutants already generated to map interaction domains of pM141 (see Chapter III) and because of the large size of the protein (509 amino acids).

The fact that pM141 localizes predominantly to the cytoplasm is a complicating factor for this strategy. Proteins are translated in the cytoplasm and will remain there unless they are small enough to enter the nucleus by passive diffusion or if they contain localization signals for subcellular targeting (137, 139, 168). It is possible that pM141 contains a NLS and is retained in the cytoplasm by complexing with a protein that masks the NLS. In this case, if one of our deletion mutants is missing the NLS, regardless of whether the mutant has a NES, we would expect to see localization similar to the full-length protein.

The deletion mutant strategy is also complicated by the fact that the mutant proteins, upon further and further deletion of N- or C-terminal amino acids, can reach a

size small enough to diffuse passively through the nucleus. Although most nuclear transit is regulated and efficient localization requires nucleocytoplasmic shuttling, proteins up to 60 kDa or more can enter the nucleus through passive diffusion (102, 137, 168, 190). The results from our localization mapping imply that we achieved passive diffusion of some of our smaller C-terminal deletion mutants. Some of our deletion mutants are small enough to conceivably diffuse into the nucleus passively. Two of our C-terminal deletion mutants, p141MostCT and p141NextCT, localized in a similar pattern to the full-length protein regardless of whether the proteins were fused to a FLAG or EGFP tag. The two smallest C-terminal mutants, p141USNLS and p141USM4, had a fairly equal distribution in the cytoplasm and nucleus, regardless of epitope tagging. However the p141DSM4 mutant displayed a localization pattern dependent on the size of the epitope tag. FLAG-tagged p141DSM4 exhibited an equal distribution between cytoplasm and nucleus similar to p141USNLS and p141USM4, while the EGFP-tagged mutant exhibited localization like the full-length protein. The FLAG tag is a small tag and only adds approximately 3 kDa to the molecular weight of pM141. However, EGFP, a 29 kDa protein, has a considerably larger molecular weight. Our results indicate that the three smallest FLAG-tagged mutants can diffuse passively into the nucleus and that addition of the EGFP tag to the p141DMS4 mutant increases the size such that the protein cannot diffuse into the nucleus. Apparently, p141USNLS and p141USM4 remain small enough for passive diffusion even with the addition of EGFP.

Another complication of a deletion strategy is the fact the protein of interest as a whole remains relatively intact and may thus retain an ability to bind to regulatory proteins. It is well documented that complexing between proteins can mask NES or NLS

and that this binding is a means of regulating the NES/NLS-containing protein (76, 137, 139, 168). The interaction domains may also be deleted or affected leading to difficulty in interpreting results. Alternatively, a localization domain may be removed, but the protein is retained in a subcellular location because it retains an ability to bind to a regulatory protein.

An alternative strategy for mapping NES/NLS is to break the protein up into small components which can passively enter the nucleus and which are then expressed fused to a protein, for example GFP, that does not contain localization signals and because of its size is diffusely distributed throughout the cell (42, 121, 186). Using this strategy the localization of each protein fragment is compared to that of GFP. If a fragment contains a localization signal then GFP will be relocalized to a distinct subcellular compartment. Future studies of pM141 localization should include this strategy for several reasons. First, although pM141 can be isolated from the nucleus, the majority of pM141 is localized to the cytoplasm (61, 82). Thus, if pM141 does contain a NLS/NES then the protein localization must be highly regulated. However, using the strategy with the GFP fusions the target protein does not remain intact and therefore the possibility that regulatory proteins can still bind is decreased. Furthermore, with this strategy results are interpreted on the basis of a protein fragment containing a signal rather than lacking one. Thus, each protein will localize to a subcellular compartment only if the fragment has a signal. This strategy also escapes the problem of passive diffusion of smaller deletion mutants as long as the protein fragments are designed to be small enough to passively enter the nucleus. Under these circumstances each mutant will localize diffusely throughout the cell with a pattern identical to GFP unless the protein

fragment contains a signal.

Hypothesis: pM141 contains a NES and enters the nucleus by passive diffusion. We hypothesized that pM141 contains a NES and NLS. Our hypothesis was based on several pieces of evidence: 1) when expressed individually pM141 localizes predominantly to the cytoplasm and to a lesser extent the nucleus while pM140 is almost entirely nuclear localized, 2) in the presence of pM141, pM140 is relocalized from the nucleus and co-localizes to a distinct perinucleur region with pM141, 3) bioinformatics analysis of pM141 revealed a putative NLS, while a NES was not predicted for pM141 or pM140 and 4) the proteins form a complex. An alternate hypothesis might be that pM140 is prevented from entering the nucleus by complexing with pM141 in the cytoplasm and that pM141 can enter the nucleus by passive diffusion, but is rapidly transported out of the nucleus by a NES.

In support of our alternate hypothesis we have demonstrated that the proteins are coordinately regulated at the transcriptional and translational levels (59, 61). If pM140 is required in the nucleus at distinct times after infection or in response to specific cellular stimuli then the proteins would need to be coordinately expressed so that they could complex immediately post-translation and remain complexed until pM140 is required in the nucleus. Upon reception of a signal, pM140 would be released from pM141, exposing the NLS, and allowing pM140 to transit the nucleus. It is intriguing that pM141 from infected cells is more rapidly degraded in the absence of pM140 (61). M141 protein levels are dependent on the concentration of pM140, but pM141 can be rapidly degraded even when the proteins retain an ability to form a complex (Chapter V). This further

demonstrates the complex interplay between the two proteins. It is tempting to speculate that pM141 retains pM140 in the cytoplasm until a signal is received causing the rapid degradation of pM141 and nuclear translocation of pM140 mediated by the exposed NLS.

CHAPTER V

REGULATION OF pM141 DEGRADATION BY pM140

Introduction

The proteasomes are the main intracellular proteolytic machinery and are responsible for proper functioning of cellular processes through regulated degradation of proteins (77). The proteasome is a large, multisubunit complex that is cylindrical in shape and lined with proteases that mediate degradation of targeted proteins (77). The most well characterized form of targeting proteins to the proteasome is by addition of polyubiquitin chains that are recognized by proteasomal components (77). Ubiquitin-independent degradation of proteins is also observed, but is less well characterized currently (77). Several degradation signals have been identified. For example, PEST domains are commonly found on rapidly-degraded proteins in general and have commonly been observed on proteins degraded in a ubiquitin-dependent and proteasome-dependent fashion (144).

We previously observed that steady-state levels of pM141 were significantly reduced in the absence of pM140 and found that the protein exhibits an increased rate of turnover in the absence of pM140 relative to that in the presence of pM140 (61). Furthermore, analysis of the protein sequence of pM141 reveals a PEST domain. These results indicate that appropriate levels of pM141 may be important for the function of the protein. We hypothesized that pM141 is degraded by the ubiquitin-proteasome system. To address the question of whether degradation is proteasome-mediated we examined steady-state levels of pM141 in the presence or absence of pharmacological proteasome

inhibitors. To assess whether ubiquitin is required for degradation of pM141 we looked for ubiquitin-conjugates of the protein and assessed steady-state levels of the protein in an E1 ubiquitin ligase temperature-sensitive cell line. Given that pM141 is stabilized in the presence of pM140 and that the proteins form a stable complex (61, 82), we further hypothesized that direct complexing of the proteins was required for stabilization of pM141. Our approach was to determine if pM141 steady-state levels are dependent on the concentration of pM140. We also constructed M140 deletion mutants in order to map the region of pM140 required to stabilize pM141 and assessed whether these mutants retained an ability to complex with the protein.

Materials and Methods

Generation of plasmids. The pMT123 plasmid which expresses HA epitope tagged ubiquitin (184) was a kind gift from Lubbertus Mulder (The Rockefeller University, New York, NY). The pCS2m-cyclin E plasmid expressing a myc epitope tagged cyclin E protein (28), was a generous gift of David Pintel (University of Missouri-Columbia, Columbia, MO).

A plasmid designed to express full-length pM140 in with an N-terminal FLAG tag, FLAG140FL, was generated by first digesting His140FL (82) with HindIII. The HindIII site was subsequently blunted by reacting 1 unit of DNA Polymerase I, Large (Klenow) Fragment (New England Biolabs) per μg of linearized DNA with 0.05 mM dNTPs for 30 minutes at room temperature. The polymerase was heat inactivated at 75°C for 10 minutes before further digesting the vector with BamHI. Meanwhile p3XFLAG-CMV-7 was digested with BamHI and SmaI. The digested DNA was resolved by

electrophoresis on a 1% agarose gel. Vector and insert fragments were purified using the QIAquick Gel Extraction Kit according to manufacturer's instructions and ligations were performed as described below.

For the purpose of mapping the domain of pM140 required to stabilize pM141 we generated plasmids designed to express pM140 C-terminal deletion fusion proteins with an N-terminal FLAG tag. FLAG140DSM3, FLAG140DSM4, and FLAG140USAcidic are deleted of 305, 179, or 105 amino acids, respectively. Each of the plasmids was generated by first digesting 140DSM3/TOPO, 140DSM4/TOPO, or 140USAcidic/TOPO with BamHI and NotI. Each fragment was ligated into BamHI/NotI-digested His140FL generating 140DSM3/HisC, 140DSM4/HisC, and 140USAcidic/HisC. Then, BamHI/ApaI-digested 140DSM3/HisC, 140DSM4/HisC, or 140USAcidic/HisC fragments were ligated into BamHI/ApaI-digested FLAG140FL vector upon purification of DNA after electrophoresis as described above.

A construct designed to express full-length pM141 as an N-terminally tagged FLAG epitope fusion protein under control of a mammalian expression promoter, FLAG-M141, was generated as previously described (82). The pM141 plasmid (referred to as M141Nat in this work) which contains full-length M141 under control of the native gene promoter was generated by inserting a BamHI to XbaI fragment of pDJI (62) into BglII/XbaI-digested pcDNA3 (Invitrogen).

Restriction Enzyme Digestion. All restriction enzymes were used according to manufacturer's directions. Typically, between 5-15 units of enzyme per ug of DNA was used in digestions which were reacted at the appropriate temperature for 3 to 5 hours.

Ligations. Ligation reactions were conducted using a minimum of a three fold molar ratio of insert to vector in the presence of 0.5 units of T4 DNA Ligase according to the manufacturer's instructions with an overnight incubation at 4°C.

Transformations. FLAG140DSM3, FLAG140DSM4, and FLAG140USAcidic plasmids were transformed into XL-1 blue cells with 1 to 2 µl of ligated DNA after a 30 minute incubation on ice. The transformations were performed with a heat shock at 42°C for 1.5 minutes. After an incubation on ice for 2 more minutes 800µl of SOC Medium (153) was added to the cells for a 1 hour recovery at 37°C with agitation. Competent cells were prepared as per Sambrook (153). The pCS2m-cyclin E and pMT123 plasmids were transformed into XL-1 blue cells with 50-100 ng DNA. FLAG140FL was transformed into NovaBlue cells (Novagen) according to manufacturer's instructions.

Amplification of plasmids. When plasmids were required for the purpose of screening cloned DNA by restriction enzyme digestion the plasmids were amplified by growing a single colony of transformed bacteria (see above) overnight at 37°C with agitation in 3 ml of Luria-Bertani Medium (LB) (153) containing either 0.2 mg/ml ampicillin (Sigma) or 50 µg/ml kanamycin (Sigma) where appropriate. Approximately 1.5 ml of overnight culture was pelleted by centrifugation at 14,000X g for 1 minute after which the resulting pellet was resuspended in 100 µl of Solution I (50 mM Tris, pH 8.0, 50 mM glucose, 10 mM EDTA). After a 5 minute incubation on ice 200 µl of Solution II (0.2 M sodium hydroxide, 1% Trition X-100) was added to the sample. Cell lysis was allowed to proceed on ice until the cloudy solution began to clear (approximately 2-3 minutes). The solutions were neutralized by addition of 150 µl of Solution III (3 M sodium acetate, pH 4.8). After a 5 minute incubation on ice the solutions were

centrifuged for 5 minutes at 14,000X g. Supernatant was collected and incubated with 1 volume of isopropanol for 5-10 minutes at room temperature. Plasmids were harvested by centrifugation at 14,000X g for 5-10 minutes. The plasmid-containing pellet was washed with 500 ml of 70% ethanol and pelleted as before. The dried pellet was resuspended in 50 μl of sterile water and then 10 μl was used per restriction digest.

To generate large scale plasmid preparations the plasmids were first amplified in 5 ml of starter culture of LB with 0.2 mg/ml ampicillin or 50 μg/ml kanamycin (where appropriate) overnight at 37°C with agitation. The starter culture was used to inoculate 250 ml of LB containing the appropriate antibiotic which was incubated at 37°C with agitation for between 14-18 hours. Plasmids were purified using the Plasmid Maxi Kit (Qiagen) according to manufacturer's instructions. In some cases the Quantum Prep Plasmid Maxiprep Kit (Bio-Rad) was used to purify DNA.

Cells. IC-21 cells (TIB-186; American Type Culture Collection, Manassas, VA), a mouse peritoneal macrophage line, were maintained in RPMI-1640 media (Mediatech Incorporated, Manassas, VA) supplemented with 1% L-glutamine and 10% heat-inactivated fetal bovine serum. NIH3T3 cells (CRL-1658; American Type Culture Collection), a mouse fibroblast line, were propagated in Dulbecco's Modified Eagle's Media supplemented with 1% L-glutamine and 10% heat-inactivated bovine calf serum. IC-21 and NIH3T3 cells were maintained in a humidified incubator at 37°C with 5% carbon dioxide. The *ts*20 cells (a generous gift from Harvey Ozer, UMDNJ-New Jersey Medical School, Newark, NJ) were derived from mouse BALB/3T3 clone A31 fibroblast cells and were propagated in Dulbecco's Modified Eagle's Media (1% L-glutamine; 10% heat-inactivated bovine calf serum) in a humidified incubator at 37°C (except where

indicated) with 5% carbon dioxide.

Viruses. Wild type MCMV (VR-194; ATCC) utilized in these experiments is Smith strain. Construction of mutant viruses disrupted of expression of M140 (RVΔ140) or M141 (RVΔ141), or deleted of M139 and M140 (RV12) was previously described (61, 82). Viruses were propagated in NIH3T3 cells and virus titers were determined by plaque assay as previously described (19).

Transient transfections. NIH3T3 cells were transfected using either TransFectin or Metafectene. When transfections were performed using Transfectin, cells were seeded into 25 cm^2 culture flasks 24 hours prior at a density of between 6-7 x 10^5 cells in 4 mls of propagation media. Cells were typically transfected with a total of 18 µl of Transfectin and a total of 9 µg of plasmid DNA, but in cases where less plasmid was used a 2:1 ratio of Transfectin volume to microgram of DNA was maintained. Plasmid DNA and Transfectin were added to 500 µl aliquots of Dulbecco's Modified Eagle's Media, mixed together, vortexed for 5 seconds, incubated at room temperature for 20 minutes, and added directly to the cells. Approximately 24 hours post-transfection cells were seeded onto 100 mm dishes which were harvested 48 hours later. In some cases the cells were infected 24 hours after seeding onto 100 mm dishes using 2 PFU/cell of virus in 2 ml of media with rocking for 1 hour. Virus-containing media was removed, replaced with fresh propagation media, and cells were incubated between 16-20 hours prior to harvesting.

When using Metafectene, cells were seeded 18 hours prior to transfection in 25 cm^2 culture flasks at a density of 3-4 x 10^5 cells. Six micrograms of plasmid DNA and 9 µl of Metafectene were added to 100 µl aliquots of Dulbecco's Modified Eagle's Media,

mixed together, vortexed for 5 seconds, and incubated at room temperature for 20 minutes. Media used to seed the cells was removed, 2 mls of media was added to the transfection mixes, and this was added to the cells. Approximately 24 hours post-transfection cells were seeded onto 100 mm dishes which were harvested 48 hours later. In some cases the cells were infected 24 hours after seeding onto 100 mm dishes using 2 PFU/cell of virus in 2 ml of media with rocking for 1 hour. Virus-containing media was removed, replaced with fresh media, and cells were incubated between 16-20 hours prior to harvesting.

Infections. Between 5-6.5 x 10^5 NIH3T3 cells, 1 x 10^6 IC-21 cells, or 6 x 10^5 ts20 cells were seeded into 60 mm dishes. Approximately 24 hours later NIH3T3 and ts20 cells were infected with 2 PFU/cell of virus in 1 ml of media with rocking for 1 hour. When infecting IC-21 cells, 4 PFU/cell of virus was used in 1 ml of media with rocking for 2 hours. After infection, virus-containing media was removed and fresh propagation media was added to the cells. Cells were harvested 16-20 hours later.

Western blotting. NIH3T3, IC-21, and ts20 cells expressing proteins of interest or control proteins were harvested, counted, and normalized based on cell numbers prior to resuspension in western lysis buffer (50 mM Tris, pH 7.5, 1% SDS). Equal volumes of cell lysates were electrophoresed on 12.5% SDS-polyacrylamide gels after boiling in the presence of 1X SDS loading dye. Transfer of proteins from the gel onto 0.45 micrometer, supported, pure nitrocellulose (GE Water and Process Technologies, Trevose, PA) was conducted at 134 milliAmps for 1 hour and 50-60 minutes using a semi-dry electroblot apparatus. The gel and nitrocellulose membrane were layered between two pieces of Whatman 3MM CHR chromatography paper soaked in cathode

buffer (25 mM Tris, pH 9.4, 40 mM 6-Aminohexanoic acid, 20% methanol) and two pieces of Whatman 3MM CHR chromatography paper soaked with either anode buffer #1 (0.3 M Tris, pH 10.4, 20% methanol) (exposed to the anode) or anode buffer #2 (25 mM Tris, pH 10.4, 20% methanol) (exposed to the nitrocellulose also soaked with anode buffer #2). Post-transfer, membranes were blocked overnight in Tris-buffered saline (TBS; 10 mM Tris, pH 7.5, 0.15 M NaCl) with 5% Carnation powdered non-fat milk and 0.1% Tween-20 (blocking solution). Membranes were probed for 1 hour in blocking solution using primary antibodies at the following concentrations: monoclonal anti-E1 (Ubiquitin Activating Enzyme) (Sigma) at 5 μg/ml, polyclonal anti-M140 or -M141 (61) diluted 1:500, and monoclonal anti-ß-Actin at 0.3 μg/ml. Membranes were washed three times in TBS with 0.1% Tween-20 for at least 10 minutes each, probed with secondary antibodies in blocking solution for 1 hour, and washed again. Secondary antibodies conjugated to infrared fluorescent dyes were used for detection with the LI-COR (Lincoln, NE) Odyssey Infrared Imaging System. IRDye 680 Conjugated goat anti-mouse IgG (LI-COR) was used at 1:20,000 and IRDye 800CW Conjugated goat anti-rabbit IgG (LI-COR) at 1:15,000 according to manufacturer's directions.

Immunoprecipitations. Immunoprecipitations were performed to detect complexing between pM141 and full-length or truncated pM140. NIH3T3 cells infected and/or transiently-transfected to express proteins of interest or control proteins were washed three times in phosphate-buffered saline, harvested in 1ml immunoprecipitation lysis buffer (50mM Tris [pH 7.5], 5mM EDTA, 150mM NaCl, 0.5% NP-40, 0.5% deoxycholate, 1mM PMSF, 10 ug of aprotinin/ml) and clarified for cellular debris at 14,000X g for 1 minute. One hundred microlitres of clarified lysate was retained as input

for SDS-PAGE. Immunoprecipitations were performed using 400-450 µl of clarified lysate and 5 µl of anti-M141 antibody or preimmune serum. Prior to immunoprecipitation all lysates were precleared with preimmune serum: 5 µl of preimmune serum was incubated with aliquots of lysate for 30 minutes at 4°C with rotation after which 60 µl Protein A-Agarose (Roche) was added and incubated for 1 hour. After centrifugation at 10,000X g for 2 minutes the supernatant containing precleared lysates was removed for specific immunoprecipitations. Precleared lysates and anti-M141 or preimmune serum was incubated at 4°C with rotation. Twenty four hours later, 60 µl of protein A-agarose was added to the protein/antibody complexes for an additional incubation of 4 hours. Immune complexes were washed three times in SNNTE buffer and three times in RIPA buffer with centrifugations of 10,000X g at 4°C for 2 minutes between each wash. Protein complexes were denatured with 5 minutes of boiling in the presence of SDS-PAGE loading dye and 2 µl ß-mercaptoethanol prior to SDS-PAGE on 12.5% acrylamide gels. Western blots were performed identical to those described above with 10 µg/ml of anti-FLAG M2 monoclonal antibody as the primary antibody.

Immunoprecipitations were also performed to detect polyubiquitinated pM141 or myc epitope-tagged cyclin E as a positive control. Infected and/or transiently-transfected NIH3T3 cells expressing proteins of interest or control proteins were washed three times in phosphate-buffered saline, harvested in 1ml immunoprecipitation lysis buffer containing 5 mM N-ethylmaleimide (Sigma), and clarified for cellular debris at 14,000X g for 1 minute. One hundred microlitres of clarified lysate was retained as input for SDS-PAGE. Immunoprecipitations were performed with a 2 hour incubation at 4°C using

400-450 µl of clarified lysate and the following antibodies: 5 µl of anti-M141 antibody or preimmune serum and 0.4 µg of Myc-Tag monoclonal antibody (Cell Signaling Technology) or IgG2a mouse isotype control. Twenty four hours later, 60 µl of protein A-agarose was added to the protein/antibody complexes for an additional incubation of 4 hours. Immune complexes were washed three times in SNNTE buffer and three times in RIPA buffer with centrifugations of 10,000X g at 4°C for 2 minutes between each wash. Protein complexes were denatured with 5 minutes of boiling in the presence of SDS-PAGE loading dye and 2 µl ß-mercaptoethanol prior to SDS-PAGE on 12.5% acrylamide gels. Western blots were performed identical to those described above with 0.8 µg/ml of anti-HA monoclonal antibody (Roche).

Inhibitors. All inhibitors were added to cells in propagation media and were used at the indicated concentrations according to manufacturers' instructions. Proteasome inhibitors, MG132 and epoxomicin, were purchased from Calbiochem (Gibbstown, NJ). The protein translation inhibitor, cycloheximide, was purchased from Sigma (Saint Louis, MI).

Results

Mechanism of pM141 Degradation. Our previous studies had indicated that the rate of pM141 degradation was enhanced in the absence of pM140 (61). As a prerequisite to understanding to what extent pM141 levels affect protein function, we wanted to determine the mechanism of pM141 degradation. Proteasome-mediated degradation is the most common method of proteolysis (27, 142) so we first asked whether pM141 would accumulate in the presence of the proteasome inhibitor, MG132.

Thus, IC-21 macrophages were infected with either WT virus or virus deleted of the M140 gene, RVΔ140 (61), and were then treated with MG132. We found that in the presence of pM140, pM141 levels accumulated to higher steady-state levels in the presence of drug treatment in a dose-dependent manner when compared to vehicle-treated cells (Fig. 24A). The relative amount of pM141 expression was 1.4 fold higher in the presence of 25 μM MG132 than vehicle and 2.5 fold higher than vehicle when 75 μM MG132 was applied to the cells (Fig. 24B). In RVΔ140 infected cells that received treatment with vehicle only, pM141 is not detectable (Fig. 24) which correlates with the increased rate of pM141 turnover when pM140 is not present (61). However, when the RVΔ140 infected cells were treated with MG132, pM141 accumulated to detectable levels in a dose-dependent manner with a 3 fold increase from 25 to 75 μM MG132 (Fig. 24). These results suggest that degradation of pM141 is proteasome-dependent. However, MG132 is a relatively non-specific proteasome inhibitor. We therefore used epoxomicin, which is among the most specific proteasome inhibitors (92), to confirm that pM141 is sensitive to degradation by the proteasome. As with MG132, pM141 from WT-infected cells accumulated in a dose-dependent manner in the presence of epoxomicin (Fig. 25). M141 protein levels were 1.2 fold higher in the presence of 5 μM epoxomicin compared to vehicle and 1.3 fold higher in the presence of 10 μM epoxomicin. As seen previously, levels of pM141 in the absence of pM140 were below the level of detection in the presence of vehicle alone while the levels were readily detectable in the presence of either 5 or 10 μM epoxomicin (Fig. 25). However, in RVΔ140-infected cells we did not observe a dose-dependent response of pM141 to epoxomicin as seen with MG132 (Fig. 25). It is possible that functionally saturating

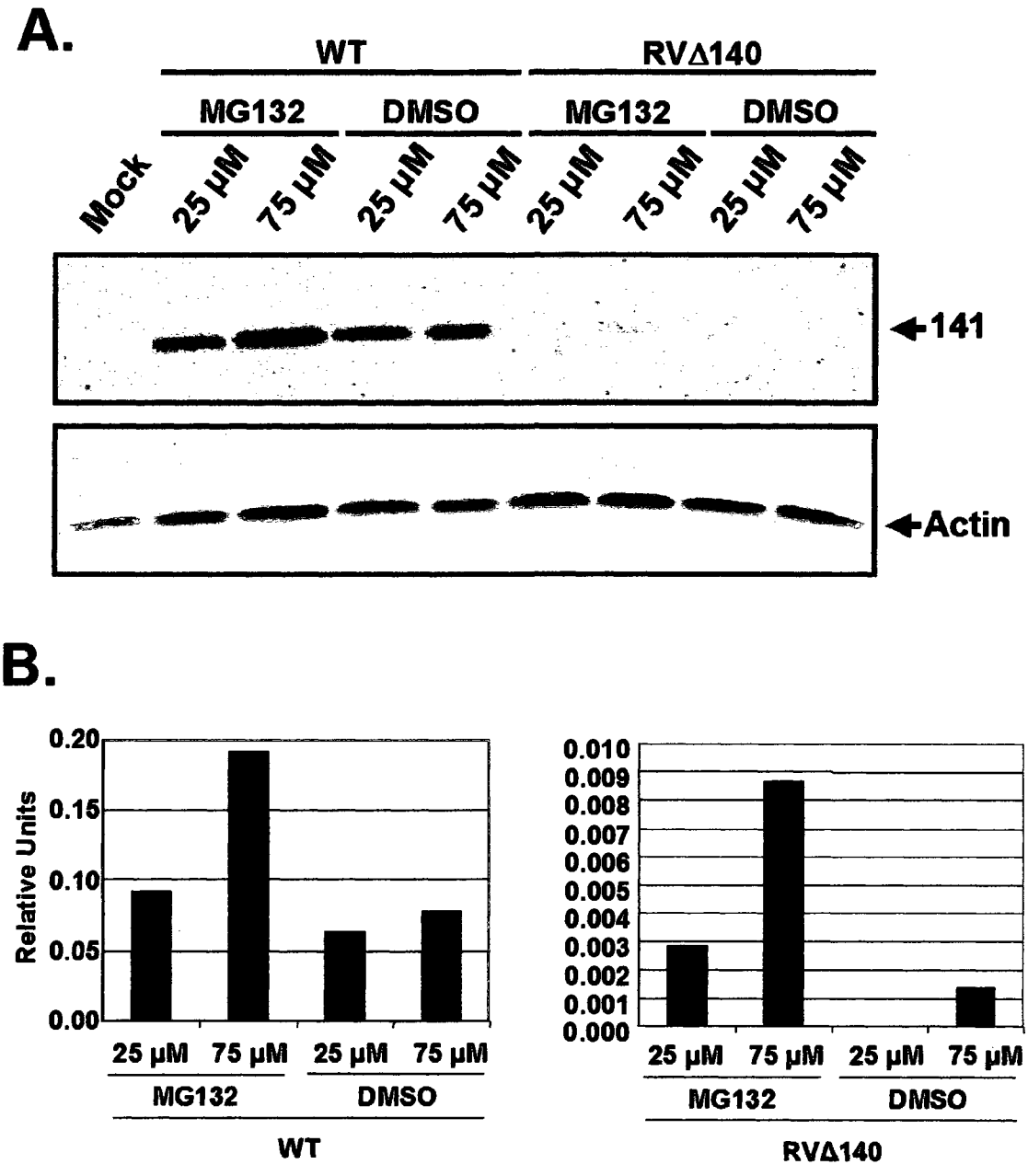

FIG. 24. Steady-state levels of pM141 from infected IC-21 macrophage cells in the presence or absence of MG132. IC-21 macrophages were mock infected or infected with 4 PFU/cell of either WT or RVΔ140. Four hours post-infection the indicated amounts of MG132 or Vehicle (DMSO) were added to the cells for approximately 18 hours. Cells were harvested, counted, and normalized based on cell number prior to electrophoresis on a 12.5% acrylamide gel. A. Western blot analysis probing for pM141 (141) or Actin as a loading control. B. Quantitation of pM141 levels of WT- (left panel) or RVΔ140-(right panel) infected cells shown in relative units after values were normalized to levels of actin.

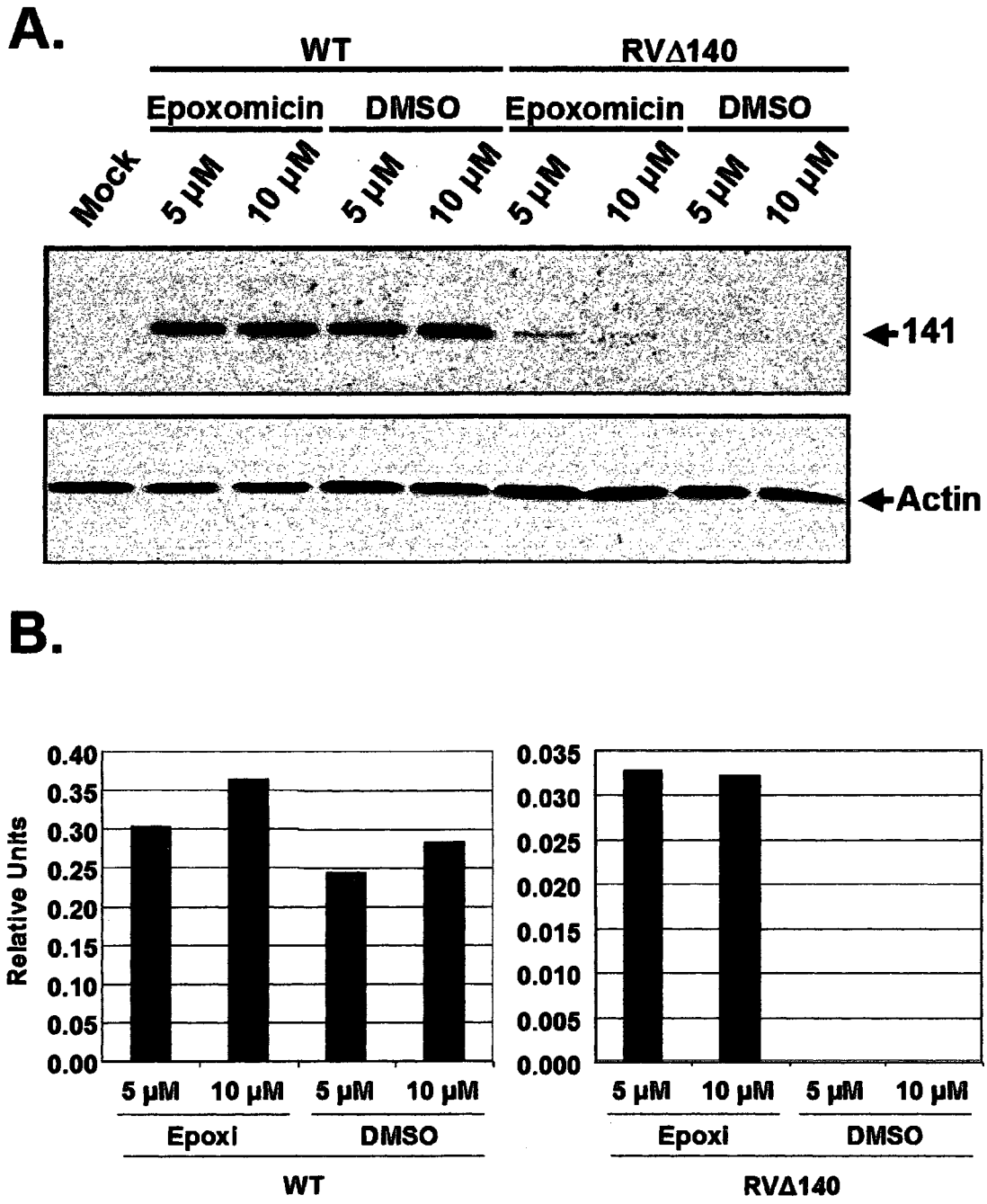

FIG. 25. Steady-state levels of pM141 from infected IC-21 macrophage cells in the presence or absence of epoxomicin. IC-21 macrophages were mock infected or infected with 4 PFU/cell of either WT or RVΔ140. Four hours post-infection the indicated amounts of epoxomicin (epoxi) or vehicle (DMSO) were added to the cells for approximately 18 hours. Cells were harvested, counted, and normalized based on cell number prior to electrophoresis on a 12.5% acrylamide gel. A. Western blot analysis probing for pM141 (141) or Actin as a loading control. B. Quantitation of pM141 levels from WT- (left panel) or RVΔ140- (right panel) infected cells are shown in relative units and after values were normalized to levels of actin.

doses of epoxomicin were achieved at 5 μM in this cell type. Regardless, pM141 levels are higher in the presence of proteasome inhibitors in WT infected cells and pM141 accumulates to detectable levels only in the presence of inhibitors in RVΔ140 infected cells. These results clearly indicate that degradation of pM141 in IC-21 macrophages is proteasome-dependent.

Given that pM141 functions in macrophage tropism, we asked whether the regulation of pM141 through proteasomal degradation was cell type specific. Therefore, NIH3T3 fibroblasts were infected with WT or RVΔ140 and then treated with proteasome inhibitors. Similar to the results in IC-21 macrophages, we observed an accumulation of pM141 from WT- or RVΔ140-infected fibroblasts treated with either MG132 (Fig. 26A) or epoxomicin (Fig. 27A) compared to that of vehicle-treated cells. M141 protein levels were 1.2 fold and 3.7 fold higher in WT-infected cells treated with 25 or 75 μM MG132, respectively, compared to vehicle-treated cells (Fig. 26B). In RVΔ140-infected cells pM141 was only detectable in the presence of MG132 and the accumulation was dose-dependent exhibiting 1.9 fold higher levels in 75 μM versus 25 μM MG132. Although we did not observe a dose-dependent increase in pM141 from WT-infected fibroblasts treated with epoxomicin the protein accumulated to greater amounts in the presence of inhibitor relative to vehicle (1.8 fold increase with 1 μM epoxomicin and 1.2 fold increase with 5 μM) (Fig. 27B). As seen with MG132 treatment, epoxomicin treatment of RVΔ140-infected fibroblasts led to the accumulation of detectable pM141 in a dose-dependent fashion with a 2.4 fold increase in the presence of 5 μM epoximicin compared to that of 1 μM inhibitor (Fig. 27B). These results demonstrate that proteasome-mediated degradation of pM141 is not cell type specific.

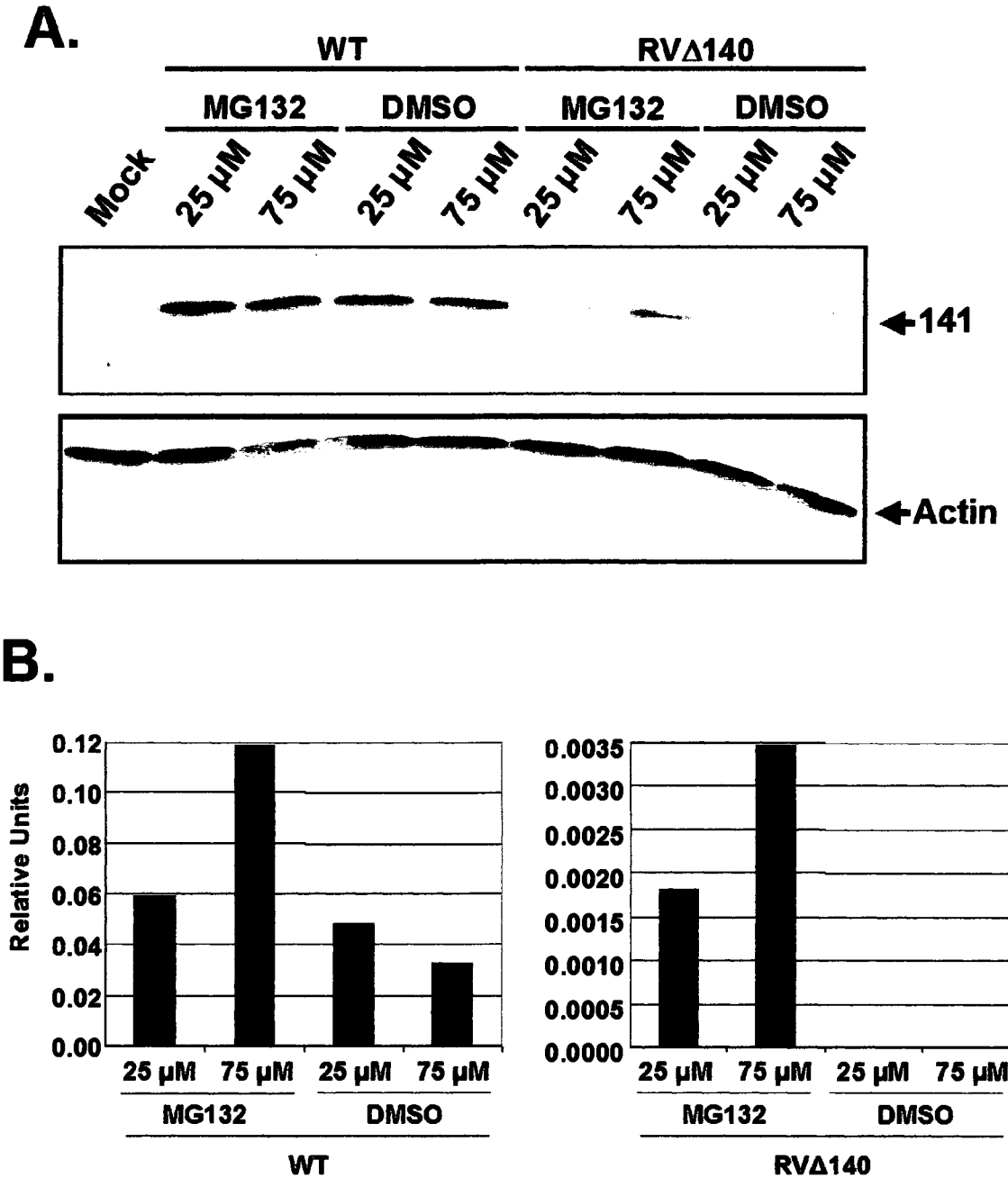

FIG. 26. Steady-state levels of pM141 from infected NIH3T3 fibroblast cells in the presence or absence of MG132. Fibroblasts were mock infected or infected with 2 PFU/cell of either WT or RVΔ140. Four hours post-infection the indicated amounts of MG132 or vehicle (DMSO) were added to the cells for approximately 18 hours. Cells were harvested, counted, and normalized based on cell number prior to electrophoresis on a 12.5% acrylamide gel. A. Results from Western blot analysis probing for pM141 (141) or Actin as a loading control. B. M141 protein levels were normalized to actin and the quantitation (shown in relative units) from each western blot is shown where WT-infected cells are represented in the left panels and RVΔ140-infected cells are represented in the right panels.

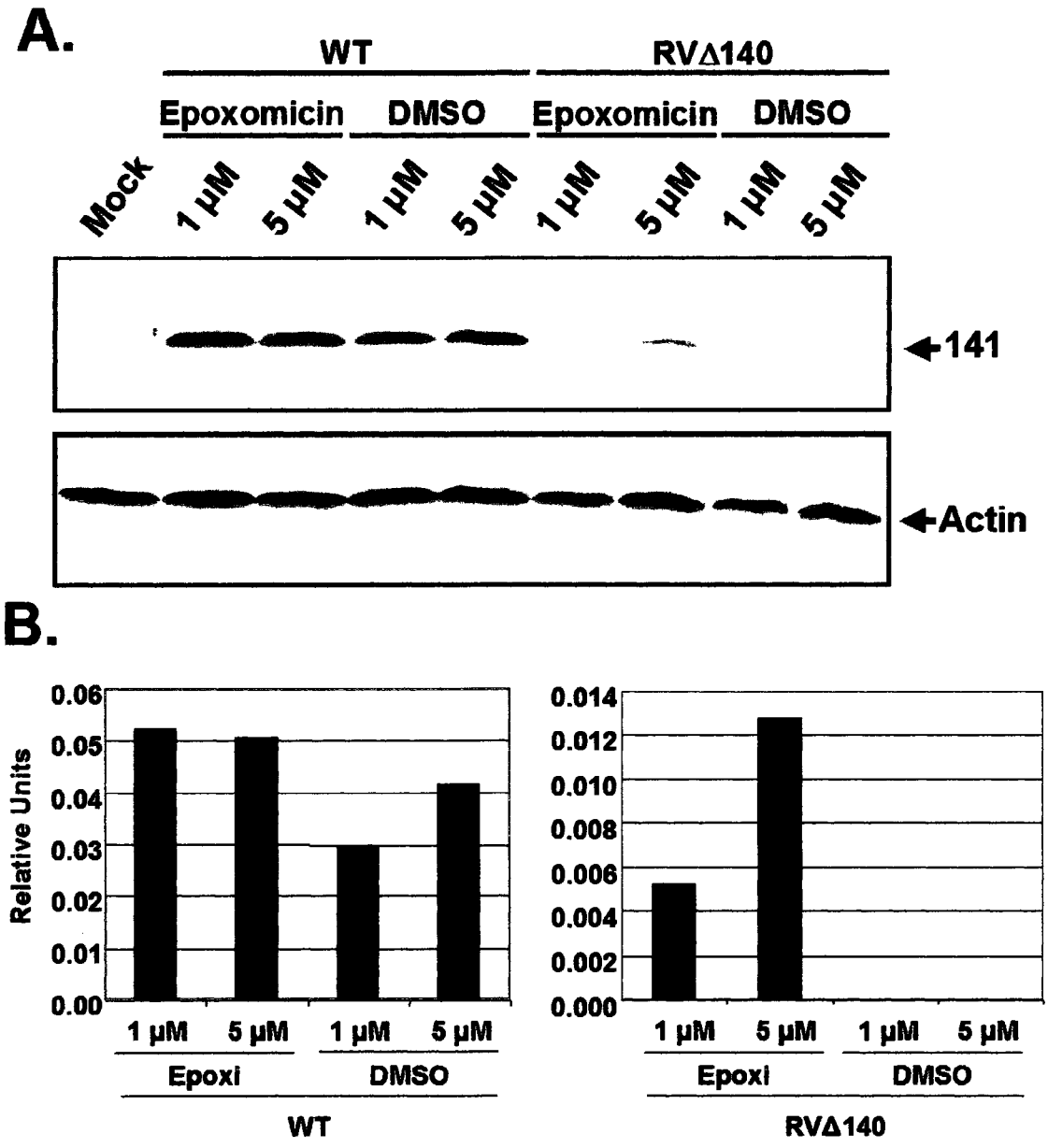

FIG. 27. Steady-state levels of pM141 from infected NIH3T3 fibroblast cells in the presence or absence of epoxomicin (epoxi). Fibroblasts were mock infected or infected with 2 PFU/cell of either WT or RVΔ140. Four hours post-infection the indicated amounts of epoxomicin or vehicle (DMSO) were added to the cells for approximately 18 hours. Cells were harvested, counted, and normalized based on cell number prior to electrophoresis on a 12.5% acrylamide gel. A. Results from Western blot analysis probing for pM141 (141) or Actin as a loading control are shown. B. M141 protein levels were normalized to actin and the quantitation (shown in relative units) from each western blot is shown where WT-infected cells are represented in the left panels and RVΔ140-infected cells are represented in the right panels.

Addition of polyubiquitin chains is the most well studied mechanism to target proteins to the proteasome for degradation. Thus, we were interested to see if pM141 degradation is ubiquitin-dependent. In order to detect polyubiquitinated forms of pM141, we transfected WT- and RVΔ140-infected cells with a plasmid expressing a HA-tagged ubiquitin. The cell lysates were subsequently subjected to immunoprecipitation with anti-M141 antibody and then Western blots were performed with anti-HA to detect the HA-tagged ubiquitin molecules that would be incorporated into polyubiquitin chains. We could not detect polyubiquitinated forms of pM141 in infected cells even in the presence of MG132 (Fig. 28, top panel) although polyubiquitinated forms of the positive control protein, myc-tagged Cyclin E, were clearly detectable under identical conditions (Fig. 28, bottom panel, lane 4).

To further investigate whether degradation of pM141 requires ubiquitin, we utilized the BALB/c 3T3-derived cell line, ts20, containing a temperature-sensitive defect in the E1 ubiquitin-activating enzyme (26, 204). At the permissive temperature of 35°C the enzyme is fully functional and proteins targeted for degradation are ubiquitinated. At the non-permissive temperature of 39°C the E1 enzyme is severely defective, ubiquitin tagging of proteins is compromised, and proteins that require ubiquitination for degradation accumulate. The feasibility of this approach was demonstrated using p53 as a positive control. As previously reported (26), p53 accumulated to high steady-state levels in ts20 cells incubated at the non-permissive temperature, but not at 35°C when the E1 enzyme is functional (Fig. 29, middle panel). We examined pM141 expression in ts20 cells infected with either WT or RVΔ140 at the permissive and non-permissive

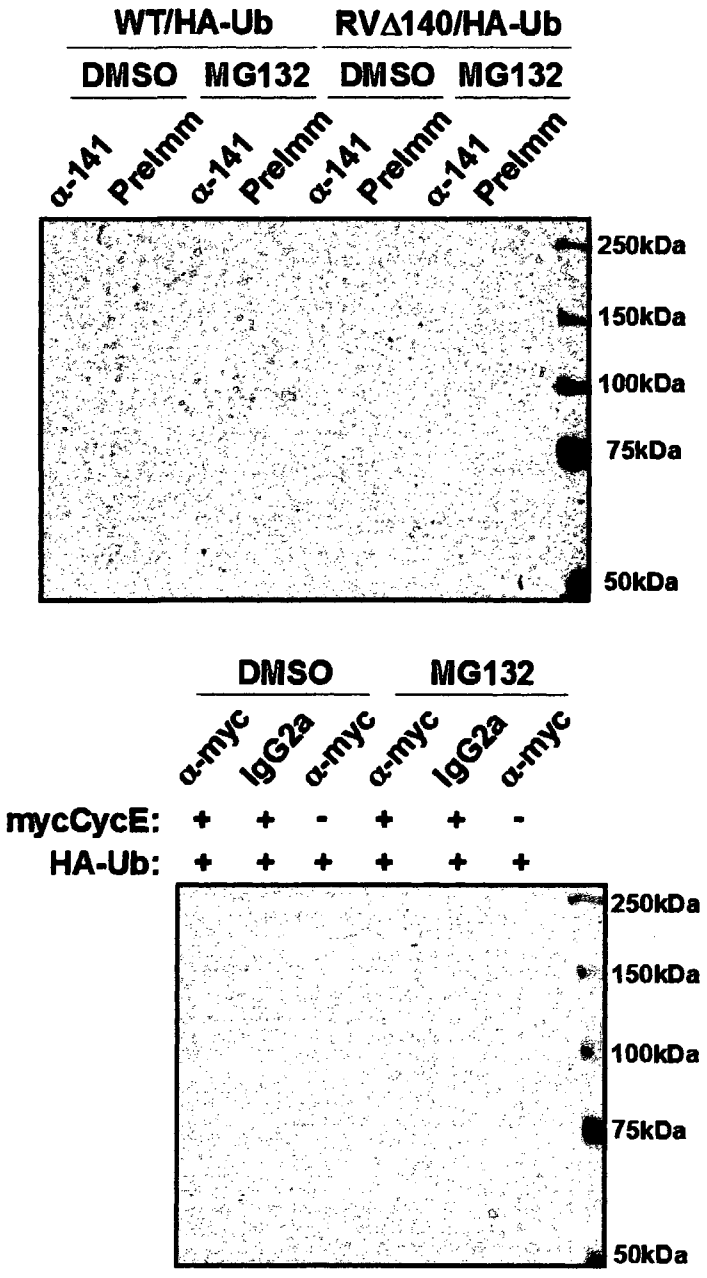

FIG. 28. Immunoprecipitation of pM141 or positive control protein from WT- or RVΔ140-infected cells expressing HA-tagged ubiquitin molecules (HA-Ub). NIH3T3 cells were transfected with HA-Ub alone (top panel) or in conjunction with a myc-epitope tagged Cyclin E construct (mycCycE). Approximately 48hours later the transfected cells were infected with 2 PFU/cell of either WT or RVΔ140 (top panel) or were mock infected (bottom panel). MG132 or vehicle (DMSO) was added to the cells 4 hours post-infection as indicated and the lysates were harvested approximately 18 hours post-treatment. Lysates were subjected to immunoprecipitations with anti-M141 or preimmune serum (preimm) in the top panel and with anti-myc or isotype-matched control antibody (IgG2a) in the bottom. Immunoprecipitates were loaded on SDS-PAGE and western blot was performed with anti-HA antibody (top and bottom panels).

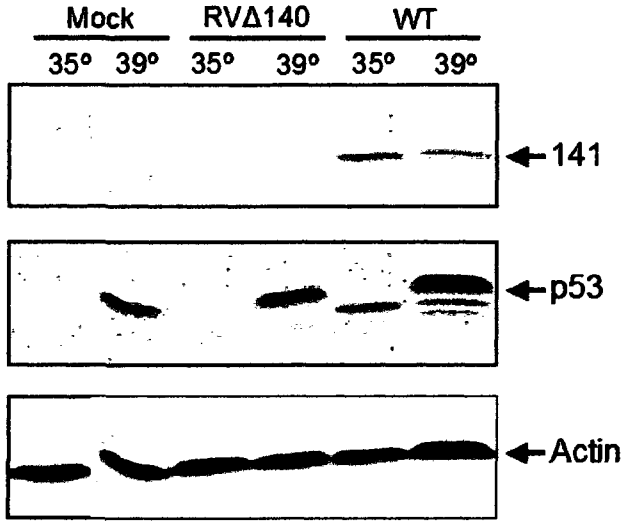

FIG. 29. Steady-state levels of pM141 from WT- or RVΔ140- infected ts20 cells. The ts20 cells were either mock infected or infected with 2 PFU/cell of either WT or RVΔ140 after which cells were incubated at the permissive (35°) or non-permissive (39°) temperatures. After approximately 18 hours the cells were harvested, counted, and normalized based on cell number prior to electrophoresis. Top panel shows expression of pM141 (141) after Western blot analysis. The membrane was reprobed with antibodies against p53 (middle) as a positive control or actin (bottom) as a loading control.

temperatures. M141 protein from WT-infected cells showed no evidence of accumulation at the non-permissive temperature (Fig. 29, top panel). Given the severe reduction of pM141 steady-state levels in RVΔ140-infected fibroblasts and macrophages we were not surprised that pM141 was undetectable in the ts20 cells at the permissive temperature. Importantly, however, we were also unable to detect pM141 at the non-permissive temperature in the absence of pM140. The inability to detect pM141 was not due to a defect in viral gene expression since RVΔ140 replicated to levels similar to WT in this cell line at either temperature (Table 4). The results from Fig. 28 and Fig. 29 demonstrate that degradation of pM141 is ubiquitin-independent.

TABLE 4. WT and RVΔ140 titers in ts20 cells. The ts20 cells were infected at 35°C with 2 PFU/cell of the viruses shown. After infection cells were maintained at 35°C or shifted to 39°C for approximately 18 hours. Supernatants were collected for plaque assays which were performed in NIH3T3 fibroblasts.

Virus	35°C	39°C
WT	9.5×10^3 PFU/ml	1.3×10^4 PFU/ml
RVΔ140	5.5×10^3 PFU/ml	1.55×10^3 PFU/ml

Mapping the degradation signal of pM141. We were also interested in mapping the degradation signal in pM141 in order to assist in defining the ubiquitin-independent mechanism of pM141 degradation. Bioinformatics analysis of the protein using the PEST-FIND program (144, 149) revealed a sequence rich in proline, glutamic acid, serine, and threonine (PEST) located at the C- terminus of M141 (Fig. 3). The PEST hypothesis was proposed by Rogers et al (149) in support of the finding that PEST motifs are found in many proteins that undergo rapid turnover. We wanted to determine if the putative PEST motif was a functional degradation signal and if not, what region of the protein is required for degradation. These experiments required us to generate deletion mutants expressed from transient transfections for the purpose of comparing their rate of degradation to that of full-length pM141. Therefore, we wanted to test whether transiently-transfected pM141 had properties comparable to that of pM141 expressed in the context of a virus infection.

First, we sought to determine if transiently-transfected pM141 was degraded via the proteasome. For this purpose we treated cells with epoxomicin and assessed steady-state levels of pM141 expressed transiently from a plasmid designed to expresses full-length pM141 as a FLAG epitope tag, FLAG-M141. Fibroblasts were transfected with FLAG-M141 and in some cases were then infected with either RVΔ141 or RVΔ140.

Cells were treated with epoxomicin or vehicle after which the steady-state levels of pM141 were compared. As expected, pM141 was not detectable when the cells were infected with RVΔ141 in the absence of FLAG-M141 expression, but pM141 accumulated in the presence of epoxomicin relative to vehicle regardless of whether the transfected cells were infected (Fig. 30). We were able to detect two bands specific to

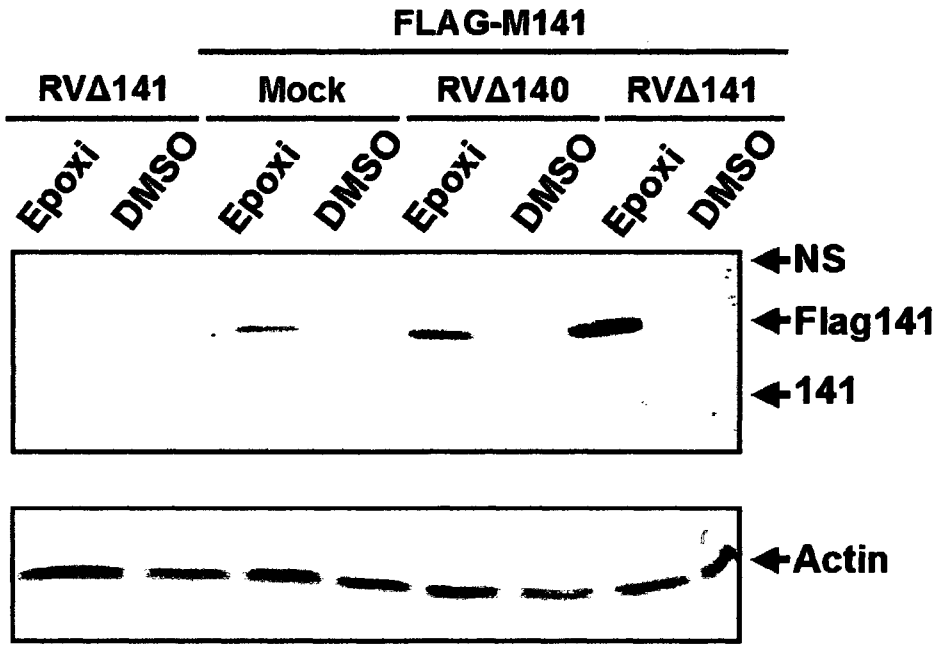

FIG. 30. Steady-state levels of pFLAG-M141 in the presence or absence of epoxomicin. NIH3T3 fibroblasts were either mock infected or infected with 2 PFU/cell of the indicated viruses. Where indicated, the cells were transfected with the FLAG-M141 plasmid. Four hours post-infection the cells were treated with 1 μM epoxomicin for approximately 18 hours. Cells were harvested, counted, and normalized based on cell number prior to loading of lysates for SDS-PAGE. Western blot analysis was performed to detect pM141 (141) or actin. Location of the FLAG epitope-tagged pM141 (FLAG141), non-tagged pM141 (141), and a non-specific band (NS) are shown.

pM141 and a higher molecular weight non-specific band as well. The specific band with a higher molecular weight corresponds to pM141 expressed as FLAG epitope fusion protein driven by the start codon upstream of the FLAG epitope sequence. The lower molecular weight pM141 band most likely corresponds to pM141 without the FLAG epitope expressed from the M141 start codon that is still present in the gene after cloning. This is supported by the fact that the lower molecular weight band is the same size as pM141 from infected cells. Results from Fig. 30 demonstrate that degradation of transiently-expressed pM141 is proteasome-dependent and these results are consistent with the results from pM141 expressed endogenously from infected cells.

We next asked if the half-life of transiently-expressed pM141 is comparable to that of pM141 expressed in infected cells. Therefore, we used cycloheximide to determine the turnover rate of transiently-expressed pFLAG-M141. Fibroblasts were transiently transfected with FLAG-M141, treated with cycloheximide, cell lysates were harvested at 2, 4, 6, and 8 hours post-treatment, and then Western blot analysis was performed. We found that pM141 expressed transiently from the FLAG-M141 construct was clearly detectable at each of the time points tested (Fig. 31A) and had a half-life of approximately 4 hours (Fig. 31B) despite the absence of pM140 expression. This finding was surprising since pM141 from RVΔ140-infected cells was below the limit of detection even at 1 hour post-cycloheximide treatment (data not shown). We considered the possibility that the stability of transfected pM141 would be altered in the presence of viral infection. We performed similar experiments with transfected FLAG-M141 except that the cells expressing the construct were also infected with RVΔ140 so that we could assess the stability of transfected pM141 in the context of infection, while still in the

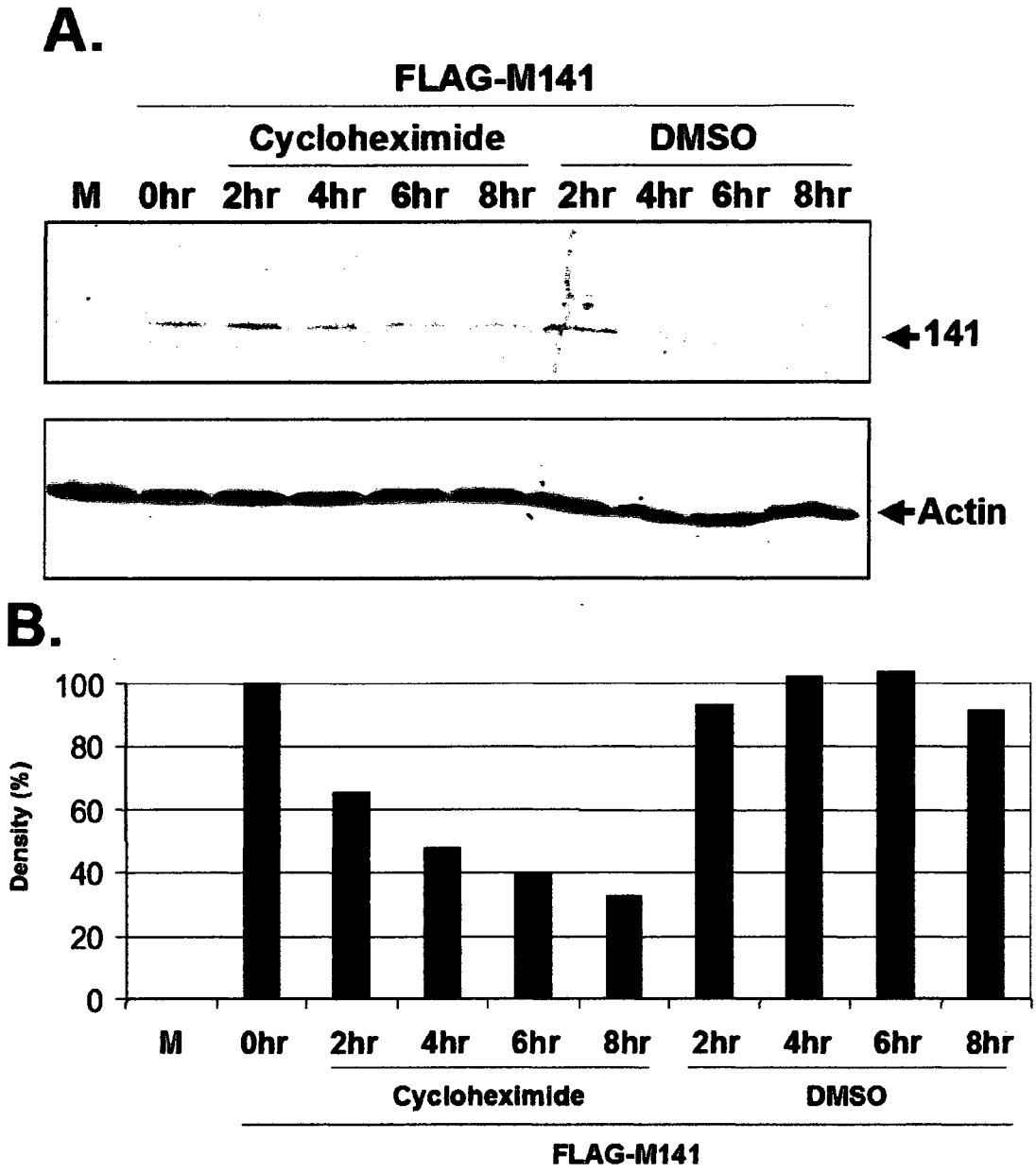

FIG. 31. Stability of transiently-expressed pFLAG-M141 from cycloheximide-treated cells. NIH3T3 fibroblasts were either mock (M) transfected or were transfected with FLAG-M141. Approximately 72 hours post-transfection the cells were treated with 100 μg/ml cycloheximide or vehicle (DMSO) and were harvested at the indicated times post-treatment. Prior to SDS-PAGE cells were counted and normalized to cell numbers. A. Western blot analysis to detect pM141 (141) or Actin which served as a loading control. B. Quantitation of pM141 Western blot shown in A after normalizing to Actin. Amount of pM141 is expressed as a percentage to the density of the protein before drug was added.

absence of pM140. As before, pM141 from RVΔ140-infected cells was clearly visible as long as 8 hours post-treatment (Fig. 32A). However, the half-life of the protein was determined to be greater than 8 hours (Fig. 32B). Therefore, we are unable to map the degradation signal of pM141 by transiently expressing deletion mutants.

Regulation of pM141 degradation by pM140. We had previously demonstrated the importance of pM140 expression on the stability of pM141 in infected cells (61) and we wanted to determine the extent to which pM141 stability was dependent on pM140. To answer this question NIH3T3 cells were transfected with increasing amounts of a plasmid that expressed full-length pM140 as a FLAG epitope fusion protein, FLAG140FL. The transfected cells were subsequently infected with RVΔ140 and the steady-state levels of pM141 were assessed by Western blot analysis of cell lysates. As shown in Fig. 33, pM141 stability was dependent on the concentration of pM140 expressed in the infected cells. Steady-state levels of pM141 increased with increasing concentrations of FLAG140FL plasmid. Steady-state levels of pM141 were barely above the limit of detection in RVΔ140-infected cells when pFLAG140FL was not expressed (Fig. 33A), but the relative amount of pM141 increased with increasing amount of M140 transfected into the cells (Fig. 33B).

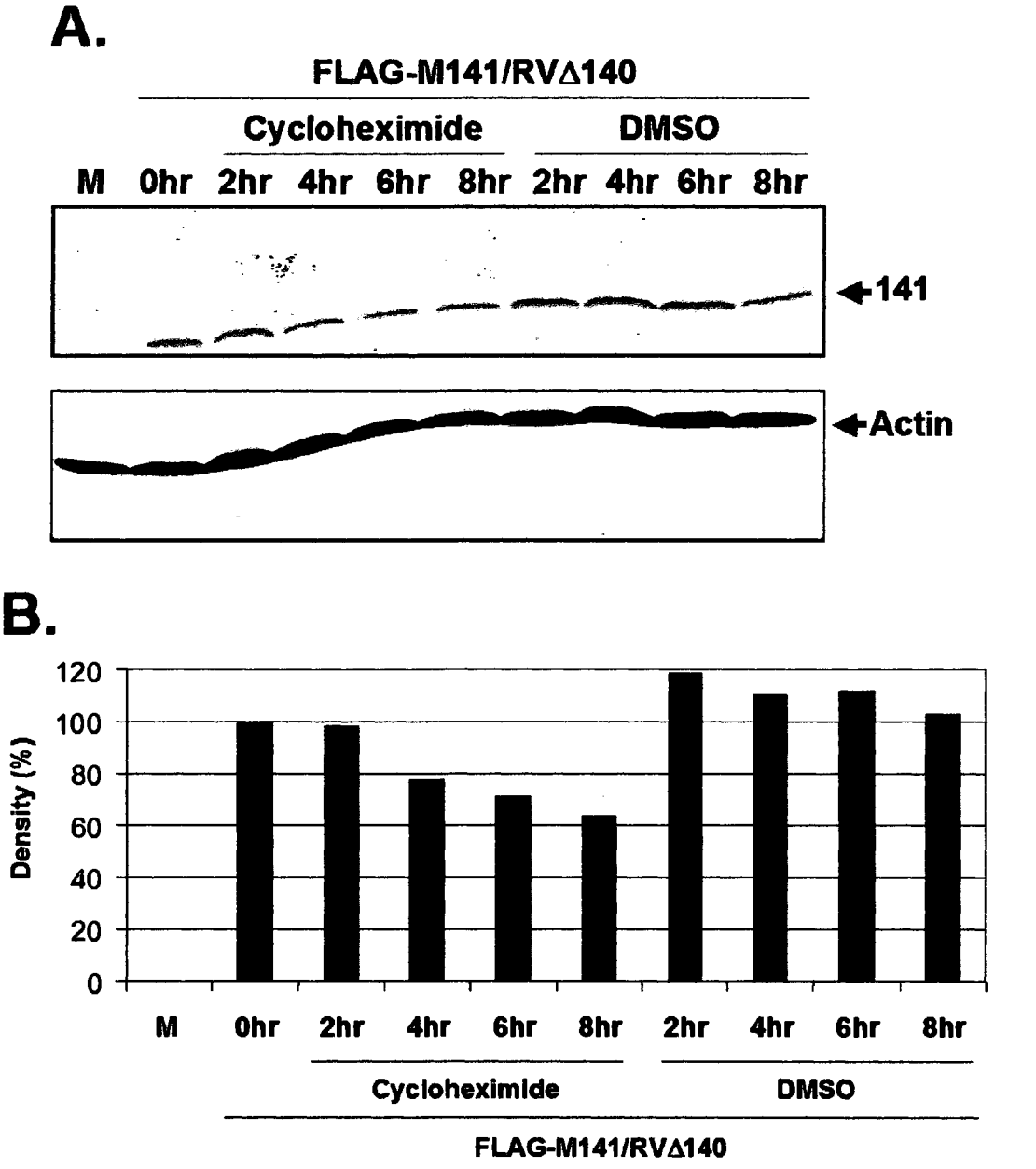

FIG. 32. Stability of pFLAG-M141 in RVΔ140-infected, cycloheximide-treated fibroblasts. NIH3T3 fibroblasts were transfected with FLAG-M141 or were mock (M) transfected and then approximately 48 hours post-transfection the cells were infected with 2 PFU/cell of RVΔ140. Eighteen hours later the cells were incubated with 100 μg/ml cycloheximide or vehicle (DMSO). Cell were harvested at the indicated times post-treatment by counting and normalizing to cell number. A. Western blot analysis of lysates from SDS-PAGE to detect either pM141 (top) or Actin as loading control (bottom). B. The relative amount of pM141 was normalized to actin and quantitated. M141 protein levels are shown as percent density relative to density prior to drug treatment.

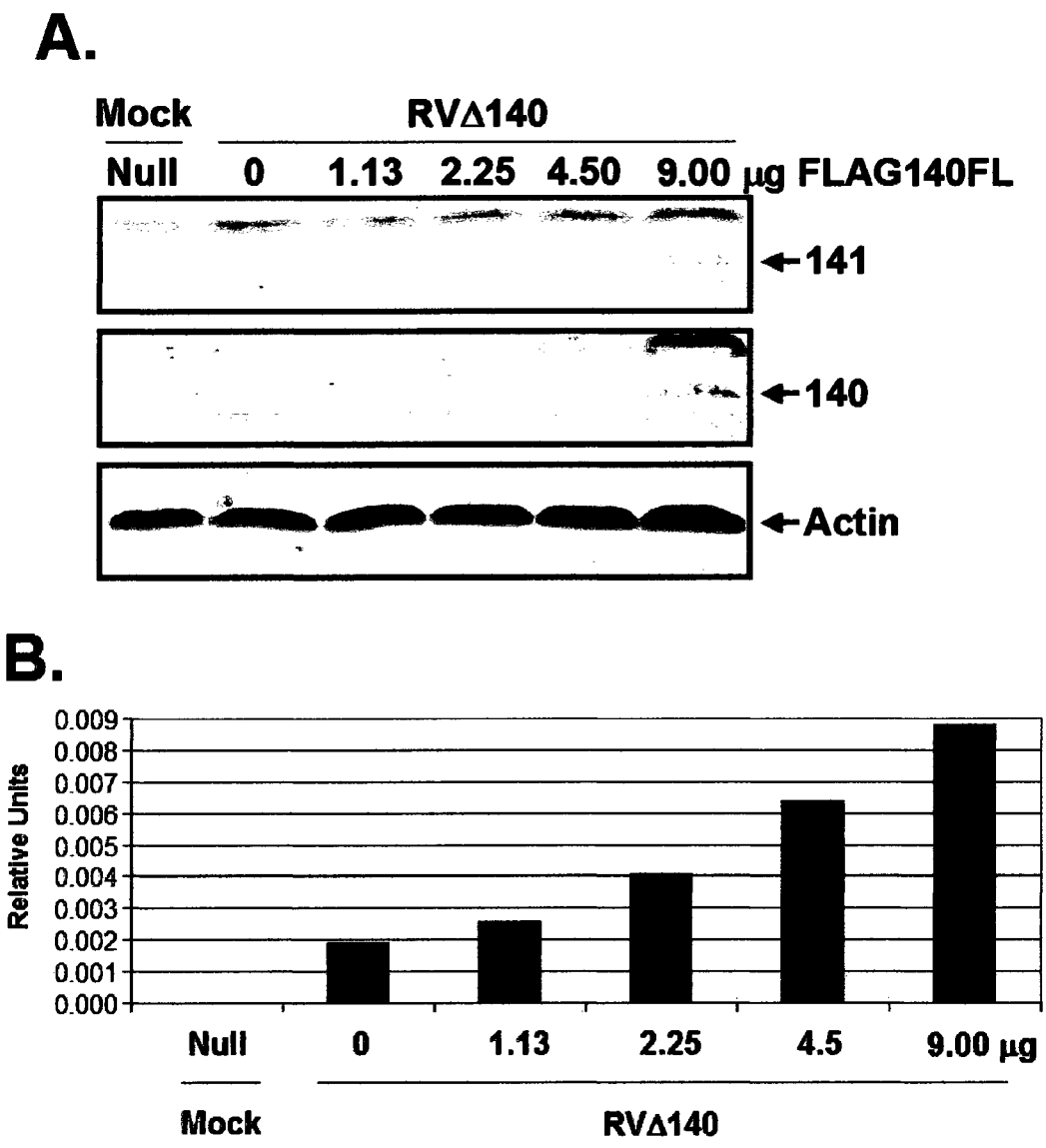

FIG. 33. Steady-state levels of pM141 in the presence of increasing amounts of pFLAG140FL. NIH3T3 fibroblasts were transfected with 0, 1.13, 2.25, 4.50, or 9.00 μg of FLAG140FL as indicated or were not transfected (Null). Approximately 48 hours later the transfected cells were infected with 2 PFU/cell of RVΔ140. Cells were harvested, counted, and normalized to cell number approximately 18 hours post-infection. A. Western blot analysis was performed after SDS-PAGE of lysates. The blot was probed with antibodies to detect pM141 (top) or Actin (bottom) as a loading control after which the blot was reprobed with anti-M140 antibodies (middle). B. M141 protein levels were normalized to levels of Actin. The quantitation is displayed in relative units.

Several pieces of evidence lead us to hypothesize that direct complexing of pM140 with pM141 was responsible for the increased stability of pM141 in WT versus RVΔ140-infected cells. First, we have previously demonstrated that pM140 and pM141 are found in complex with each other and in a larger complex (82). Furthermore, M140 and M141 are coordinately expressed at the transcript and protein levels (59, 61). Finally, pM140 protects pM141 from degradation in a concentration-dependent manner as shown above. To test this hypothesis we took advantage of two of the pM140 mutants, p140DSM4/TOPO and p140DSM3/TOPO that exhibited significantly reduced binding to pM141 from the GST pulldown assays (Fig. 18). The mutant constructs were subcloned so that they would be expressed as FLAG-epitope-tagged proteins (Fig. 34) and then each of the plasmids was individually titrated into RVΔ140-infected fibroblasts to determine whether they retained an ability to stabilize the pM141 protein. Although expression of

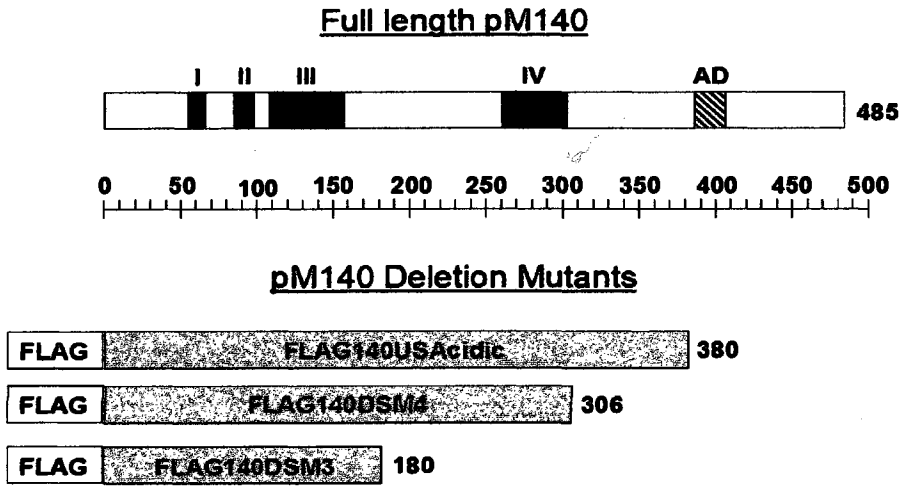

FIG. 34. Diagram of the panel of pM140 C-terminal deletion mutants screened for an ability to stabilize pM141. Full-length pM140 is shown at the top along with the location of the US22 Motifs (filled blocks) and the acidic domain (AD). The ruler is shown for reference with each tick mark corresponding to 10 amino acids. Each pM140 C-terminal deletion mutant is shown drawn to scale with the location of the FLAG epitope tag (not drawn to scale).

each of the truncated proteins increased with increasing amounts of transfected plasmid, neither one of the mutants was able to stabilize pM141 (Fig. 35). These data were consistent with our hypothesis that pM141 stability is conferred by pM140 binding. The inability to stabilize pM141 was not due to decreased expression of the mutant proteins since each of the truncated pM140 products was expressed to a higher level than pFLAG140FL when a comparable quantity of plasmid was used for transfection. The viral protein, m142 (pm142), was used as a control to demonstrate that all transfected cells were infected at a comparable level since pm142 levels are not influenced by pM140 (unpublished data).

Given these results we next asked whether the pM140 truncation mutants were able to complex with pM141 in transiently-transfected cells since the mutants had only previously been tested in *in vitro* assays. To perform these experiments we transfected each of the mutants or full-length pM140 into RVΔ140-infected fibroblasts and then immunoprecipitated the cell lysates with anti-M141 antibody. The immunoprecipitates were then subjected to SDS-PAGE and western blotting to detect the FLAG epitope expressed on each of the constructs (Fig. 36). Interestingly, we found the even though the truncated proteins had significantly reduced binding in the *in vitro* assay (Fig. 18), each of the mutants was immunoprecipitated with pM141 to levels comparable to the full-length pM140 product (Fig. 36). Since pFLAG140DSM3 and pFLAG140DSM4 retained an ability to complex with pM141 (Fig. 36), but could no longer stabilize the protein (Fig. 35), we conclude that direct complexing is insufficient to protect pM141 from degradation.

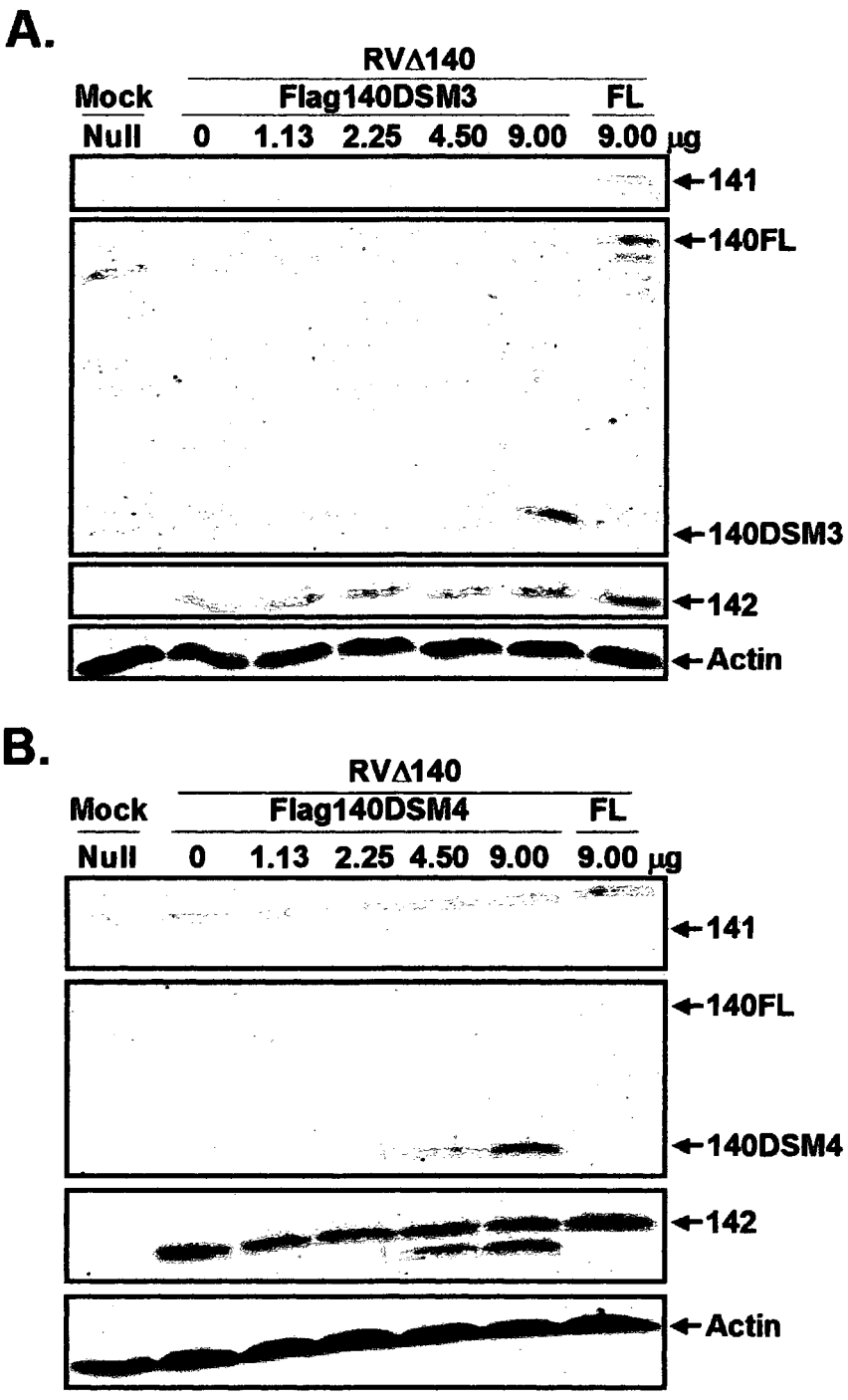

FIG. 35. Steady-state levels of pM141 in the presence of increasing amounts of pFLAG140DSM3 and pFLAG140DSM4. NIH3T3 fibroblasts were either transfected with transfection reagent in the absence of plasmid (null) or were transfected with 0, 1.13, 2.25, 4.50, or 9.00 μg of FLAG140DSM3 (A) or FLAG140DSM4 (B) and 9.00 μg of FLAG140FL as a positive control as indicated. Approximately 48 hours later the transfected cells were infected with 2 PFU/cell of RVΔ140. Cells were harvested, counted, and normalized to cell number approximately 18 hours post-infection. Shown is western blot analysis of lysates after SDS-PAGE. The blot was probed with antibodies to detect pM141 (top) and actin as a loading control (bottom) after which the blot was reprobed with either anti-M140 antibodies or anti-m142 antibodies as indicated.

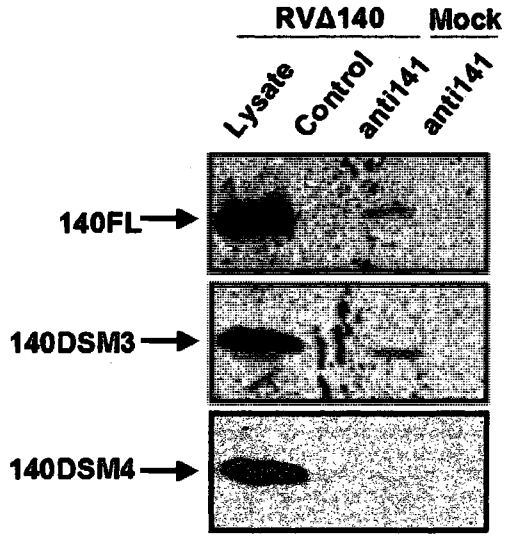

FIG. 36. Anti-M141 immunoprecipitations of RVΔ140-infected cell lysates transiently-expressing pFLAG140FL (top), pFLAG140DS3 (middle), or pFLAG140DSM4 (bottom). NIH3T3 cells were transfected with either FLAG140FL, FLAG140DSM3, or FLAG140DSM4. Approximately 48hours later the cells were infected with 2 PFU/cell of RVΔ140 or were mock infected where indicated. Cell lysates were harvested approximately 18hours later and the lysates were either loaded directly on SDS-PAGE (lysate) or were first subjected to immunoprecipitations with anti-M141 or preimmune sera as shown. Displayed is the western blot probed with anti-FLAG antibody to detect the FLAG epitope fused to each of the constructs.

The results from Fig. 35 revealed that a region proximal to the C terminus of pM140 was strictly required to protect pM141 from degradation. We wanted to map the boundary of pM140 are required to protect pM141 from degradation. Therefore, we tested the adjacent mutant, 140USAcidic/HisC, in our stability assay after the construct had been subcloned as a FLAG-epitope fusion, pFLAG140USAcidic (Fig. 37). The mutant was titrated into NIH3T3 cells using increasing amounts of the FLAG140USAcidic-expressing plasmid after which the cells were subsequently infected with RVΔ140. Steady-state levels of pM141 were assessed by Western blot analysis of cell lysates. We found that the mutant was expressed to levels comparable to the full-

length protein. As the levels of pFLAG140USAcidic increased so did the levels of pM141 expressed from the infected cells (Fig. 37A). Upon quantitation of pM141 levels after normalization to the loading control (actin) it was clearly evident that pFLAG140USAcidic was able to stabilize pM141 to levels similar to the full-length protein (Fig 37B). These results demonstrate that the region of pM140 that is required to stabilize pM141 lies within amino acids 306-380.

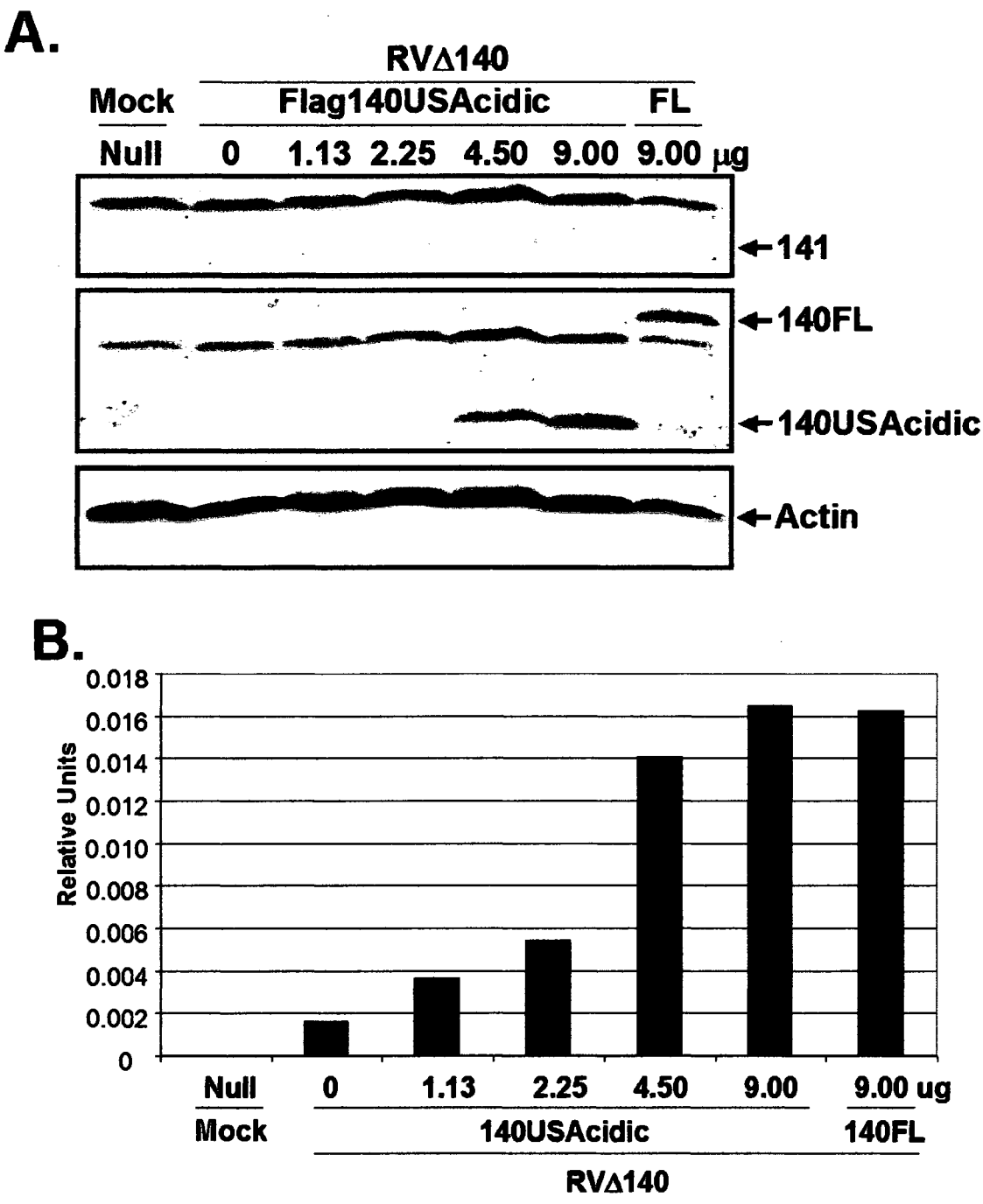

FIG. 37. Steady-state levels of pM141 in the presence of increasing amounts of pFLAG140USAcidic. NIH3T3 cells were transfected with either transfection reagent in the absence of plasmid (null), 9.00 μg of FLAG140FL (140FL), or with 0, 1.13, 2.25, 4.50, or 9.00 μg of FLAG140USAcidic (140USAcidic). Approximately 48hours later the cells were infected with 2 PFU/cell of RVΔ140 where indicated and then approximately 18hours later the cells were harvested, counted, and normalized to cell number. A. Western blot analysis of lysates subjected to SDS-PAGE after the blot was probed for pM141 (top) and actin (bottom). The blot was subsequently reprobed to detect pM140 (middle panel). B. M141 protein levels were normalized to levels of actin and the quantitation is shown in relative units.

Discussion

Degradation of pM141 is enhanced in the absence of pM140 (61) suggesting that appropriate levels of pM141 are required for proper protein function. We have now demonstrated at least one mechanism by which pM141 is degraded. The data indicate that pM141 is degraded via the proteasomal pathway in two independent cell types.

It is possible that pM141 is degraded by other mechanisms in addition to the proteasome. Although we have demonstrated that pM141 degradation is proteasome-dependent, pM141 levels in the presence of proteasome inhibitors from RVΔ140 infected cells never reached levels like those found in WT-infected cells regardless of whether proteasome inhibitor was added. The most likely explanation for these findings is that pharmacological inhibition of the proteasomal activity is incomplete. Alternately, pM141 may also be degraded by a second mechanism. We did not examine alternate mechanisms of protein degradation, but it would be of interest to see if pM141 is also degraded by lysosomal enzymes or by autophagy.

We have demonstrated that proteasomal degradation of pM141 is ubiquitin-independent. The most well-studied mechanism by which proteins are targeted to the proteasome is by ubiquitin tagging. However, numerous cellular (69, 77, 128) and viral proteins (109, 187, 202) have been shown to be degraded by the proteasomes in an ubiquitin-independent fashion. Although ubiquitin-independent mechanisms are less well understand at this time, it appears that proteins containing unstructured regions may be directed to the proteasome (4, 77). Bioinformatics analysis of pM141 did reveal an unstructured region in the form of a PEST motif. We were unable to determine if the PEST domain is required to target pM141 for degradation. In order to do this we would

need to compare half-lives of pM141 constructs that contain or are deleted of the PEST motif and are expressed from transiently transfected cells. Unfortunately, transiently-transfected full-length pM141 is significantly more stable than pM141 expressed from infected cells despite the fact that degradation of transiently-transfected pM141 is also proteasome-mediated. This was the case even when transiently-transfected M141 was expressed from its native promoter and the pM141 construct was expressed in the absence or presence of infection.

We have found that direct complexing between pM140 and pM141 is not sufficient to stabilize pM141. We previously found that in addition to forming a larger complex with the MCMV pM139, a separate complex composed of only pM140 and pM141 is found in infected cells (82). Furthermore, we have shown that the half-life of pM141 is reduced in the absence of pM140 while the half-life is similar to WT levels in the absence of pM139 (61). Based on this evidence we hypothesized that binding of pM140 to pM141 restricted access to a degradation signal or otherwise stabilized the protein. In our current study, we found that although pM140 stabilizes pM141 in a concentration-dependent fashion, complexing between the proteins is not sufficient to protect pM141 from degradation. These results imply that there may a third binding partner that is recruited to the complex through pM140 and this protein stabilizes pM141 directly. At present, we have identified two pM140 binding partners, MCMV pM139 and an unknown protein of 98kDa. Our previous data implies that pM139 is not able to stabilize pM141 since the half-life of pM141 is similar in the presence or absence of pM139 (61). Several experiments that are ongoing would allow us to test the hypothesis that an additional pM140 binding partner is required to stabilize pM141. First, we are in

the process of trying to identify the 98kDa protein. In addition, we are attempting to identify other binding partners of pM140.

Another explanation of these results is that stabilization of pM141 is dependent on the conformation of pM140. In this scenario, the pM140 mutants that retain an ability to bind to pM141 might not be able to fold in a way that allows the pM141 degradation signal to be masked. There is additional evidence that this region of pM140 may be important for proper conformation. This region was also found to contain the interaction domain of pM140 required for complexing with pM141 using *in vitro* translated pM140 with GST pulldowns of GST141FL (see chapter III). Interestingly, we found that the same pM140 deletion mutants that displayed significantly reduced binding to pM141 using *in vitro* assays (Chapter III) were able to bind pM141 to levels comparable to the full-length protein when the constructs were co-expressed in transiently-transfected cells (Chapter V). These results imply that mutants deleted of this region can only reach the proper conformation for pM141 binding under certain conditions (i.e. in the presence of intact cells). Similarly, it is possible that mutants deleted of this region may not be able to acquire the proper conformation to stabilize pM141 and that additional amino acids are required for this function.

We have determined the specific region of pM140 required to stabilize pM141. Interestingly, this region, between amino acids 306 and 380, does not contain any of the US22 motifs or the acidic domain of M140. Furthermore, this region of the protein does not share any significant sequence homology to the HCMV homologue, US23.

M140 has been shown to regulate the degradation of other MCMV proteins including the major capsid protein (MCP) and the tegument protein, M25 (60). Similar to

the results seen with pM141, steady-state levels of MCP and M25 are significantly reduced in RVΔ140-infected cells relative to that of WT-infected cells and the half-life of the MCP is reduced in the absence of pM140 (60). However, unlike our results with pM141, regulation of MCP and M25 proteins levels by pM140 have been demonstrated to be cell type specific. Levels of MCP and M25 protein are reduced specifically in macrophage cells, but not in fibroblasts. Interestingly, we have demonstrated that proteasomal degradation of pM141 is cell type independent. Since pM140 has a function in macrophage tropism it seems likely that regulation of the MCP and M25 protein levels in macrophages may be related to the specific function of the protein while regulation of pM141 may be a more general function of pM140.

CHAPTER VI

CONCLUSIONS

The M140 and M141 proteins form a stable complex inside infected cells (82). We wanted to determine if the proteins function in macrophage tropism as a complex or as individual proteins. Thus, we attempted to map interaction domains of the proteins with the long term goal of generating MCMV with an interaction-defective allele. We were unable to map the interaction domain(s) of pM141 using a strategy of *in vitro* expression of the protein. We found that the protein, expressed *in vitro*, appeared to be globular in nature and bound non-specifically to pM140 and to our negative controls. Since we have successfully demonstrated specific complexing between pM141 and pM140 from transiently-expressed proteins, we will use a strategy of transient expression of the proteins in cultured cells for future experiments to map the interaction domain(s) of pM141.

In the present study we were able to identify an interaction domain at the extreme N terminus of pM140 expressed *in vitro*. The amino acids in this region do not contain any of the US22 motifs and exhibit a fairly even distribution of polar and nonpolar residues. In future studies we will determine if the identified region of pM140 is required for complexing with pM141 when the proteins are expressed transiently in cultured cells. If the region is strictly required for complexing of proteins expressed under native conditions then we will generate a MCMV mutant with a pM140 interaction-defective allele to determine if pM140/pM141 complexing is required for optimal viral replication inside cultured macrophages or macrophage-dense organs from infected mice.

The M141 protein is localized diffusely throughout the cytoplasm and, to a lesser extent, the nucleus while pM140 is localized predominantly to the nucleus (61, 82). However, when the proteins are co-expressed they co-localize to a perinuclear region adjacent to aggresomes (60, 82). We hypothesized that pM141 contains a NLS and NES and relocalizes pM140 from the nucleus to the perinuclear locale and we wanted to determine where the protein functions. Thus, we wanted to map the localization signals of pM141 with the long term goal of generating MCMV with alleles defective in M141 localization domains. Using a strategy of increasing deletions at each terminus of pM141, we were unable to determine if the protein contains a functional NLS or NES. Future experiments to map the localization domain(s) of pM141 will examine specific protein subdomains fused to a neutral protein that contains no localization signals and is also small enough to enter the nucleus by passive diffusion such as GFP. The localization of each fusion protein will be assessed to determine if the protein domain contains a specific subcellular localization signal.

In the absence of pM140 steady-state levels of pM141 are significantly decreased and the half-life of pM141 is reduced from approximately 2 hours to 1 hour (61). We wanted to determine the mechanism of pM141 degradation and assess the contribution of pM140 in protecting the protein from degradation with the long term goal of understanding how regulation of pM141 by pM140 contributes to the function of the proteins. In the present study we determined that pM141 degradation is proteasome-dependent, but ubiquitin-independent. Due to the fact that transiently-expressed pM141 is significantly more stable than pM141 expressed from infected cells, we were unable to map the degradation signal of the protein using a strategy of deletion analysis with

pM141 constructs that were designed to express proteins transiently in cultured cells. However, we were able to determine that stability of pM141 is dependent on the concentration of pM140. We were able to map the region in pM140 required to stabilize pM141. Interestingly, the region does not contain US22 motifis or the pM140 acidic domain and it does not overlap with a pM141 interaction domain demonstrating that direct complexing between the proteins is not sufficient to protect pM141 from degradation. These results suggest a model (Fig. 38) where pM141 can be targeted for degradation even when pM140/pM141 complexing can occur. However, under native conditions pM140 recruits a third protein of unknown origin to the complex and this protein prevents rapid degradation of pM141. In future studies we will map the degradation signal of pM141 by generating mutations in the M141 gene in mutant MCMV. We will also compare viral titers in infected cultured macrophages and macrophage-dense organs from infected mice of WT MCMV, RVΔ140, and a MCMV mutant expressing pM140 that is unable to stabilize pM141.

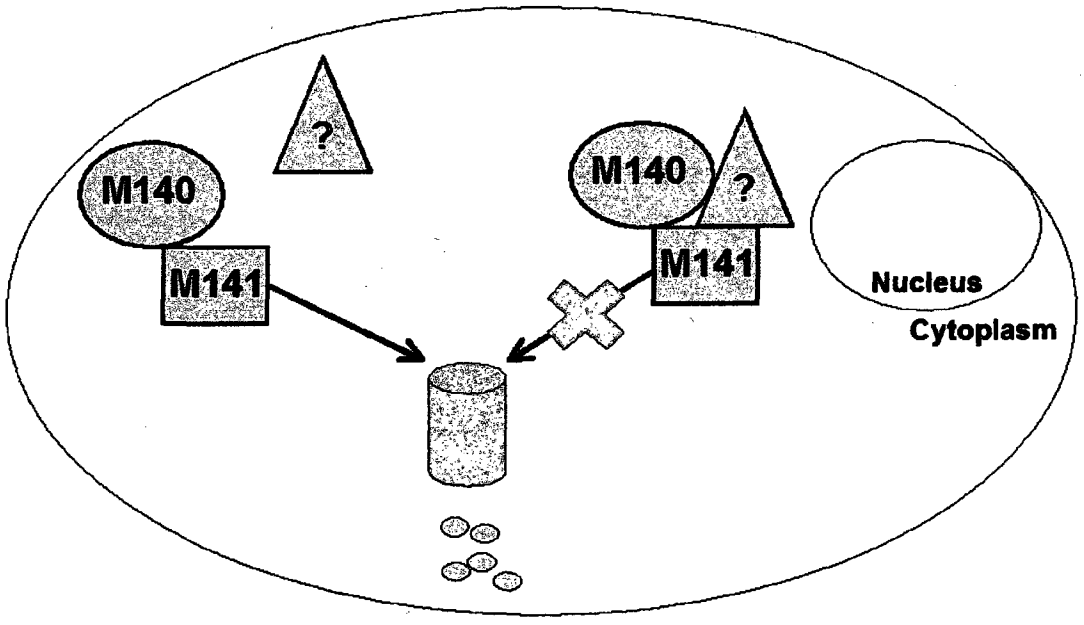

FIG. 38. Model of regulation of pM141 stability by pM140. The M141 protein can be targeted for degradation by the proteasome (blue cylinder) under circumstances where pM140 and pM141 can form a complex (left). However, inside WT infected cells pM140 recruits an, as yet unidentified, third protein to the pM140/pM141 complex that is able to directly stabilize pM141 and prevents its rapid degradation (right). The location of the nucleus and cytoplasm are shown.

REFERENCES

1. **Adamo, J. E., J. Schroer, and T. Shenk.** 2004. Human cytomegalovirus TRS1 protein is required for efficient assembly of DNA-containing capsids. J. Virol. **78:**10221-10229.

2. **Akopian, T. N., A. F. Kisselev, and A. L. Goldberg.** 1997. Processive degradation of proteins and other catalytic properties of the proteasome from Thermoplasma acidophilum. J. Biol. Chem. **272:**1791-1798.

3. **Alberts, B.** 1998. The cell as a collection of protein machines: preparing the next generation of molecular biologists. Cell **92:**291-294.

4. **Asher, G., N. Reuven, and Y. Shaul.** 2006. 20S proteasomes and protein degradation "by default". Bioessays **28:**844-849.

5. **Asher, G., and Y. Shaul.** 2006. Ubiquitin-independent degradation: lessons from the p53 model. Isr. Med. Assoc. J. **8:**229-232.

6. **Baboshina, O. V., and A. L. Haas.** 1996. Novel multiubiquitin chain linkages catalyzed by the conjugating enzymes E2EPF and RAD6 are recognized by 26 S proteasome subunit 5. J. Biol. Chem. **271:**2823-2831.

7. **Bayliss, R., H. M. Kent, A. H. Corbett, and M. Stewart.** 2000. Crystallization and initial X-ray diffraction characterization of complexes of FxFG nucleoporin repeats with nuclear transport factors. J. Struct. Biol. **131:**240-247.

8. **Bayliss, R., T. Littlewood, and M. Stewart.** 2000. Structural basis for the interaction between FxFG nucleoporin repeats and importin-beta in nuclear trafficking. Cell **102:**99-108.

9. **Bayliss, R., T. Littlewood, L. A. Strawn, S. R. Wente, and M. Stewart.** 2002. GLFG and FxFG nucleoporins bind to overlapping sites on importin-beta. J. Biol. Chem. **277:**50597-50606.

10. **Bayliss, R., K. Ribbeck, D. Akin, H. M. Kent, C. M. Feldherr, D. Gorlich, and M. Stewart.** 1999. Interaction between NTF2 and xFxFG-containing nucleoporins is required to mediate nuclear import of RanGDP. J. Mol. Biol. **293:**579-593.

11. **Belizario, J. E., J. Alves, M. Garay-Malpartida, and J. M. Occhiucci.** 2008. Coupling caspase cleavage and proteasomal degradation of proteins carrying PEST motif. Curr. Protein Pept. Sci. **9:**210-220.

12. **Bodaghi, B., O. Goureau, D. Zipeto, L. Laurent, J. L. Virelizier, and S. Michelson.** 1999. Role of IFN-gamma-induced indoleamine 2,3 dioxygenase and

inducible nitric oxide synthase in the replication of human cytomegalovirus in retinal pigment epithelial cells. J. Immunol. **162:**957-964.

13. **Boehme, K. W., and T. Compton.** 2006. Virus entry and activation of innate immunity, p. 111-130. *In* M. Reddehase (ed.), Cytomegaloviruses. Caister Academic Press.

14. **Borissenko, L., and M. Groll.** 2007. Diversity of proteasomal missions: fine tuning of the immune response. Biol. Chem. **388:**947-955.

15. **Boutet, S. C., M. H. Disatnik, L. S. Chan, K. Iori, and T. A. Rando.** 2007. Regulation of Pax3 by proteasomal degradation of monoubiquitinated protein in skeletal muscle progenitors. Cell **130:**349-362.

16. **Budt, M., L. Niederstadt, R. S. Valchanova, S. Jonjic, and W. Brune.** 2009. Specific inhibition of the PKR-mediated antiviral response by the murine cytomegalovirus proteins m142 and m143. J. Virol. **83:**1260-1270.

17. **Cadwell, K., and L. Coscoy.** 2005. Ubiquitination on nonlysine residues by a viral E3 ubiquitin ligase. Science **309:**127-130.

18. **Campbell, A. E.** 1999. Murine cytomegalovirus, p. 447-466. *In* R. A. a. I. Chen (ed.), Persistent viral infections. John Wiley & Sons Ltd.

19. **Campbell, A. E., J. S. Slater, and W. S. Futch.** 1989. Murine cytomegalovirus-induced suppression of antigen-specific cytotoxic T lymphocyte maturation. Virology **173:**268-275.

20. **Camus, S., S. Menendez, C. F. Cheok, L. F. Stevenson, S. Lain, and D. P. Lane.** 2007. Ubiquitin-independent degradation of p53 mediated by high-risk human papillomavirus protein E6. Oncogene **26:**4059-4070.

21. **Chee, M. S., A. T. Bankier, S. Beck, R. Bohni, C. M. Brown, R. Cerny, T. Horsnell, C. A. Hutchison, 3rd, T. Kouzarides, J. A. Martignetti, and et al.** 1990. Analysis of the protein-coding content of the sequence of human cytomegalovirus strain AD169. Curr. Top. Microbiol. Immunol. **154:**125-169.

22. **Child, S. J., and A. P. Geballe.** 2009. Binding and relocalization of protein kinase R by murine cytomegalovirus. J. Virol. **83:**1790-1799.

23. **Child, S. J., M. Hakki, K. L. De Niro, and A. P. Geballe.** 2004. Evasion of cellular antiviral responses by human cytomegalovirus TRS1 and IRS1. J. Virol. **78:**197-205.

24. **Child, S. J., L. K. Hanson, C. E. Brown, D. M. Janzen, and A. P. Geballe.** 2006. Double-stranded RNA binding by a heterodimeric complex of murine cytomegalovirus m142 and m143 proteins. J. Virol. **80:**10173-10180.

25. **Chin, K. C., and P. Cresswell.** 2001. Viperin (cig5), an IFN-inducible antiviral protein directly induced by human cytomegalovirus. Proc. Natl. Acad. Sci. USA **98:**15125-15130.

26. **Chowdary, D. R., J. J. Dermody, K. K. Jha, and H. L. Ozer.** 1994. Accumulation of p53 in a mutant cell line defective in the ubiquitin pathway. Mol. Cell Biol. **14:**1997-2003.

27. **Ciechanover, A.** 2006. Intracellular protein degradation: from a vague idea thru the lysosome and the ubiquitin-proteasome system and onto human diseases and drug targeting. Hematology Am. Soc. Hematol. Educ. Program:1-12, 505-506.

28. **Clurman, B. E., R. J. Sheaff, K. Thress, M. Groudine, and J. M. Roberts.** 1996. Turnover of cyclin E by the ubiquitin-proteasome pathway is regulated by cdk2 binding and cyclin phosphorylation. Genes Dev. **10:**1979-1990.

29. **Colugnati, F. A., S. A. Staras, S. C. Dollard, and M. J. Cannon.** 2007. Incidence of cytomegalovirus infection among the general population and pregnant women in the United States. BMC Infect. Dis. **7:**71-81.

30. **Compton, T., D. M. Nowlin, and N. R. Cooper.** 1993. Initiation of human cytomegalovirus infection requires initial interaction with cell surface heparan sulfate. Virology **193:**834-841.

31. **Corboy, M. J., P. J. Thomas, and W. C. Wigley.** 2005. Aggresome formation. Methods Mol. Biol. **301:**305-327.

32. **Cronshaw, J. M., A. N. Krutchinsky, W. Zhang, B. T. Chait, and M. J. Matunis.** 2002. Proteomic analysis of the mammalian nuclear pore complex. J. Cell Biol. **158:**915-927.

33. **D'Angelo, M. A., and M. W. Hetzer.** 2008. Structure, dynamics and function of nuclear pore complexes. Trends Cell Biol. **18:**456-466.

34. **Dalod, M., T. Hamilton, R. Salomon, T. P. Salazar-Mather, S. C. Henry, J. D. Hamilton, and C. A. Biron.** 2003. Dendritic cell responses to early murine cytomegalovirus infection: subset functional specialization and differential regulation by interferon alpha/beta. J. Exp. Med. **197:**885-898.

35. **Dankner, W. M., J. A. McCutchan, D. D. Richman, K. Hirata, and S. A. Spector.** 1990. Localization of human cytomegalovirus in peripheral blood leukocytes by in situ hybridization. J. Infect. Dis. **161:**31-36.

36. **Delannoy, A. S., D. Hober, A. Bouzidi, and P. Wattre.** 1999. Role of interferon alpha (IFN-alpha) and interferon gamma (IFN-gamma) in the control of the infection of monocyte-like cells with human cytomegalovirus (HCMV). Microbiol. Immunol. **43:**1087-1096.

37. **Dunn, W., C. Chou, H. Li, R. Hai, D. Patterson, V. Stolc, H. Zhu, and F. Liu.** 2003. Functional profiling of a human cytomegalovirus genome. Proc. Natl. Acad. Sci. USA **100:**14223-14228.

38. **Ebeling, A., G. M. Keil, E. Knust, and U. H. Koszinowski.** 1983. Molecular cloning and physical mapping of murine cytomegalovirus DNA. J. Virol. **47:**421-433.

39. **Efstathiou, S., G. L. Lawrence, C. M. Brown, and B. G. Barrell.** 1992. Identification of homologues to the human cytomegalovirus US22 gene family in human herpesvirus 6. J. Gen. Virol. **73 (Pt 7):**1661-1671.

40. **Eickmann, M., D. Gicklhorn, and K. Radsak.** 2006. Glycoprotein trafficking in virion morphogenesis, p. 245-264. *In* M. J. Reddehase (ed.), Cytomegalovirus. Lippincott-Raven, Philadelphia, PA.

41. **Einhorn, L., and A. Ost.** 1984. Cytomegalovirus infection of human blood cells. J. Infect. Dis. **149:**207-214.

42. **Eulalio, A., I. Nunes-Correia, A. L. Carvalho, C. Faro, V. Citovsky, J. Salas, M. L. Salas, S. Simoes, and M. C. de Lima.** 2006. Nuclear export of African swine fever virus p37 protein occurs through two distinct pathways and is mediated by three independent signals. J. Virol. **80:**1393-1404.

43. **Feire, A. L., H. Koss, and T. Compton.** 2004. Cellular integrins function as entry receptors for human cytomegalovirus via a highly conserved disintegrin-like domain. Proc. Natl. Acad. Sci. USA **101:**15470-15475.

44. **Feng, X., J. Schroer, D. Yu, and T. Shenk.** 2006. Human cytomegalovirus pUS24 is a virion protein that functions very early in the replication cycle. J. Virol. **80:**8371-8378.

45. **Fish, K. N., A. S. Depto, A. V. Moses, W. Britt, and J. A. Nelson.** 1995. Growth kinetics of human cytomegalovirus are altered in monocyte-derived macrophages. J. Virol. **69:**3737-3743.

46. **Fornerod, M., M. Ohno, M. Yoshida, and I. W. Mattaj.** 1997. CRM1 is an export receptor for leucine-rich nuclear export signals. Cell **90:**1051-1060.

47. **Fukuda, M., S. Asano, T. Nakamura, M. Adachi, M. Yoshida, M. Yanagida, and E. Nishida.** 1997. CRM1 is responsible for intracellular transport mediated by the nuclear export signal. Nature **390:**308-311.

48. **Gibson, W.** 2006. Assembly and maturation of the capsid, p. 231-243. *In* M. J. Reddehase (ed.), Cytomegaloviruses. Lippincott-Raven, Philadelphia, PA.

49. **Goodrum, F. D., C. T. Jordan, K. High, and T. Shenk.** 2002. Human cytomegalovirus gene expression during infection of primary hematopoietic progenitor cells: a model for latency. Proc. Natl. Acad. Sci. USA **99:**16255-16260.

50. **Gorlich, D., P. Henklein, R. A. Laskey, and E. Hartmann.** 1996. A 41 amino acid motif in importin-alpha confers binding to importin-beta and hence transit into the nucleus. EMBO J. **15:**1810-1817.

51. **Gorlich, D., S. Kostka, R. Kraft, C. Dingwall, R. A. Laskey, E. Hartmann, and S. Prehn.** 1995. Two different subunits of importin cooperate to recognize nuclear localization signals and bind them to the nuclear envelope. Curr. Biol. **5:**383-392.

52. **Gredmark, S., W. B. Britt, X. Xie, L. Lindbom, and C. Soderberg-Naucler.** 2004. Human cytomegalovirus induces inhibition of macrophage differentiation by binding to human aminopeptidase N/CD13. J. Immunol. **173:**4897-4907.

53. **Groll, M., M. Bajorek, A. Kohler, L. Moroder, D. M. Rubin, R. Huber, M. H. Glickman, and D. Finley.** 2000. A gated channel into the proteasome core particle. Nat. Struct. Biol. **7:**1062-1067.

54. **Groll, M., L. Ditzel, J. Lowe, D. Stock, M. Bochtler, H. D. Bartunik, and R. Huber.** 1997. Structure of 20S proteasome from yeast at 2.4 A resolution. Nature **386:**463-471.

55. **Hakki, M., E. E. Marshall, K. L. De Niro, and A. P. Geballe.** 2006. Binding and nuclear relocalization of protein kinase R by human cytomegalovirus TRS1. J. Virol. **80:**11817-11826.

56. **Han, J. D., N. Bertin, T. Hao, D. S. Goldberg, G. F. Berriz, L. V. Zhang, D. Dupuy, A. J. Walhout, M. E. Cusick, F. P. Roth, and M. Vidal.** 2004. Evidence for dynamically organized modularity in the yeast protein-protein interaction network. Nature **430:**88-93.

57. **Hanson, L. K., and A. E. Campbell.** 2006. Determinants of Macrophage Tropism, p. 419-443. *In* M. J. Reddehase (ed.), Cytomegaloviruses. Caister Academic Press.

58. **Hanson, L. K., B. L. Dalton, L. F. Cageao, R. E. Brock, J. S. Slater, J. A. Kerry, and A. E. Campbell.** 2005. Characterization and regulation of essential murine cytomegalovirus genes m142 and m143. Virology **334:**166-177.

59. **Hanson, L. K., B. L. Dalton, Z. Karabekian, H. E. Farrell, W. D. Rawlinson, R. M. Stenberg, and A. E. Campbell.** 1999. Transcriptional analysis of the murine cytomegalovirus HindIII-I region: identification of a novel immediate-early gene region. Virology **260:**156-164.

60. **Hanson, L. K., J. S. Slater, V. J. Cavanaugh, W. W. Newcomb, L. L. Bolin, C. N. Nelson, L. D. Fetters, Q. Tang, J. C. Brown, G. Maul, and A. E. Campbell.** Murine cytomegalovirus capsid stability is dependent upon M140 in infected macrophages. J. Virol. In Press.

61. **Hanson, L. K., J. S. Slater, Z. Karabekian, G. Ciocco-Schmitt, and A. E. Campbell.** 2001. Products of US22 genes M140 and M141 confer efficient replication of murine cytomegalovirus in macrophages and spleen. J. Virol. **75:**6292-6302.

62. **Hanson, L. K., J. S. Slater, Z. Karabekian, H. W. t. Virgin, C. A. Biron, M. C. Ruzek, N. van Rooijen, R. P. Ciavarra, R. M. Stenberg, and A. E. Campbell.** 1999. Replication of murine cytomegalovirus in differentiated macrophages as a determinant of viral pathogenesis. J. Virol. **73:**5970-5980.

63. **Heise, M. T., M. Connick, and H. W. t. Virgin.** 1998. Murine cytomegalovirus inhibits interferon gamma-induced antigen presentation to CD4 T cells by macrophages via regulation of expression of major histocompatibility complex class II-associated genes. J. Exp. Med. **187:**1037-1046.

64. **Henry, S. C., K. Schmader, T. T. Brown, S. E. Miller, D. N. Howell, G. G. Daley, and J. D. Hamilton.** 2000. Enhanced green fluorescent protein as a marker for localizing murine cytomegalovirus in acute and latent infection. J. Virol. Methods **89:**61-73.

65. **Herbein, G., and W. A. O'Brien.** 2000. Tumor necrosis factor (TNF)-alpha and TNF receptors in viral pathogenesis. Proc. Soc. Exp. Biol. Med. **223:**241-257.

66. **Ho, M.** 2008. The history of cytomegalovirus and its diseases. Med. Microbiol. Immunol. **197:**65-73.

67. **Hofmann, R. M., and C. M. Pickart.** 2001. In vitro assembly and recognition of Lys-63 polyubiquitin chains. J. Biol. Chem. **276:**27936-27943.

68. **Homman-Loudiyi, M., K. Hultenby, W. Britt, and C. Soderberg-Naucler.** 2003. Envelopment of human cytomegalovirus occurs by budding into Golgi-

derived vacuole compartments positive for gB, Rab 3, trans-golgi network 46, and mannosidase II. J. Virol. **77:**3191-3203.

69. **Hoyt, M. A., and P. Coffino.** 2004. Ubiquitin-free routes into the proteasome. Cell. Mol. Life Sci. **61:**1596-1600.

70. **Hwang, J., and R. F. Kalejta.** 2007. Proteasome-dependent, ubiquitin-independent degradation of Daxx by the viral pp71 protein in human cytomegalovirus-infected cells. Virology **367:**334-338.

71. **Ibanez, C. E., R. Schrier, P. Ghazal, C. Wiley, and J. A. Nelson.** 1991. Human cytomegalovirus productively infects primary differentiated macrophages. J. Virol. **65:**6581-6588.

72. **Imamoto, N., T. Shimamoto, S. Kose, T. Takao, T. Tachibana, M. Matsubae, T. Sekimoto, Y. Shimonishi, and Y. Yoneda.** 1995. The nuclear pore-targeting complex binds to nuclear pores after association with a karyophile. FEBS Lett. **368:**415-419.

73. **Imamoto, N., T. Tachibana, M. Matsubae, and Y. Yoneda.** 1995. A karyophilic protein forms a stable complex with cytoplasmic components prior to nuclear pore binding. J. Biol. Chem. **270:**8559-8565.

74. **Isaacson, M. K., A. L. Feire, and T. Compton.** 2007. Epidermal growth factor receptor is not required for human cytomegalovirus entry or signaling. J. Virol. **81:**6241-6247.

75. **Izaurralde, E., U. Kutay, C. von Kobbe, I. W. Mattaj, and D. Gorlich.** 1997. The asymmetric distribution of the constituents of the Ran system is essential for transport into and out of the nucleus. EMBO J. **16:**6535-6547.

76. **Jans, D. A., C. Y. Xiao, and M. H. Lam.** 2000. Nuclear targeting signal recognition: a key control point in nuclear transport? Bioessays **22:**532-544.

77. **Jariel-Encontre, I., G. Bossis, and M. Piechaczyk.** 2008. Ubiquitin-independent degradation of proteins by the proteasome. Biochim. Biophys. Acta **1786:**153-177.

78. **Jarvis, M. A., and J. A. Nelson.** 2002. Human cytomegalovirus persistence and latency in endothelial cells and macrophages. Curr. Opin. Microbiol. **5:**403-407.

79. **Johnstone, R. W., J. A. Kerry, and J. A. Trapani.** 1998. The human interferon-inducible protein, IFI 16, is a repressor of transcription. J. Biol. Chem. **273:**17172-17177.

80. **Kalderon, D., B. L. Roberts, W. D. Richardson, and A. E. Smith.** 1984. A short amino acid sequence able to specify nuclear location. Cell **39:**499-509.

81. **Kalejta, R. F., and T. Shenk.** 2003. Proteasome-dependent, ubiquitin-independent degradation of the Rb family of tumor suppressors by the human cytomegalovirus pp71 protein. Proc. Natl. Acad. Sci. USA **100:**3263-3268.

82. **Karabekian, Z., L. K. Hanson, J. S. Slater, N. K. Krishna, L. L. Bolin, J. A. Kerry, and A. E. Campbell.** 2005. Complex formation among murine cytomegalovirus US22 proteins encoded by genes M139, M140, and M141. J. Virol. **79:**3525-3535.

83. **Kari, B., and R. Gehrz.** 1992. A human cytomegalovirus glycoprotein complex designated gC-II is a major heparin-binding component of the envelope. J. Virol. **66:**1761-1764.

84. **Karin, M., and Y. Ben-Neriah.** 2000. Phosphorylation meets ubiquitination: the control of NF-[kappa]B activity. Annu. Rev. Immunol. **18:**621-663.

85. **Kattenhorn, L. M., R. Mills, M. Wagner, A. Lomsadze, V. Makeev, M. Borodovsky, H. L. Ploegh, and B. M. Kessler.** 2004. Identification of proteins associated with murine cytomegalovirus virions. J. Virol. **78:**11187-11197.

86. **Kerry, J. A., M. A. Priddy, T. Y. Jervey, C. P. Kohler, T. L. Staley, C. D. Vanson, T. R. Jones, A. C. Iskenderian, D. G. Anders, and R. M. Stenberg.** 1996. Multiple regulatory events influence human cytomegalovirus DNA polymerase (UL54) expression during viral infection. J. Virol. **70:**373-382.

87. **Keskin, O., N. Tuncbag, and A. Gursoy.** 2008. Characterization and prediction of protein interfaces to infer protein-protein interaction networks. Curr. Pharm. Biotechnol. **9:**67-76.

88. **Khan, S., A. Zimmermann, M. Basler, M. Groettrup, and H. Hengel.** 2004. A cytomegalovirus inhibitor of gamma interferon signaling controls immunoproteasome induction. J. Virol. **78:**1831-1842.

89. **Kim, J. H., S. Y. Sohn, T. S. Benedict Yen, and B. Y. Ahn.** 2008. Ubiquitin-dependent and -independent proteasomal degradation of hepatitis B virus X protein. Biochem. Biophys. Res. Commun. **366:**1036-1042.

90. **Kirkpatrick, D. S., N. A. Hathaway, J. Hanna, S. Elsasser, J. Rush, D. Finley, R. W. King, and S. P. Gygi.** 2006. Quantitative analysis of in vitro ubiquitinated cyclin B1 reveals complex chain topology. Nat. Cell Biol. **8:**700-710.

91. **Kisselev, A. F., T. N. Akopian, K. M. Woo, and A. L. Goldberg.** 1999. The sizes of peptides generated from protein by mammalian 26 and 20 S proteasomes.

Implications for understanding the degradative mechanism and antigen presentation. J. Biol. Chem. **274:**3363-3371.

92. **Kisselev, A. F., and A. L. Goldberg.** 2001. Proteasome inhibitors: from research tools to drug candidates. Chem. Biol. **8:**739-758.

93. **Kohler, A., P. Cascio, D. S. Leggett, K. M. Woo, A. L. Goldberg, and D. Finley.** 2001. The axial channel of the proteasome core particle is gated by the Rpt2 ATPase and controls both substrate entry and product release. Mol. Cell **7:**1143-1152.

94. **Kouzarides, T., A. T. Bankier, S. C. Satchwell, E. Preddy, and B. G. Barrell.** 1988. An immediate early gene of human cytomegalovirus encodes a potential membrane glycoprotein. Virology **165:**151-164.

95. **Krmpotic, A., I. Bubic, B. Polic, P. Lucin, and S. Jonjic.** 2003. Pathogenesis of murine cytomegalovirus infection. Microbes Infect. **5:**1263-1277.

96. **Larsson, S., C. Soderberg-Naucler, F. Z. Wang, and E. Moller.** 1998. Cytomegalovirus DNA can be detected in peripheral blood mononuclear cells from all seropositive and most seronegative healthy blood donors over time. Transfusion **38:**271-278.

97. **Lee, C. H., G. C. Lee, Y. J. Chan, C. J. Chiou, J. H. Ahn, and G. S. Hayward.** 1999. Factors affecting human cytomegalovirus gene expression in human monocyte cell lines. Mol. Cells **9:**37-44.

98. **Link, H., K. Battmer, and C. Stumme.** 1993. Cytomegalovirus infection in leucocytes after bone marrow transplantation demonstrated by mRNA in situ hybridization. Br. J. Haematol. **85:**573-577.

99. **Loh, L. C., V. D. Keeler, and J. D. Shanley.** 1999. Sequence requirements for the nuclear localization of the murine cytomegalovirus M44 gene product pp50. Virology **259:**43-59.

100. **LoPiccolo, D. M., M. C. Gold, D. G. Kavanagh, M. Wagner, U. H. Koszinowski, and A. B. Hill.** 2003. Effective inhibition of K(b)- and D(b)-restricted antigen presentation in primary macrophages by murine cytomegalovirus. J. Virol. **77:**301-308.

101. **Lowe, J., D. Stock, B. Jap, P. Zwickl, W. Baumeister, and R. Huber.** 1995. Crystal structure of the 20S proteasome from the archaeon T. acidophilum at 3.4 A resolution. Science **268:**533-539.

102. **Macara, I. G.** 2001. Transport into and out of the nucleus. Microbiol. Mol. Biol. Rev. **65:**570-574.

103. **Magnani, M., R. Crinelli, M. Bianchi, and A. Antonelli.** 2000. The ubiquitin-dependent proteolytic system and other potential targets for the modulation of nuclear factor-kB (NF-kB). Curr. Drug Targets **1:**387-399.

104. **Mathes, E., E. L. O'Dea, A. Hoffmann, and G. Ghosh.** 2008. NF-kappaB dictates the degradation pathway of IkappaBalpha. EMBO J. **27:**1357-1367.

105. **Menard, C., M. Wagner, Z. Ruzsics, K. Holak, W. Brune, A. E. Campbell, and U. H. Koszinowski.** 2003. Role of murine cytomegalovirus US22 gene family members in replication in macrophages. J. Virol. **77:**5557-5570.

106. **Mendelson, M., S. Monard, P. Sissons, and J. Sinclair.** 1996. Detection of endogenous human cytomegalovirus in CD34+ bone marrow progenitors. J. Gen. Virol. 77 **(Pt 12):**3099-3102.

107. **Mercer, J. A., J. R. Marks, and D. H. Spector.** 1983. Molecular cloning and restriction endonuclease mapping of the murine cytomegalovirus genome (Smith Strain). Virology **129:**94-106.

108. **Meyer-Konig, U., F. T. Hufert, and D. M. von Laer.** 1997. Infection of blood and bone marrow cells with the human cytomegalovirus in vivo. Leuk. Lymphoma **25:**445-454.

109. **Miller, C. L., and D. J. Pintel.** 2001. The NS2 protein generated by the parvovirus minute virus of mice is degraded by the proteasome in a manner independent of ubiquitin chain elongation or activation. Virology **285:**346-355.

110. **Miller, D. M., B. M. Rahill, J. M. Boss, M. D. Lairmore, J. E. Durbin, J. W. Waldman, and D. D. Sedmak.** 1998. Human cytomegalovirus inhibits major histocompatibility complex class II expression by disruption of the Jak/Stat pathway. J. Exp. Med. **187:**675-683.

111. **Miller, D. M., Y. Zhang, B. M. Rahill, K. Kazor, S. Rofagha, J. J. Eckel, and D. D. Sedmak.** 2000. Human cytomegalovirus blocks interferon-gamma stimulated up-regulation of major histocompatibility complex class I expression and the class I antigen processing machinery. Transplantation **69:**687-690.

112. **Miller, D. M., Y. Zhang, B. M. Rahill, W. J. Waldman, and D. D. Sedmak.** 1999. Human cytomegalovirus inhibits IFN-alpha-stimulated antiviral and immunoregulatory responses by blocking multiple levels of IFN-alpha signal transduction. J. Immunol. **162:**6107-6113.

113. **Mitchell, B. M., A. Leung, and J. G. Stevens.** 1996. Murine cytomegalovirus DNA in peripheral blood of latently infected mice is detectable only in monocytes and polymorphonuclear leukocytes. Virology **223:**198-207.

114. **Mocarski, E. S., and C. T. Courcelle.** 2001. Cytomegaloviruses and their replication, p. 2629-2673. *In* P. M. H. D. M. Knipe, D. E. Griffin, R. A. Lamb, M. A. Martin, B. Roizmon, and S. E. Straus (ed.), Fields virology, Fourth ed, vol. 2. Lippincott-Raven, Philadelphia, PA.

115. **Morell, M., F. X. Aviles, and S. Ventura.** 2009. Detecting and interfering protein interactions: towards the control of biochemical pathways. Curr. Med. Chem. **16:**362-379.

116. **Murphy, E., D. Yu, J. Grimwood, J. Schmutz, M. Dickson, M. A. Jarvis, G. Hahn, J. A. Nelson, R. M. Myers, and T. E. Shenk.** 2003. Coding potential of laboratory and clinical strains of human cytomegalovirus. Proc. Natl. Acad. Sci. USA **100:**14976-14981.

117. **Myerson, D., R. C. Hackman, J. A. Nelson, D. C. Ward, and J. K. McDougall.** 1984. Widespread presence of histologically occult cytomegalovirus. Hum. Pathol. **15:**430-439.

118. **Narlikar, G. J., H. Y. Fan, and R. E. Kingston.** 2002. Cooperation between complexes that regulate chromatin structure and transcription. Cell **108:**475-487.

119. **Nicholas, J.** 1996. Determination and analysis of the complete nucleotide sequence of human herpesvirus. J. Virol. **70:**5975-5989.

120. **Nicholas, J., and M. E. Martin.** 1994. Nucleotide sequence analysis of a 38.5-kilobase-pair region of the genome of human herpesvirus 6 encoding human cytomegalovirus immediate-early gene homologs and transactivating functions. J. Virol. **68:**597-610.

121. **Niu, Y., F. Roy, F. Saltel, C. Andrieu-Soler, W. Dong, A. L. Chantegrel, R. Accardi, A. Thepot, N. Foiselle, M. Tommasino, P. Jurdic, and B. S. Sylla.** 2006. A nuclear export signal and phosphorylation regulate Dok1 subcellular localization and functions. Mol. Cell. Biol. **26:**4288-42301.

122. **Noda, S., K. Tanaka, S. Sawamura, M. Sasaki, T. Matsumoto, K. Mikami, Y. Aiba, H. Hasegawa, N. Kawabe, and Y. Koga.** 2001. Role of nitric oxide synthase type 2 in acute infection with murine cytomegalovirus. J. Immunol. **166:**3533-3541.

123. **Nussbaum, A. K., T. P. Dick, W. Keilholz, M. Schirle, S. Stevanovic, K. Dietz, W. Heinemeyer, M. Groll, D. H. Wolf, R. Huber, H. G. Rammensee, and H. Schild.** 1998. Cleavage motifs of the yeast 20S proteasome beta subunits deduced from digests of enolase 1. Proc. Natl. Acad. Sci. USA **95:**12504-12509.

124. **Odeberg, J., and C. Soderberg-Naucler.** 2001. Reduced expression of HLA class II molecules and Iinterleukin-10- and transforming growth factor beta1-independent suppression of T-cell proliferation in human cytomegalovirus-infected macrophage cultures. J. Virol. **75:**5174-5181.

125. **Oh, W., M. R. Yang, E. W. Lee, K. M. Park, S. Pyo, J. S. Yang, H. W. Lee, and J. Song.** 2006. Jab1 mediates cytoplasmic localization and degradation of West Nile virus capsid protein. J. Biol. Chem. **281:**30166-30174.

126. **Okada, K., K. Tanaka, S. Noda, M. Okazaki, and Y. Koga.** 1999. Nitric oxide increases the amount of murine cytomegalovirus-DNA in mice latently infected with the virus. Arch. Virol. **144:**2273-2290.

127. **Onno, M., C. Pangault, G. Le Friec, V. Guilloux, P. Andre, and R. Fauchet.** 2000. Modulation of HLA-G antigens expression by human cytomegalovirus: specific induction in activated macrophages harboring human cytomegalovirus infection. J. Immunol. **164:**6426-6434.

128. **Orlowski, M., and S. Wilk.** 2003. Ubiquitin-independent proteolytic functions of the proteasome. Arch. Biochem. Biophys. **415:**1-5.

129. **Ouchi, M., and T. Ouchi.** 2008. Role of IFI16 in DNA damage and checkpoint. Front. Biosci. **13:**236-239.

130. **Pass, R. F.** 2001. Cytomegaloviruses, p. 2675-2705. *In* P. M. H. D. M. Knipe, D. E. Griffin, R. A. Lamb, M. A. Martin, B. Roizmon, and S. E. Straus (ed.), Fields Virology, vol. 2. Lippincott-Raven, Philadelphia, PA.

131. **Pawson, T., and P. Nash.** 2003. Assembly of cell regulatory systems through protein interaction domains. Science **300:**445-452.

132. **Pawson, T., M. Raina, and P. Nash.** 2002. Interaction domains: from simple binding events to complex cellular behavior. FEBS Lett. **513:**2-10.

133. **Penfold, M. E., D. J. Dairaghi, G. M. Duke, N. Saederup, E. S. Mocarski, G. W. Kemble, and T. J. Schall.** 1999. Cytomegalovirus encodes a potent alpha chemokine. Proc. Natl. Acad. Sci. USA **96:**9839-9844.

134. **Petropoulos, L., and J. Hiscott.** 1998. Association between HTLV-1 Tax and I kappa B alpha is dependent on the I kappa B alpha phosphorylation state. Virology **252:**189-199.

135. **Pines, J., and C. Lindon.** 2005. Proteolysis: anytime, any place, anywhere? Nat. Cell Biol. **7:**731-735.

136. **Pollock, J. L., R. M. Presti, S. Paetzold, and H. W. t. Virgin.** 1997. Latent murine cytomegalovirus infection in macrophages. Virology **227:**168-179.

137. **Poon, I. K., and D. A. Jans.** 2005. Regulation of nuclear transport: central role in development and transformation? Traffic **6:**173-186.

138. **Popkin, D. L., and H. W. t. Virgin.** 2003. Murine cytomegalovirus infection inhibits tumor necrosis factor alpha responses in primary macrophages. J. Virol. **77:**10125-10130.

139. **Pouton, C. W., K. M. Wagstaff, D. M. Roth, G. W. Moseley, and D. A. Jans.** 2007. Targeted delivery to the nucleus. Adv. Drug Deliv. Rev. **59:**698-717.

140. **Presti, R. M., D. L. Popkin, M. Connick, S. Paetzold, and H. W. t. Virgin.** 2001. Novel cell type-specific antiviral mechanism of interferon gamma action in macrophages. J. Exp. Med. **193:**483-496.

141. **Radu, A., G. Blobel, and M. S. Moore.** 1995. Identification of a protein complex that is required for nuclear protein import and mediates docking of import substrate to distinct nucleoporins. Proc. Natl. Acad. Sci. USA **92:**1769-1773.

142. **Ravid, T., and M. Hochstrasser.** 2008. Diversity of degradation signals in the ubiquitin-proteasome system. Nat. Rev. Mol. Cell Biol. **9:**679-690.

143. **Rawlinson, W. D., H. E. Farrell, and B. G. Barrell.** 1996. Analysis of the complete DNA sequence of murine cytomegalovirus. J. Virol. **70:**8833-8849.

144. **Rechsteiner, M., and S. W. Rogers.** 1996. PEST sequences and regulation by proteolysis. Trends Biochem. Sci. **21:**267-271.

145. **Redpath, S., A. Angulo, N. R. Gascoigne, and P. Ghazal.** 1999. Murine cytomegalovirus infection down-regulates MHC class II expression on macrophages by induction of IL-10. J. Immunol. **162:**6701-6707.

146. **Reichelt, R., A. Holzenburg, E. L. Buhle, Jr., M. Jarnik, A. Engel, and U. Aebi.** 1990. Correlation between structure and mass distribution of the nuclear pore complex and of distinct pore complex components. J. Cell Biol. **110:**883-894.

147. **Rexach, M., and G. Blobel.** 1995. Protein import into nuclei: association and dissociation reactions involving transport substrate, transport factors, and nucleoporins. Cell **83:**683-692.

148. **Rice, G. P., R. D. Schrier, and M. B. Oldstone.** 1984. Cytomegalovirus infects human lymphocytes and monocytes: virus expression is restricted to immediate-early gene products. Proc. Natl. Acad. Sci. USA **81:**6134-6138.

149. **Rogers, S., R. Wells, and M. Rechsteiner.** 1986. Amino acid sequences common to rapidly degraded proteins: the PEST hypothesis. Science **234:**364-368.

150. **Roizman, B.** 1996. *Herpesviridae*, p. 2221-2230. *In* D. M. K. B. N. Fields, P. M. Howley (ed.), Fields Virology, Third ed, vol. 2. Lippincott-Raven, Philadelphia, PA.

151. **Romanowski, M. J., and T. Shenk.** 1997. Characterization of the human cytomegalovirus irs1 and trs1 genes: a second immediate-early transcription unit within irs1 whose product antagonizes transcriptional activation. J. Virol. **71:**1485-1496.

152. **Saederup, N., Y. C. Lin, D. J. Dairaghi, T. J. Schall, and E. S. Mocarski.** 1999. Cytomegalovirus-encoded beta chemokine promotes monocyte-associated viremia in the host. Proc. Natl. Acad. Sci. USA **96:**10881-10886.

153. **Sambrook, J. F., E.F.; Maniatis, T.** 1989. Molecular Cloning Second Edition ed. Cold Spring Harbor Laboratory Press.

154. **Sanchez, V., P. C. Angeletti, J. A. Engler, and W. J. Britt.** 1998. Localization of human cytomegalovirus structural proteins to the nuclear matrix of infected human fibroblasts. J. Virol. **72:**3321-3329.

155. **Sanchez, V., K. D. Greis, E. Sztul, and W. J. Britt.** 2000. Accumulation of virion tegument and envelope proteins in a stable cytoplasmic compartment during human cytomegalovirus replication: characterization of a potential site of virus assembly. J. Virol. **74:**975-986.

156. **Schroder, K., P. J. Hertzog, T. Ravasi, and D. A. Hume.** 2004. Interferon-gamma: an overview of signals, mechanisms and functions. J. Leukoc. Biol. **75:**163-189.

157. **Scott, M. L., T. Fujita, H. C. Liou, G. P. Nolan, and D. Baltimore.** 1993. The p65 subunit of NF-kappa B regulates I kappa B by two distinct mechanisms. Genes Dev. **7:**1266-1276.

158. **Seo, J. Y., and W. J. Britt.** 2006. Sequence requirements for localization of human cytomegalovirus tegument protein pp28 to the virus assembly compartment and for assembly of infectious virus. J. Virol. **80:**5611-5626.

159. **Sinclair, J., and P. Sissons.** 2006. Latency and reactivation of human cytomegalovirus. J. Gen. Virol. **87:**1763-1779.

160. **Sinzger, C., and G. Jahn.** 1996. Human cytomegalovirus cell tropism and pathogenesis. Intervirology **39:**302-319.

161. **Skaletskaya, A., L. M. Bartle, T. Chittenden, A. L. McCormick, E. S. Mocarski, and V. S. Goldmacher.** 2001. A cytomegalovirus-encoded inhibitor of apoptosis that suppresses caspase-8 activation. Proc. Natl. Acad. Sci. USA **98:**7829-7834.

162. **Smith, M. S., G. L. Bentz, J. S. Alexander, and A. D. Yurochko.** 2004. Human cytomegalovirus induces monocyte differentiation and migration as a strategy for dissemination and persistence. J. Virol. **78:**4444-4453.

163. **Smith, M. S., G. L. Bentz, P. M. Smith, E. R. Bivins, and A. D. Yurochko.** 2004. HCMV activates PI(3)K in monocytes and promotes monocyte motility and transendothelial migration in a PI(3)K-dependent manner. J. Leukoc. Biol. **76:**65-76.

164. **Soderberg-Naucler, C., K. Fish, and J. A. Nelson.** 1999. Cytomegalovirus, p. 209-242. *In* R. A. a. I. Chen (ed.), Persistent Viral Infections. John Wiley & Sons Ltd.

165. **Soderberg-Naucler, C., D. N. Streblow, K. N. Fish, J. Allan-Yorke, P. P. Smith, and J. A. Nelson.** 2001. Reactivation of latent human cytomegalovirus in CD14(+) monocytes is differentiation dependent. J. Virol. **75:**7543-7554.

166. **Soderberg, C., S. Larsson, S. Bergstedt-Lindqvist, and E. Moller.** 1993. Definition of a subset of human peripheral blood mononuclear cells that are permissive to human cytomegalovirus infection. J. Virol. **67:**3166-175.

167. **Soroceanu, L., A. Akhavan, and C. S. Cobbs.** 2008. Platelet-derived growth factor-alpha receptor activation is required for human cytomegalovirus infection. Nature **455:**391-395.

168. **Sorokin, A. V., E. R. Kim, and L. P. Ovchinnikov.** 2007. Nucleocytoplasmic transport of proteins. Biochemistry (Mosc) **72:**1439-1457.

169. **Spaete, R. R., R. C. Gehrz, and M. P. Landini.** 1994. Human cytomegalovirus structural proteins. J. Gen. Virol. **75 (Pt 12):**3287-3308.

170. **Stade, K., C. S. Ford, C. Guthrie, and K. Weis.** 1997. Exportin 1 (Crm1p) is an essential nuclear export factor. Cell **90:**1041-1050.

171. **Stasiak, P. C., and E. S. Mocarski.** 1992. Transactivation of the cytomegalovirus ICP36 gene promoter requires the alpha gene product TRS1 in addition to IE1 and IE2. J. Virol. **66:**1050-1058.

172. **Stewart, M.** 2007. Molecular mechanism of the nuclear protein import cycle. Nat. Rev. Mol. Cell Biol. **8:**195-208.

173. **Stinski, M. F., and D. T. Petrik.** 2008. Functional roles of the human cytomegalovirus essential IE86 protein. Curr. Top. Microbiol. Immunol. **325:**133-152.

174. **Stoddart, C. A., R. D. Cardin, J. M. Boname, W. C. Manning, G. B. Abenes, and E. S. Mocarski.** 1994. Peripheral blood mononuclear phagocytes mediate dissemination of murine cytomegalovirus. J. Virol. **68:**6243-6253.

175. **Strawn, L. A., T. Shen, N. Shulga, D. S. Goldfarb, and S. R. Wente.** 2004. Minimal nuclear pore complexes define FG repeat domains essential for transport. Nat. Cell Biol. **6:**197-206.

176. **Streblow, D. N., S. M. Varnum, R. D. Smith, and J. A. Nelson.** 2006. A proteomics analysis of human cytomegalovirus particles, p. 91-110. *In* M. J. Reddehase (ed.), Cytomegaloviruses. Caister Academic Press.

177. **Strehl, B., U. Seifert, E. Kruger, S. Heink, U. Kuckelkorn, and P. M. Kloetzel.** 2005. Interferon-gamma, the functional plasticity of the ubiquitin-proteasome system, and MHC class I antigen processing. Immunol. Rev. **207:**19-30.

178. **Suzuki, R., K. Moriishi, K. Fukuda, M. Shirakura, K. Ishii, I. Shoji, T. Wakita, T. Miyamura, Y. Matsuura, and T. Suzuki.** 2009. Proteasomal turnover of hepatitis C virus core protein is regulated by two distinct mechanisms: a ubiquitin-dependent mechanism and a ubiquitin-independent but PA28gamma-dependent mechanism. J. Virol. **83:**2389-2392.

179. **Tait, S. W., E. de Vries, C. Maas, A. M. Keller, C. S. D'Santos, and J. Borst.** 2007. Apoptosis induction by Bid requires unconventional ubiquitination and degradation of its N-terminal fragment. J. Cell Biol. **179:**1453-1466.

180. **Taylor-Wiedeman, J., G. P. Hayhurst, J. G. Sissons, and J. H. Sinclair.** 1993. Polymorphonuclear cells are not sites of persistence of human cytomegalovirus in healthy individuals. J. Gen. Virol. **74 (Pt 2):**265-268.

181. **Taylor-Wiedeman, J., J. G. Sissons, L. K. Borysiewicz, and J. H. Sinclair.** 1991. Monocytes are a major site of persistence of human cytomegalovirus in peripheral blood mononuclear cells. J. Gen. Virol. **72 (Pt 9):**2059-2064.

182. **Taylor-Wiedeman, J., P. Sissons, and J. Sinclair.** 1994. Induction of endogenous human cytomegalovirus gene expression after differentiation of monocytes from healthy carriers. J. Virol. **68:**1597-1604.

183. **Terry, L. J., E. B. Shows, and S. R. Wente.** 2007. Crossing the nuclear envelope: hierarchical regulation of nucleocytoplasmic transport. Science **318:**1412-1416.

184. **Treier, M., L. M. Staszewski, and D. Bohmann.** 1994. Ubiquitin-dependent c-Jun degradation in vivo is mediated by the delta domain. Cell **78:**787-798.

185. **Valchanova, R. S., M. Picard-Maureau, M. Budt, and W. Brune.** 2006. Murine cytomegalovirus m142 and m143 are both required to block protein kinase R-mediated shutdown of protein synthesis. J. Virol. **80:**10181-10190.

186. **Velichkova, M., and T. Hasson.** 2005. Keap1 regulates the oxidation-sensitive shuttling of Nrf2 into and out of the nucleus via a Crm1-dependent nuclear export mechanism. Mol. Cell. Biol. **25:**4501-4513.

187. **Voigt, A., U. Salzmann, U. Seifert, M. Dathe, A. Soza, P. M. Kloetzel, and U. Kuckelkorn.** 2007. 20S proteasome-dependent generation of an IEpp89 murine cytomegalovirus-derived H-2L(d) epitope from a recombinant protein. Biochem. Biophys. Res. Commun. **355:**549-554.

188. **von Laer, D., U. Meyer-Koenig, A. Serr, J. Finke, L. Kanz, A. A. Fauser, D. Neumann-Haefelin, W. Brugger, and F. T. Hufert.** 1995. Detection of cytomegalovirus DNA in CD34+ cells from blood and bone marrow. Blood **86:**4086-4090.

189. **von Laer, D., A. Serr, U. Meyer-Konig, G. Kirste, F. T. Hufert, and O. Haller.** 1995. Human cytomegalovirus immediate early and late transcripts are expressed in all major leukocyte populations in vivo. J. Infect. Dis. **172:**365-370.

190. **Wang, R., and M. G. Brattain.** 2007. The maximal size of protein to diffuse through the nuclear pore is larger than 60kDa. FEBS Lett. **581:**3164-3170.

191. **Wang, X., R. A. Herr, W. J. Chua, L. Lybarger, E. J. Wiertz, and T. H. Hansen.** 2007. Ubiquitination of serine, threonine, or lysine residues on the cytoplasmic tail can induce ERAD of MHC-I by viral E3 ligase mK3. J. Cell Biol. **177:**613-624.

192. **Wang, X., D. Y. Huang, S. M. Huong, and E. S. Huang.** 2005. Integrin alphavbeta3 is a coreceptor for human cytomegalovirus. Nat. Med. **11:**515-521.

193. **Wang, X., S. M. Huong, M. L. Chiu, N. Raab-Traub, and E. S. Huang.** 2003. Epidermal growth factor receptor is a cellular receptor for human cytomegalovirus. Nature **424:**456-461.

194. **Wenzel, T., and W. Baumeister.** 1995. Conformational constraints in protein degradation by the 20S proteasome. Nat. Struct. Biol. **2:**199-204.

195. **Whitby, F. G., E. I. Masters, L. Kramer, J. R. Knowlton, Y. Yao, C. C. Wang, and C. P. Hill.** 2000. Structural basis for the activation of 20S proteasomes by 11S regulators. Nature **408:**115-120.

196. **Wileman, T.** 2007. Aggresomes and pericentriolar sites of virus assembly: cellular defense or viral design? Annu. Rev. Microbiol. **61:**149-167.

197. **Yeow, W. S., C. M. Lawson, and M. W. Beilharz.** 1998. Antiviral activities of individual murine IFN-alpha subtypes in vivo: intramuscular injection of IFN expression constructs reduces cytomegalovirus replication. J. Immunol. **160:**2932-2939.

198. **Yerkovich, S. T., S. D. Olver, J. C. Lenzo, C. D. Peacock, and P. Price.** 1997. The roles of tumour necrosis factor-alpha, interleukin-1 and interleukin-12 in murine cytomegalovirus infection. Immunology **91:**45-52.

199. **Yoneda, Y.** 2000. Nucleocytoplasmic protein traffic and its significance to cell function. Genes Cells **5:**777-787.

200. **Yoneda, Y., M. Hieda, E. Nagoshi, and Y. Miyamoto.** 1999. Nucleocytoplasmic protein transport and recycling of Ran. Cell Struct. Funct. **24:**425-433.

201. **Yu, D., M. C. Silva, and T. Shenk.** 2003. Functional map of human cytomegalovirus AD169 defined by global mutational analysis. Proc. Natl. Acad. Sci. USA **100:**12396-123401.

202. **Yuksek, K., W. L. Chen, D. Chien, and J. H. Ou.** 2009. Ubiquitin-independent degradation of hepatitis C virus F protein. J. Virol. **83:**612-621.

203. **Yurochko, A. D., and E. S. Huang.** 1999. Human cytomegalovirus binding to human monocytes induces immunoregulatory gene expression. J. Immunol. **162:**4806-4816.

204. **Zeng, G. C., J. Donegan, H. L. Ozer, and R. Hand.** 1984. Characterization of a ts mutant of BALB/3T3 cells and correction of the defect by in vitro addition of extracts from wild-type cells. Mol. Cell. Biol. **4:**1815-1822.

205. **Zhou, H. X., and S. Qin.** 2007. Interaction-site prediction for protein complexes: a critical assessment. Bioinformatics **23:**2203-2209.

206. **Zhu, H., J. P. Cong, and T. Shenk.** 1997. Use of differential display analysis to assess the effect of human cytomegalovirus infection on the accumulation of cellular RNAs: induction of interferon-responsive RNAs. Proc. Natl. Acad. Sci. USA **94:**13985-13990.

207. **Zimmermann, A., M. Trilling, M. Wagner, M. Wilborn, I. Bubic, S. Jonjic, U. Koszinowski, and H. Hengel.** 2005. A cytomegaloviral protein reveals a dual role for STAT2 in IFN-{gamma} signaling and antiviral responses. J. Exp. Med. **201:**1543-1553.

VITA

Lisa L. Bolin

Education:

2009	Doctor of Philosophy, Biomedical Sciences Eastern Virginia Medical School (EVMS) and Old Dominion University Department of Microbiology and Molecular Cell Biology, EVMS
2002	Bachelor of Science, Biology and Biochemistry Old Dominion University
1999	Associate in Science Tidewater Community College

Publications:

1) Hanson, L.K., Slater, J.S., Cavanaugh, V.J., Newcomb, W.W., Bolin, L.L., Nelson, C.N., Fetters, L.D., Tang, Q., Brown, J.C., Maul, G., Campbell, A.E. Murine cytomegalovirus capsid stability is dependent upon M140 in infected macrophages. (2009) J. Virol. In press.

2) Karabekian, Z., Hanson, L.K., Slater, J.S., Krishna, N.K., Bolin, L.L., Kerry, J.A., Campbell, A.E. Complex formation among murine cytomegalovirus US22 proteins encoded by genes M139, M140, and M141. (2005) J. Virol. 79:3525-3535.

Awards:

2006	Second Place Graduate Research Award for Oral Presentation, Virginia Branch American Society for Microbiology
2005	Honorable Mention for Graduate Student Poster Presentation, Old Dominion University Annual Research Exposition
2002	Undergraduate Research Award for Poster Presentation, Virginia Branch American Society for Microbiology
2002	First Place Undergraduate Award for Poster Presentation, Fourth Annual Student Poster Session Tidewater Virginia Chapter of Sigma Xi